

MICROPALEONTOLOGICAL ANALYSIS AND SEQUENCE
STRATIGRAPHY THROUGH THE UPPER TOURNAISIAN SUBSTAGE
IN ALADAĞ UNIT
(CENTRAL TAURIDES, TURKEY)

A THESIS SUBMITTED TO
THE GRADUATE SCHOOL OF NATURAL AND APPLIED SCIENCES
OF
MIDDLE EAST TECHNICAL UNIVERSITY

BY

AKSEL TUĞBA DİNÇ

IN PARTIAL FULFILLMENT OF THE REQUIREMENTS
FOR
THE DEGREE OF MASTER OF SCIENCE
IN
GEOLOGICAL ENGINEERING

DECEMBER 2009

Approval of the thesis:

**MICROPALEONTOLOGICAL ANALYSIS AND SEQUENCE
STRATIGRAPHY THROUGH UPPER TOURNAISIAN SUBSTAGE
IN ALADAĞ UNIT
(CENTRAL TAURIDES, TURKEY)**

submitted by **AKSEL TUĞBA DİNÇ** in partial fulfillment of the requirements
for the degree of **Master of Science in Geological Engineering Department,**
Middle East Technical University by,

Prof. Dr. Canan Özgen _____
Dean, Graduate School of **Natural and Applied Sciences**

Prof. Dr. M. Zeki Çamur _____
Head of Department, **Geological Engineering**

Prof. Dr. Demir Altıner _____
Supervisor, **Geological Engineering Dept., METU**

Examining Committee Members:

Prof. Dr. Asuman Türkmenoğlu _____
Geological Engineering Dept., METU

Prof. Dr. Demir Altıner _____
Geological Engineering Dept., METU

Assoc. Prof. Dr. Bora Rojay _____
Geological Engineering Dept., METU

Assoc. Prof. Dr. İsmail Ömer Yılmaz _____
Geological Engineering Dept., METU

Dr. Zühtü Batı _____
TPAO, ANKARA

Date: 03. 12. 2009

I hereby declare that all information in this document has been obtained and presented in accordance with academic rules and ethical conduct. I also declare that, as required by these rules and conduct, I have fully cited and referenced all material and results that are not original to this work.

Name, Last Name: Aksel Tuğba DİNÇ

Signature:

ABSTRACT

MICROPALEONTOLOGICAL ANALYSIS AND SEQUENCE STRATIGRAPHY THROUGH UPPER TOURNAISIAN SUBSTAGE IN ALADAĞ UNIT (CENTRAL TAURIDES, TURKEY)

Dinç, Aksel Tuğba

M.Sc., Department of Geological Engineering

Supervisor : Prof. Dr. Demir Altıner

Co-Supervisor: Prof. Dr. Sevinç Özkan Altıner

December 2009, 121 pages

The purpose of this study is to investigate the Upper Tournaisian substage within the Carboniferous carbonate deposits of the Aladağ Unit in the Hadım region (Central Taurides) based on foraminiferal diversity and to study the meter scale cyclicity in order to explain the sequence stratigraphic evolution of the carbonate succession.

In this study, a 27.01 m thick stratigraphic section consisting of limestones and shales was measured and 89 samples, collected along this section, were analyzed. Micropaleontological analyses are based on benthic foraminifera. According to the benthic foraminiferal assemblages, two biozones were identified as Zone Ut1 and Zone Ut2 within the Upper Tournaisian. Zone Ut1 is characterized by a poor foraminiferal assemblage while the Zone Ut2 consists of a diverse Upper Tournaisian foraminiferal fauna.

In order to construct a sequence stratigraphic framework and appreciate depositional environmental changes, microfacies studies were carried out. Seven microfacies types were recognized and depending on the stacking patterns of these microfacies types, two fundamental types of cycles, A and B, were identified. Through the measured section, twenty-five shallowing-upward meter scale cycles

and two sequence boundaries were determined. Quantitative analysis of benthic foraminifera was used to demonstrate the biological response to cyclicity. Since foraminifers are very sensitive to sea level changes, the abundance of benthic foraminifera displays a good response to sedimentary cyclicity.

In order to apply a worldwide sequence stratigraphic correlation, the sequence boundaries and the meter scale cycles of this study were compared with those described in South China and Western European platform and the Moscow Syncline. An Early Tournaisian transgression was followed by a major fall in relative sea level during the Late Tournaisian. Two sequence boundaries recognized in the measured section correspond to global sea level falls in the Late Tournaisian.

Keywords: Tournaisian, Carboniferous, Carbonate platform, Sequence stratigraphy, Taurides, Foraminifera

ÖZ

ALADAĞ BİRİMİNİN ÜST TURNEZİYEN ASKATI BOYUNCA MİKROPALEONTOLOJİK ANALİZLER VE SEKANS STRATİGRAFİSİ (ORTA TOROSLAR, TÜRKİYE)

Dinç, Aksel Tuğba

Yüksek Lisans, Jeoloji Mühendisliği Bölümü

Tez Yöneticisi : Prof. Dr. Demir Altıner

Ortak Tez Yöneticisi: Prof. Dr. Sevinç Özkan Altıner

Aralık 2009, 121 sayfa

Bu çalışmanın amacı, Hadim (Orta Toroslar) bölgesinde yer alan Aladağ Birliği'ne ait Karbonifer karbonat çökeltilerinde bulunan Üst Turneziyen askatını, foraminifer çeşitliliğine dayanarak araştırmak ve bu karbonat istifinin sekans stratigrafik evrimini açıklayabilmek için metre ölçeğindeki devirselliğini çalışmaktır.

Bu çalışmada, kireçtaşı ve şeyller içeren 27.01 metrelik bir stratigrafik kesit ölçülmüş ve bu kesit boyunca alınan 89 adet örnek çalışılmıştır. Mikropaleontoloji analizleri bentik foraminifere dayanılarak yapılmıştır. Bentik foraminifer topluluklarına göre, Üst Turneziyen'de, Ut1 Zonu ve Ut2 Zonu olarak 2 adet biyozon ayırtlanmıştır. Ut1 Zonu, foraminifer faunasının ender gözlemlendiği bir zon iken, Ut2 Zonu ise Üst Turneziyen foraminifer faunasının çeşitliliği ile tanımlanmıştır.

Sekans stratigrafi çatısını oluşturabilmek ve çökelim ortamı değişimlerini kavrayabilmek için, mikrofasiyes çalışmaları yapılmıştır. Yedi adet mikrofasiyes tipi ayıklanmış ve bu mikrofasiyeslerin üst üste depolanma şekline göre, A ve B olarak iki tane temel devir tanımlanmıştır. Ölçülen kesit boyunca, yirmi beş adet

yukarı doğru sığlaşan metre ölçekli devir ve 2 sekans sınırı belirlenmiştir. Biyolojik tepkinin, devirsellik üzerindeki etkilerini ortaya koyabilmek için bentik foraminiferlerin sayısal analizleri kullanılmıştır. Foraminiferlerin deniz seviyesi değişimlerine çok duyarlı olmalarından dolayı, bentik foraminiferlerin bolluğu, sedimanter devirselliğe uyumlu tepki göstermektedir.

Evrensel bir sekans stratigrafi korelasyonu uygulayabilmek için, bu çalışmadaki metre ölçekli devirler ve sekans sınırları, Güney Çin ve Batı Avrupa platformları ve Moskova Syneclise'ndakiler ile karşılaştırılmıştır. Erken Turneziyen transgresyonu, Geç Turneziyen boyunca göreceli deniz seviyesindeki büyük bir düşüşle takip edilmiştir. Ölçülen kesitte tespit edilen iki sekans sınırı Geç Turneziyen'de tanınan iki global deniz seviyesine karşılık gelmektedir. Bu deniz seviyesi değişimlerinin küresel etkileri, çalışılan Üst-Turneziyen karbonat istifinde teşhis edilmiştir.

Anahtar kelimeler: Turneziyen, Karbonifer, Karbonat platformu, Sekans stratigrafisi, Toroslar, Foraminifer

ACKNOWLEDGEMENTS

I feel most grateful to my supervisor Prof. Dr. Demir Altıner for his precious suggestions, support, endless patience. He always encouraged me at every stage of this study and this thesis could not be accomplished without him; I feel really lucky to have the chance to work with him.

I would like to express my eternal thanks to my parents Hamide Dinç and Yaşar Dinç, my lovely brother Cem Dinç, my cousins Aylin Özcan, Serhat Akçabayırlı, Erkut Akdedmir, my aunt Zeliha Akdemir and my uncle Ali Akdemir for their lifetime support and love. All of you are my major reason in achieving this goal.

Special thanks to Prof. Dr. Sevinç Altıner for sharing her valuable ideas and I am grateful for all the mentoring and recommendations I have received. I would like to thank to Dr. Zühtü Batı for his help and technical support during my thesis.

I have received a lot of help from Ayşe Atakul and I am grateful to her for her valuable recommendations.

I would like to thank all the jury members, namely Prof. Dr. Asuman Türkmenoğlu, Assoc. Prof. Dr. Bora Rojaj, Assoc. Prof. Dr. İ. Ömer Yılmaz, Dr. Zühtü Batı, who spared their valuable time for this study. I am greatly thankful for their comments and critics which improved the text.

I would like to thank my dear friends Onur Karacaoğlu, Elif Medetoğulları, Gaye Oztepe, Dilhan Aydın, Pınar Kasımoğlu, Hilal Sevindik, Meral Bacanak, Hayriye Çakmak, Bükay Sardoğan, Özge Gürhan, Selen Esmeray for being there for me whenever I need.

I would like to thank to Ender Özaydın and Beytullah Demirtaş for their endless help and motivation during my study.

I would also like to thank Tayfun Cerrah, Nurettin Ahi, Uğur Kızıltepe, Özgür Sönmez, Ayla Bıyık, Özlem Sarp, Müge Çimen, Özgür Sarp, İlker Korkutlar for their understanding, tolerance and guidance through this study.

To my beloved parents and brother

TABLE OF CONTENTS

ABSTRACT	iv
ÖZ	vi
ACKNOWLEDGEMENTS	viii
TABLE OF CONTENTS	xi
LIST OF TABLES	xiii
LIST OF FIGURES	xiv

CHAPTERS

1 INTRODUCTION	1
1.1. Purpose and Scope	1
1.2. Geographic Setting	2
1.3. Method of Study	2
1.4. Previous Works	3
1.5. Regional Geology	9
2 LITHOSTRATIGRAPHY AND BIOSTRATIGRAPHY	13
2.1. Lithostratigraphy	13
2.1.1. Yarıcak Formation	14
2.1.1.1. Çityayla Member	14
2.1.1.2. Mantar Tepe Member	16
2.2. Biostratigraphy	22
3 SEQUENCE STRATIGRAPHY	28
3.1. Microfacies Types	28
3.1.1. Mudstone to Siltstone Microfacies	30
3.1.2. Silty Peloidal Mudstone Microfacies	30
3.1.3. Silty Peloidal Packstone Microfacies	33
3.1.4. Peloidal and Crinoidal Wackestone-Packstone Microfacies	33
3.1.5. Crinoidal Wackestone- Packstone Microfacies	35
3.1.6. Crinoidal and Foraminiferal Packstone-Grainstone	38

3.1.7. Foraminiferal Grainstone-Packstone Microfacies	41
3.2. Meter Scale Cycles Through the Upper-Tournaisian.....	41
3.3. Lateral Relationship of Meter-Scale Cycles	48
3.4. Sequence Stratigraphic Interpretation	50
3.5. Sequence Stratigraphic Correlations With Well-Known Tournaisian Sections of the World.....	53
3.6. Interpretation of Response of Benthic Foraminifers.....	60
4 SYTEMATIC PALEONTOLOGY.....	64
5 DISCUSSION AND CONCLUSION.....	89
REFERENCES.....	96
APPENDICES	
A: EXPLANATION OF PLATES.....	111
PLATE I.....	111
PLATE II.....	113
PLATE III.....	115
PLATE IV.....	117
PLATE V.....	119
B: NUMBER OF BENTHIC FORAMINIFERA COUNTED IN THE MEASURED SECTION.....	121

LIST OF TABLES

TABLES

Table 2.1. Foraminiferal zones in different studies.....	26
Table 3.1. Carbonate and siliciclastic facies and their depositional environments in the studied section.....	29
Table 3.2. Sequence stratigraphic correlation with bizozones and sequence boundaries between Belgium and Northern France and this study.....	58

LIST OF FIGURES

FIGURES

Figure 1.1. Location map of the study area where the stratigraphic section is taken.	2
Figure 1.2. Location of the 27.01 m thick stratigraphic section (A: layers from TD-51 to TD-71; B: layers from TD-72 to TD-78; C: layers from TD-79 to TD-129).	4
Figure 1.3. Geological subdivision of the Tauride Belt (modified from Özgül, 1984)	9
Figure 1.4. Tectonic map of the study area (modified from Altner and Özgül, 2001)	10
Figure 1.5. Allochthonous and allochthonous units in the Hadim-Taşkent area (Altner and Özgül, 2001). The stratigraphic position of the studied section is shown as a short vertical bar in the Aladağ Unit stratigraphy.....	11
Figure 2.1. Generalized columnar section of the Aladağ Unit in the Hadim-Taşkent area (simplified from Özgül, 1997). TD is the symbol of the measured section in the Yarıcak Formation.	15
Figure 2.2. Lithostratigraphy of the measured section with biozones	17
Figure 2.3. Photograph of the level consisting of coral corresponding to the sample TD-74 (C:Coral)	20
Figure 2.4. The beds corresponding to the samples TD-53 and TD-117 measure 17 cm and 110 cm respectively in the measured section....	21
Figure 2.5. Fossil ranges and biozonation in the measured section	24
Figure 2.6. The dashed line show the boundary of the biozones Ut1 and Ut2 within the Upper Tournaisian.....	25

Figure 2.7. The study areas of Upper Tournaisian foraminiferal zones are shown on the Early Carboniferous World map (taken from www.scotese.com).	26
Figure 3.1. Photomicrographs of mudstone to siltstone lithofacies (MS). (Q: Quartz grain), (1: TD-68; 2: TD-70)	31
Figure 3.2. Photomicrographs of silty peloidal mudstone lithofacies (MS-P1). (Q: Quartz grain, P: Peloid), (1: TD-60, 2: TD-64)	32
Figure 3.3. Photomicrographs of silty peloidal packstone lithofacies (P1). (Q: Quartz grain, P: Peloid), (1: TD-59; 2: TD-62)	34
Figure 3.4. Photomicrographs of peloidal and crinoidal wackestone-packstone lithofacies (P1-P2). (Cr: Crinoid fragment, Q: Quartz grain, P: Peloid), (1: TD-66; 2: TD-69)	36
Figure 3.5. Photomicrographs of crinoidal wackestone-packstone lithofacies (P2). (Br: Bryzoa fragment, Cr: Crinoid fragment), (1: TD-74; 2: TD-75)	37
Figure 3.6. Photomicrographs of foraminiferal and crinoidal packstone-grainstone lithofacies (P2-P3). (Bv: Bivalve fragment, C: Coral, F: Foraminifer), (1: TD-77; 2: TD-103)	39
Figure 3.7. The coral level (sample TD-77) in crinoidal and foraminiferal packstone-grainstone microfacies. The photomicrograph of the sample TD-77 is viewed in figure 3.6	40
Figure 3.8. Photomicrographs of foraminiferal grainstone-packstone lithofacies (P3). (Cr: Crinoidal fragment; F: Foraminifer; P: Peloid), (1-2: TD-107)	42
Figure 3.9. Meter scale cycles derived from microfacies analysis in the measured section	44
Figure 3.10. Types of cycles based on microfacies stacking patterns	47

Figure 3.11. Composite model illustrating the microfacies distribution of Upper Tournaisian beds in the investigated section (A1, A2, A3, B1, B2 are parasequence type illustrated in Figure 3.10). Note that parasequence organization illustrated in Figure 3.10 fit well to the lateral facies change illustrated in the figure with the exception of A4-type parasequence which requires a rather abrupt facies change model	49
Figure 3.12. The levels of sequence boundaries, namely SB1 and SB2, are interpreted as top of the layers corresponding to sample TD-51 and TD-100	54
Figure 3.13. Sequence stratigraphic correlation scheme for the Upper Tournaisian and Lower Visean starata in the Guangxi region (South China). LST: Lowstand system tract, TST: Transgressive system tract, HST: Highstand system tract, SB: Sequence Boundary, MFZ: Maximum flooding surface, A-F: Foraminiferal associations (modified from Hance <i>et al.</i> , 1997)	56
Figure 3.14. Carboniferous sea-level changes in the Moscow Syncline and comparison with the Carboniferous curves of Ross and Ross (1988) and this study (modified from Alekseev <i>et al.</i> (1996))	59
Figure 3.15. Benthic foraminiferal countings and response of foraminiferal abundance to meter-scale cycles.	62

CHAPTER 1

INTRODUCTION

1.1. Purpose and Scope

The purpose of this study is to delineate the Upper Tournaisian substage within the Carboniferous carbonate deposits of the Aladağ Unit in the Hadim region (Central Taurides) based on benthic foraminifers and to define the shallowing-upward meter scale cycles in order to explain the sequence stratigraphic evolution of the carbonate succession. A 27.01 m thick stratigraphic section has been measured across the well-exposed carbonate deposits of the Çityayla Member and the Mantar Tepe Member of the Yarıcak Formation which is one of the fundamental lithostratigraphic units of the Upper Paleozoic of the Aladağ Unit.

To investigate the Upper Tournaisian substage within the measured section, the biostratigraphical frame has been established based on foraminiferal diversity. According to the foraminiferal fauna, the measured section has been divided into two biozones. Moreover, detailed microfacies analysis has been carried out by using standard microfacies models of Flügel (2004) and Wilson (1975). Meter-scale shallowing-upward cycles have been determined by using the stacking pattern of microfacies types. The Upper Tournaisian sequence stratigraphic evolution along the section is explained by the successive development of two third-order sequences correlated with the Western European and Southern Chinese equivalents. Since foraminifers are very sensitive to sea level changes, a study was carried out on the response of foraminiferal abundance to sea level fluctuations. Furthermore, a broad taxonomic work has also been carried out by giving an account on the morphological description, distribution and occurrence of the foraminiferal fauna.

1.2. Geographic Setting

The study area is located at approximately 15 km southwest of the town of Hadim (Figure 1.1). The studied section was measured along a road cut on the way of Taşkent-Alanya. It is situated on the topographic map of O28-b2 of 1/25.000 scale. The section starts at coordinates 0457255 E and 4081848 N and finishes at 0457194 E and 4081850 N.



Figure 1.1: Location map of the study area where the stratigraphic section is taken.

1.3. Method of Study

In this study, both the field work and the laboratory work were carried out. Along the measured section each bed was analyzed in terms of lithology and faunal content. A sequence stratigraphic analysis was carried out by examining the

stacking patterns of meter-scale cycles which were defined by the stacking of vertical microfacies changes and changes in benthic foraminiferal population.

A total number of 89 oriented samples were collected along the measured section measuring 27.01 m in thickness (Figure 1.2). To investigate the benthic foraminiferal content and microfacies evolution, thin sections were prepared for the laboratory work. Thin sections were analyzed under the microscope and the foraminiferal content of each bed was determined by using the descriptions in previous works and the catalogue of foraminifers giving the original descriptions of taxa. According to the foraminiferal assemblages two biozones were defined within the Upper Tournaisian. Moreover, benthic foraminifers were counted in order to understand their responses to environmental variations caused by sea level oscillations reflected in the anatomy of shallowing-upward cycles.

1.4. Previous Works

Taurides has been studied by various researchers over the last century. The first studies in the Taurides were aiming to describe the evolution of the Tauride carbonate platform including stratigraphy and structural geology. Through these studies, Blumenthal (1944, 1947, 1951 and 1956) defined the basic geologic and the geomorphologic features of Seydişehir–Beyşehir region. Blumenthal (1944) investigated exposure of the Aladağ unit around Beyşehir, Bozkır and Northern Alanya region and named these exposures as the “Hadim Nappe”. Moreover, Blumenthal (1944) represented maps illustrating the tectonic structures of the Western Taurides. After Blumenthal, Monod (1967) tried to investigate the stratigraphic evolution of Tauride carbonate platform. Brunn et al. (1971) described the detailed geology and stratigraphy of Taurides. Among these studies, Özgül (1971) carried out very significant studies related to the structural evolution of Central Taurides. He defined the importance of block movements in structural evolution of the northern part of Central Taurides and mentioned that the lithological units of Paleozoic and younger ages, deposited in different basins,

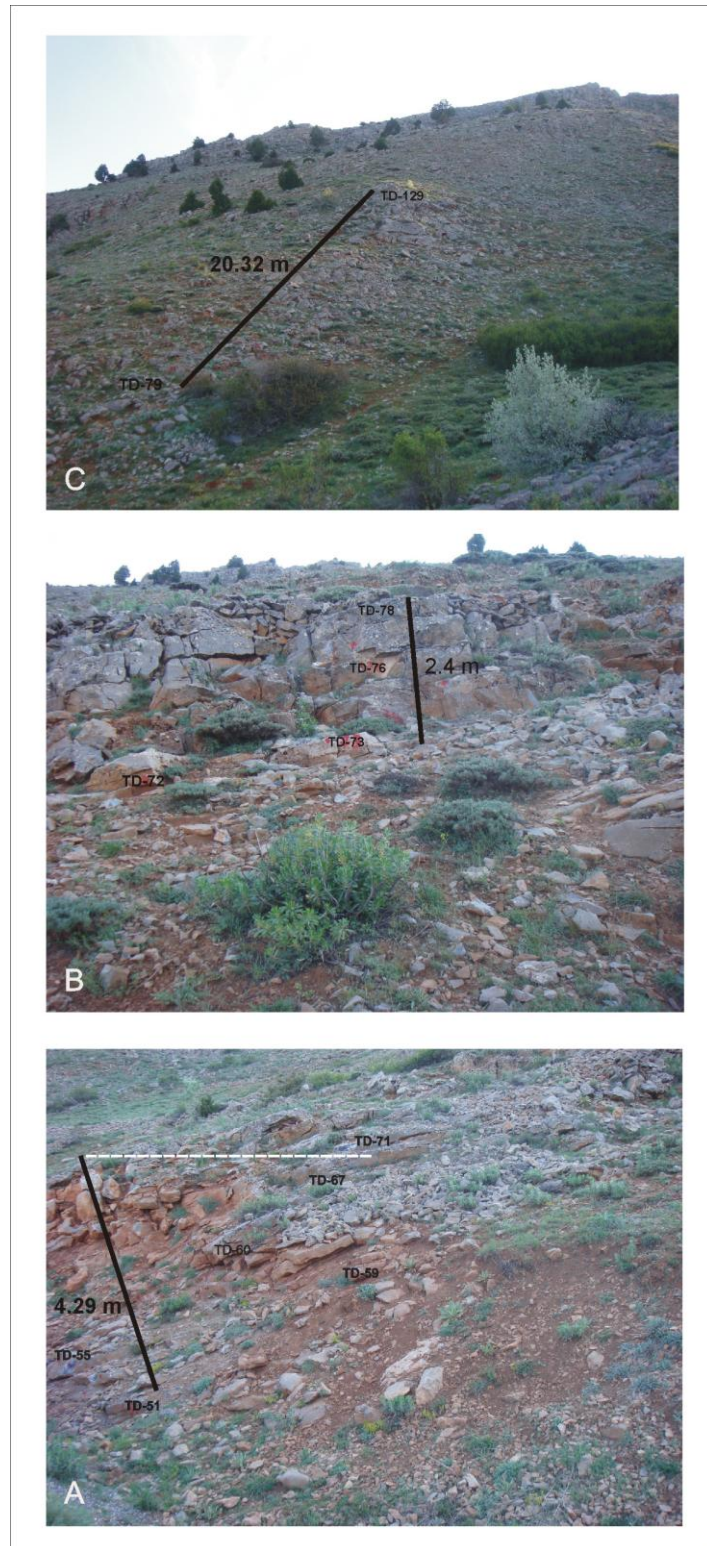


Figure 1.2: Location of the 27.01 m thick stratigraphic section (A: layers from TD-51 to TD-71; B: layers from TD-72 to TD-78; C: layers from TD-79 to TD-129).

were in faulted contact. He also defined the Hadim and Geyikdağı units as autochthonous and South Central Anatolia and Central Taurides units as allochthonous. Moreover, Özgül (1971) proposed that the allochthonous Central Taurus Unit - named as the “Hadim Nappe” by Blumenthal (1944) - was not a whole nappe but moved both in northern and southern direction. Özgül and Gedik (1973) studied the detailed stratigraphy of the Lower Paleozoic Çaltepe Limestone and Seydişehir Formation which crop out near Hadim (Konya) through a tectonic fenestral in Central Taurides. Özgül (1976) reported some geological aspects of the Taurides orogenic belt. According to Özgül (1976), the Taurus Mountains contain rock units which are deposited from Cambrian to Tertiary and within these belts there are different units representing basin conditions. He described six tectonostratigraphic units within Central Taurides and named these units as Bozkır Unit, Bolkar Dağı Unit, Aladağ Unit, Antalya Unit and Alanya Unit from north to south. He distinguished and differentiated these units from each other by their stratigraphic position, character of metamorphism, the rock units which they contain and their present structural position. According to Özgül (1976), the Aladağ Unit, Bolkar Dağı Unit, Geyik Dağı Unit and Alanya Units consisting of carbonates and detrial rocks were deposited in a shelf environment whereas the Bozkır Dağı Unit and Antalya Unit contain of deep sea sediments, ophiolites and submarine basic volcanic rocks. After Özgül, Monod (1977) described the Paleozoic unit of Bademli and reported the Carboniferous units consisting of carbonates and interclated quartz arenitic sandstones and dolomites. He also named the Aladağ and Bozkır Units as “Beyşehir Hoyran Nappes” and the rock units belonging to the Aladağ Units as the “Bademli-Cevizli Unit”. The Bademli-Cevizli Units of Monod (1977) are also equivalent of the “Hadim Nappe” of Blumenthal (1944). After Monod, Gutnic et al. (1979) also studied the Carboniferous units of Bademli and documented the Carboniferous units consisting of shales with brachiopods and neritic carbonate deposits. Özgül (1984) carried out a very important study in terms of the stratigraphy and tectonic evolution of the Central Taurides. According to Özgül (1984), the geographical subdivision of the Tauride Belt consists of three main sectors, namely Western, Central and Eastern Taurides. Özgül (1984) defined the Bozkır, Bolkar Dağı,

Aladağ, Antalya and Alanya Units as allochthonous and the Geyik Dağı as the main autochthon. He mentioned that the allochthonous units were emplaced onto the main autochthon during the Cretaceous to Eocene times from south to north resulting in the formation of several rock packages piled on top of each other as nappes. Demirtaşlı (1984) studied the stratigraphy and tectonics of the area between Silifke and Anamur within Central Taurus Mountains. He recognized four tectonostratigraphic units as the Autochthonous Southern Zone, the Intermediate Zone (Lower Allochthon), the Northern Zone (Middle Allochthon) and the Hadim Nappe (Upper Allochthon; the Aladağ Unit of Özgül, 1976) and mentioned that the stratigraphic sequences of each of these units show considerable differences indicating a contrasting tectonic development of each unit.

Özgül (1997) carried out a detailed study related to stratigraphical frameworks of tectonic units of Hadim-Taşkent region in the Central Taurides. He divided the Aladağ Unit into six formations and named these formations as Gölboğazı Formation (Devonian), Yarıcak Formation (Carboniferous), Çekiç Dağı Formation (Permian), Gevne Formation (Triassic), Çambaşı Formation (Jurassic-Cretaceous) and Zekeriya Formation (Maastrichtian). He divided the Yarıcak Formation into two members and named these members as Çityayla Member and Mantar Tepe Member. The subdivision of this formation proposed in this study were very important in terms of lithostratigraphy of the study area, since the stratigraphic section analyzed in this study was measured within the carbonates of Yarıcak Formation.

The micropaleontological studies play an important role in the investigation of Tournaisian-Visean boundary. Many researchers have been studying the Upper Tournaisian to define the Tournaisian-Visean boundary in recent years. The Carboniferous Namur-Dinant Basin (Southern Belgium) is one of the best documented basin in the world since it is the type area for the Tournaisian and Visean stages. Therefore, outcrops in Namur-Dinant Basin have been used as worldwide references for the Mississippian Subsystem (Lower Carboniferous). In

1967, the 6th International Carboniferous Congress adopted Conil's proposal for defining the lower boundary of the Visean in the Dinant Bastion section (Subcommission of Carboniferous Stratigraphy 1969). Conil and Lys (1968) studied the Dinantian foraminifers in Belgium. After these studies, Conil and Lys (1977), documented the effect of transgressions on Dinantian foraminifers. Conil (1988) studied the Tournaisian-Visean boundary and documented the foraminifers in Dinant Basin. According to Conil (1989), the distribution of the principal fossil guides in the Tournaisian-Visean transitional strata of the Dinant type area appears to be ecologically controlled because of restricted sedimentation conditions. Conil et al. (1991) defined a Mississippian and Devonian foraminiferal zonation in Namur-Dinant Basin. After Conil et al. (1991), Hance et al. (1994) studied Moliniacien in Belgium Dinant. Among these studies, Hance and Muech (1995) presented a proposal at the 13th International Congress on the Carboniferous-Permian at Krakow (Poland). They suggested placing the lower boundary of the Visean at the entry of *Eoparastaffella* with a subangular outer periphery (morphotype 1) succeeding the primitive specimens with a rounded periphery (morphotype 2). Hance et al. (1997) carried out a detailed micropaleontological study to investigate the evolution of the T-V transitional strata in South China (Guangxi). They distinguished six foraminiferal associations (A-F) in the Tournaisian-Visean transitional strata and they carried out a careful examination of the evolutionary stages of the foraminifer *Eoparastaffella*. Poty et al. (2006) studied the Mississippian foraminiferal zonation of Belgium and Northern France. They differentiated sixteen Mississippian Foraminifer Zones from MFZ1 to MFZ16. Devuyst et al. (2006) studied the early evolution of the genus *Eoparastaffella* in Eurasia and carried out a detailed taxonomic study for the *interiacta* group and related forms in the Late Tournaisian and Early Visean.

The biostratigraphical data was also used to realize the biostratigraphical evolution of Tauride Belt in Carboniferous age by many researchers. Altner (1981, 1984) carried out many biostratigraphical studies on the Triassic, Permian and Carboniferous rock bodies in the Tauride Belt. Altner et al. (2000) discussed the Upper Permian foraminiferal biofacies belts and investigated several

similarities in lithology and fossil assemblages between the upper Permian deposits of the Tauride-Anatolide platform in the south and the Arabian platform in the southeast Anatolia. Among these studies, Altiner and Özgül (2001) studied on foraminiferal associations of Carboniferous and Permian units and several biozones were investigated in Hadim region. Peynircioğlu (2005) carried out a micropaleontological analysis across the Tournaisian-Visean boundary in Aladağ Unit within Central Taurides. Atakul (2006) delineated the effective boundary between Lower and Middle Carboniferous and studied the foraminiferal evolution across a stratigraphic section comprising this boundary. Kobayashi and Altiner (2008) studied the Late Carboniferous and Early Permian Fusulinoideans in Hadim area within the Central Taurides.

The cyclostratigraphic and sequence stratigraphic studies in Carboniferous units of Central Taurides were carried out by several researchers. Şen (2002) defined the meter-scale cycles of the Middle Carboniferous subtidal carbonates and studied the responses of fusulinacean foraminifers to sedimentary cyclicity and examined the evolutionary pattern of the biofacies and lithofacies. Peynircioğlu (2005) identified shallowing-upward meter scale cycles across the Tournaisian-Visean boundary within the Aladağ Unit (Central Taurides). Atakul (2006) carried out detailed microfacies and sequence stratigraphic studies in the Hadim region of Central Taurides. Sequence stratigraphical studies within the Tournaisian-Visean carbonate deposits were also carried by foreign researchers worldwide. Alekseev et al. (1996) described the Carboniferous sea-level changes within the Moscow Syncline. They construct new relative sea-level curves for the Carboniferous of the Moscow Syncline and they marked an early Tournaisian transgression followed by a prominent early Visean regression. After Alekseev et al., Hance et al. (1997) also carried out a detailed study in order to construct a sequence stratigraphical approach within the Tournaisian-Visean starata in South China. According to Hance et al. (1997), a major fall in relative sea-level occurred during Late Tournaisian time in the Guangxi region and the resulting unconformity in the platform area forms a classic type 1 sequence boundary predated by the entry of the Visean *Eoparastaffella* (morphotype 2).

1.5. Regional Geology

According to Özgül (1984) the geographical subdivision of the Tauride Belt consists of three main sectors, namely Western, Central and Eastern Taurides (Figure 1.3). Our study locality falls into the Central Taurides which comprise several tectonic units. Özgül (1976) described and named these tectonic units as Bozkır, Bolkar Dağı, Aladağ, Geyik Dağı, Antalya and Alanya Units from north to south (Figure 1.4). Bozkır, Bolkar Dağı, Aladağ, Antalya and Alanya Units are allochthonous whereas the Geyik Dağı Unit is the main autochthon (Özgül, 1984) (Figure 1.5). The allochthonous units were emplaced onto the autochthon during the Late Cretaceous to Eocene times both from the south and the north. These movements resulted finally in the formation of several rock packages piled on top of each other as nappes constituting the typical tectonic structure of the Tauride Belt (Özgül, 1984). When the lithological, biostratigraphical and geochronological data are examined, many similarities are found between the Paleozoic to Tertiary sequences of the tectonic units of the Central Taurides. This suggests that Geyikdağı, Aladağ, Bolkar Dağı and Bozkır Units were representing the northern part of a huge platform which probably remained undisturbed at least up to the Late Cretaceous times (Özgül, 1984).

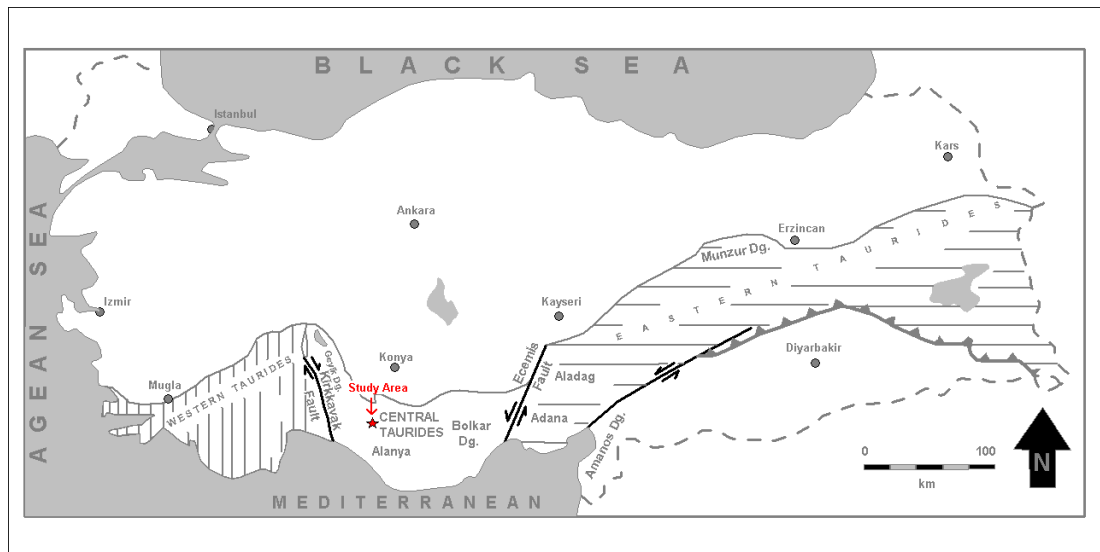


Figure 1.3: Geographical subdivision of the Tauride Belt (modified from Özgül, 1984).

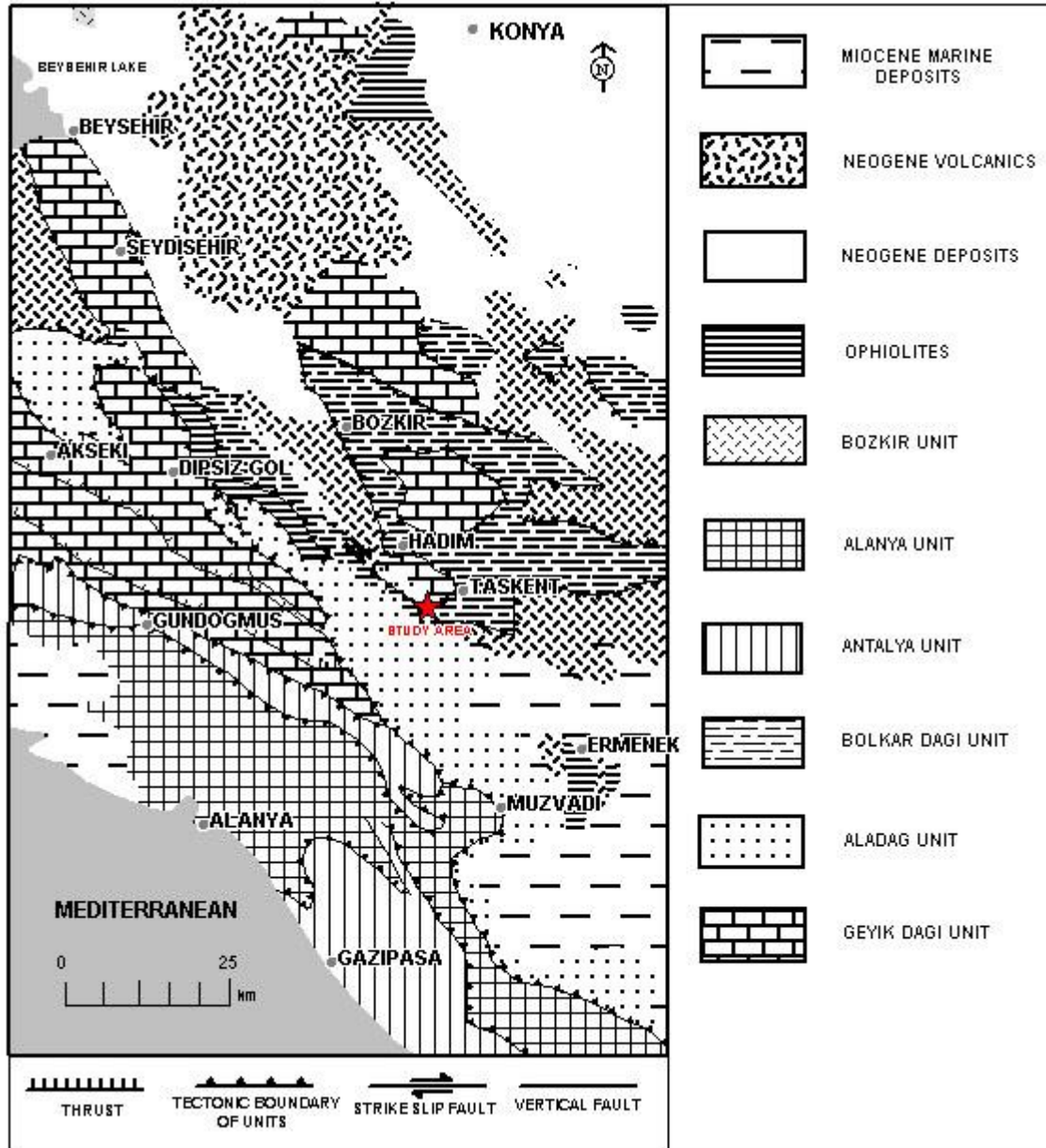


Figure 1.4: Tectonic map of the study area (modified from Altıner and Özgül, 2001).

The study area is located within the allochthonous Aladağ Unit and it is well exposed in the Hadim-Taşkent Region (Figure 1.4). The Aladağ Unit is characterized by shelf type carbonates and clastic rocks of Late Devonian-Late Cretaceous age (Figure 1.5). Aladağ Unit is divided into six formations in the Hadim-Taşkent Region as Gölboğazı Formation (Devonian), Yarıcak Formation (Carboniferous), Çekiç Dağı Formation (Permian), Gevne Formation (Triassic), Çambaşı Formation (Jurassic-Cretaceous) and Zekeriya Formation (Maastrichtian) (Özgül, 1997). Among these formations, mostly composed of

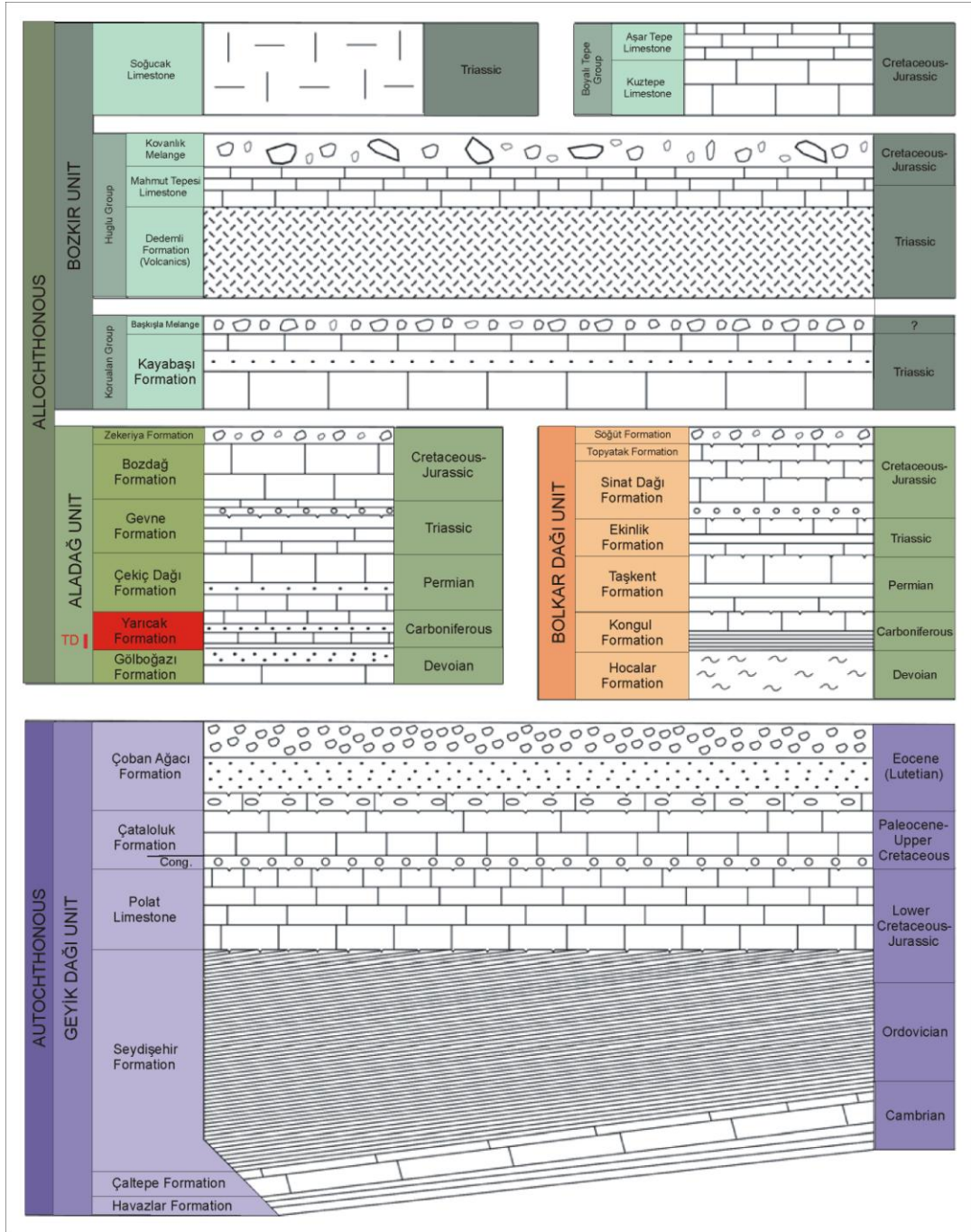


Figure 1.5: Autochthonous and allochthonous units in the Hadim-Taşkent area (Altner and Özgül, 2001). The stratigraphic position of the studied section is shown as a short vertical bar in the Aladağ Unit stratigraphy (TD is the symbol of the measured section in the Yarıcak Formation).

carbonates and subordinate quartz arenites, the Yarıcak Formation constitutes the main subject of this thesis. This formation consists of dark shales of Tournaisian age at the bottom and a main limestone unit corresponding to the Upper Tournaisian to Viséan carbonates in the middle of the formation. The upper part of the formation is basically composed of sandstone and limestone interclations ranging in age from Serpukhovian to Late Carboniferous. Within this general stratigraphic frame, our studied section corresponds to the Mississippian portion of the section, located at the base of Upper Tournaisian to Viséan carbonates (Figure 1.5).

CHAPTER 2

LITHOSTRATIGRAPHY AND BIOSTRATIGRAPHY

2.1. Lithostratigraphy

The study area is located on the exposures of the Aladağ unit which is one of the tectonic units of the Central Taurides. Aladağ Unit consists of shelf type clastics and carbonates of Late Devonian-Late Cretaceous age (Özgül, 1984). Özgül (1984) defined the Aladağ Unit as the equivalent of the “Hadim Nappe” of Blumenthal (1944) and “Bademli-Cevizli Unit” of Monod (1977). It is subdivided into six formations named as Gölboğazı Formation (Devonian), Yarıcak Formation (Carboniferous), Çekiç Dağı Formation (Permian), Gevne Formation (Triassic), Çambaşı Formation (Jurassic- Cretaceous) and Zekeriya Formation (Maastrichtian) (Özgül, 1997) (Figure 2.1). The Upper Paleozoic of the Aladağ Unit comprises three of these rock formations and starts at the base with the Gölboğazı Formation of Late Devonian age consisting of dolomites, quartz sandstones, reefal limestones and shales. The quartz sandstones representing the uppermost levels of the Gölboğazı Formation are overlain by the Tournaisian shales of the Çityayla Member of the Yarıcak Formation. The rest of the Yarıcak Formation continues with limestone and quartz sandstone- limestone alternations of Late Tournaisian to Late Carboniferous age. The Paleozoic of the Aladağ Unit is capped by the Permian carbonates and quartz arenites of Çekiç Dağı Formation. The studied Upper Tournaisian carbonates in this study are located in the Carboniferous Yarıcak Formation whose stratigraphy is treated in detail below.

2.1.1. Yarıcak Formation

The Yarıcak Formation takes its name from the type section which passes through the Yarıcak Plateau. Along its type section, located 9-10 km southwest of the Hadim Town, the formation mainly consists of shallow water limestones interclated with quartz arenitic sandstone layers at the top and dark colored shale layers at the base (Özgül, 1997). The thickness of the type section and reference section are measured 860 m and 600 m, respectively (Özgül, 1997). It overlies conformably the Gölboğazı Formation and is overlain unconformably by the Çekiç Dağı Formation (Figure 2.1). The underlying Gölboğazı Formation of Late Devonian age consists of dolomites, quartz arenitic sandstone, shale and reefal limestone including fragments of coral, brachiopod, crinoid, alg and bryzoa (Özgül, 1997). Overlying Çekiç Dağı Formation of Permian age is mainly characterized by carbonates consisting of benthic foraminifers and algae at the top and quartz arenitic sandstone at the base. The Çekiç Dağ Formation is divided into 4 members from bottom to top and named as Keltaş Limestone Member, Çamalanı Limestone Member, Kızılgiriş Member, Yellice Limestone Member, respectively. Çekiç Dağı Member overlies the Yarıcak Formation unconformably (Özgül, 1997). The Yarıcak formation is subdivided into two members named as Çityayla Limestone Member and Mantar Tepe Member from bottom to top.

2.1.1.1. Çityayla Member

The Çityayla Member overlies conformably the Gölboğazı Formation of Devonian age and is overlain by the Mantar Tepe Member of latest Tournaisian to Late Carboniferous age. The member takes its name from the Çityayla Plateau. The thickness of the type section and the reference section are 107 m and 50 m, respectively (Özgül, 1997). The fossil groups recorded in the member comprise Tournaisian brachiopods, crinoids, bryozoa and rarely trilobites and lesser amount

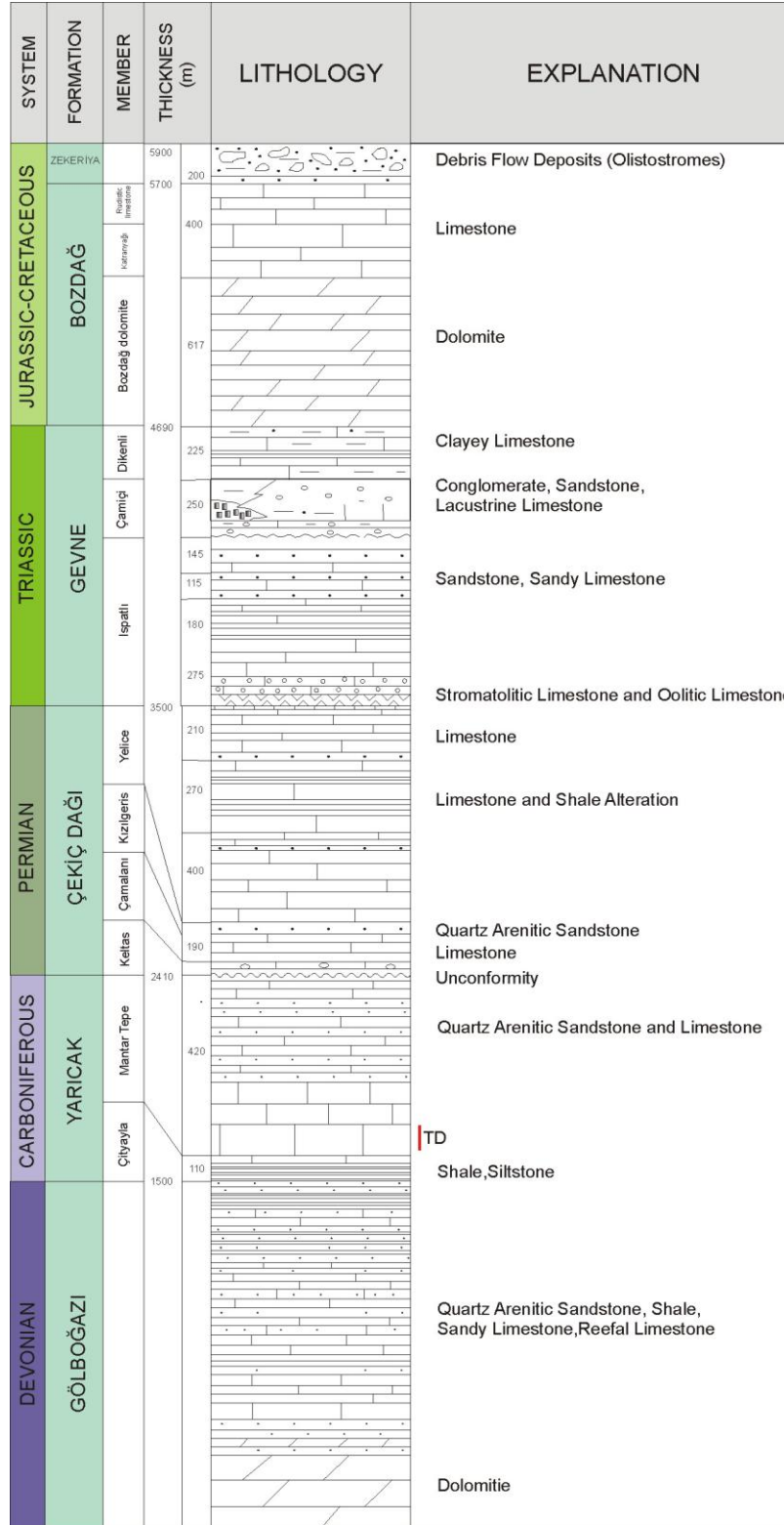


Figure 2.1: Generalized columnar section of the Aladağ Unit in the Hadim Taşkent area (simplified from Özgül, 1997). TD is the symbol of the measured section in the Yarıcak Formation.

of microfossils. It includes a foraminiferal fauna comprising *Earlandia minor*, *Earlandia elegans* and a brachiopod fauna comprising *Productus productus*, *Tomiproductus vaughani*, *Ripidomella michelini*, *Spifer tornacensis*, *Marginifera* sp. (Özgül, 1997). The Çityayla Member is characterized by dark colored shales with limestone and sandstone interrelations which indicate the deposition of Çityayla Member in low energy shelf conditions below the wave base level (Özgül, 1997). The lower part of the measured section presented in this study comprises the top of the Çityayla Member.

2.1.1.2. Mantar Tepe Member

The Mantar Tepe Member comprises most of the Yarıcak Formation and takes its name from the Mantar Tepe. It overlies the Çityayla Member and is overlain unconformably by the Çekiç Dağı Formation. The member is characterized by bioclastic, oolitic and micritic limestones at the bottom and quartz arenitic sandstones interclated with fusuline-rich limestone levels at the top (Altınır and Özgül, 2001). The thickness of the type section and reference section are 860 m and 600 m, respectively (Özgül, 1997). The lower part of the Mantar Tepe Member comprises a level of limestone including *Siphonophyllia cylindrica* which characterizes the Upper Tournaisian- Lower Visean interval (Özgül, 1997). Özgül (1997) recognized Visean, Serpukhovian, Bashkirian, Moscovian stages within the type section of the Mantar Tepe Member based on foraminiferal and algal zones. The Visean consists of *Pseudoendothyra struvei*, *Eostaffella parastruvei*, *Archaediscus* spp., *Mediocris mediocris*, *Dainella tujmasensis*, *Endothyra* spp., *Omphalotis samarica*, *Rectodiscus rotundus*, *Eoparastaffella simplex*, *Plectogyranopsis convexa*, *Siphonophylla clindrica*, *Syringopora* sp., *Lithostrotion* sp., *Paleosmilla* sp. A Serpukhovian age was assigned on the lossis of a fossil assemblage of *Plectostaffella jakhensis*, *Eostafella postmosquensis*, *E. pseudotruvei*, *Globivalvulina moderata*, *Pseudoendothyra suppressa*, *Pseudoglomospira subquadrata*, *Neoarchaediscus incertus*, *N. ovoides*. The Bashkirian stage is characterized by *Profusulinella parva*, *P. spp.*, *Ozowainella*

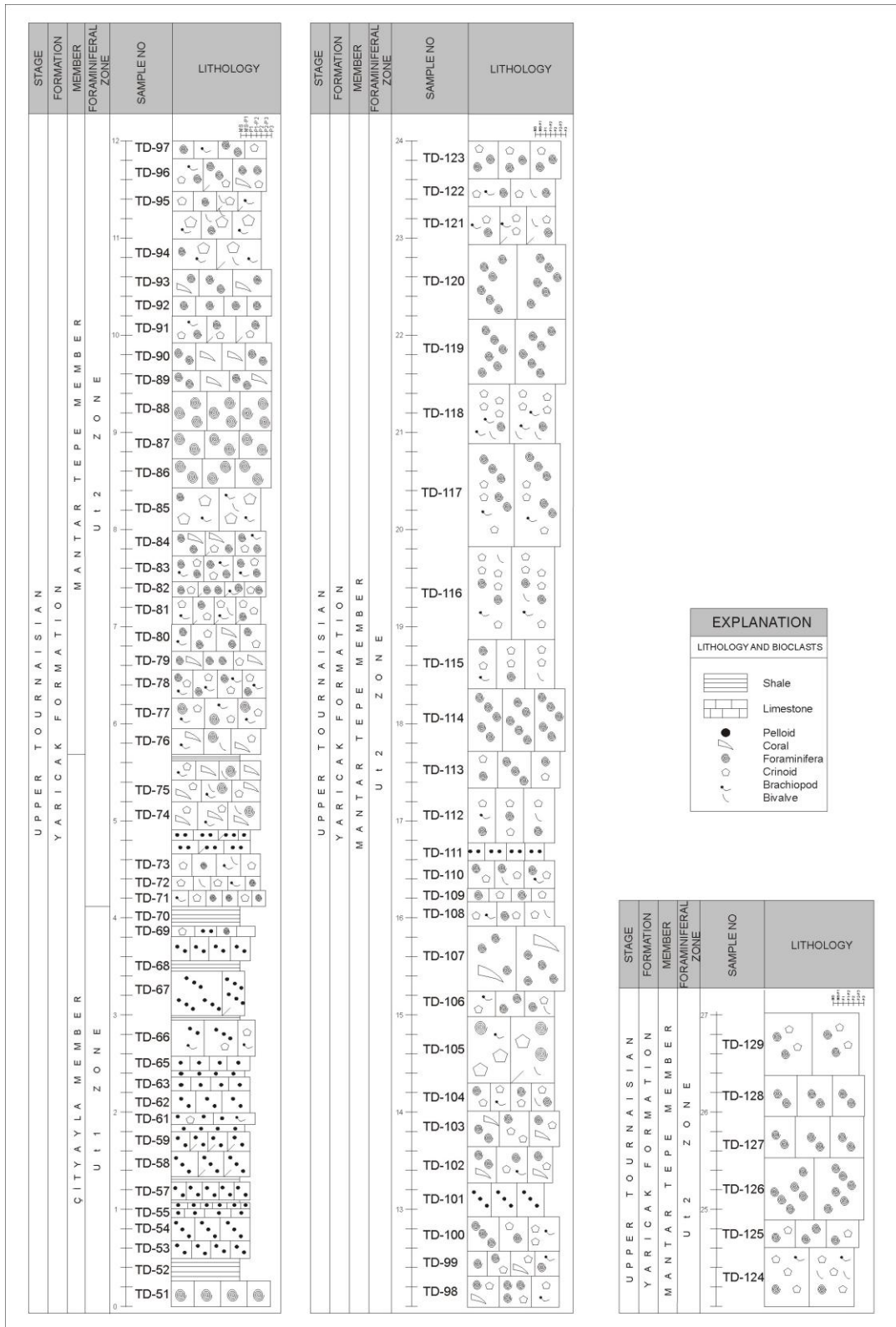


Figure 2.2: Lithostratigraphy of the measured section with biozones.

rhomboformis, *Eostaffela* spp., *Millerella concinna*, *Pseudostaffella antiqua*, *Asteroarchaediscus bashkiricus*, *Endothyra bashkirica*, *Globivalvulina scaphoidea*, *Bradyina cribrostomata*. The upper most part of the member of Moscovian age consists of *Fusulinella* ex. gr. *bocki*, *Eofusulina triangula*, *Bradyina samarica*, *B. pauciseptata*, *Eoschubertella* sp., *Neostaffella subquadrata*, *Eofusulina triangula*, *Globivalvulina granulosa* (Özgül, 1997). The Mantar Tepe Member was probably deposited in a relatively high energy environment of shallow shelf receiving high amount of sediment influx from the land (Özgül, 1997).

A considerable part of the measured section presented in this study comprises the top of the Çityayla Member and the base of the Mantar Tepe Member corresponding to the Upper Tournaisian. It starts with the shale-limestone alternations at the base (layers from sample TD-51 to TD-76) and then continues with the shallow subtidal carbonates (layers from sample TD-77 to TD-129, Figure 2.2). The shale-limestone alternation is observed at the boundary of Çityayla and Mantar Tepe Members of Özgül (1997) (Figure 2.1). We have also interpreted the interval represented by the shale-limestone alternation as the Çityayla Member (layers from sample TD-51 to TD-76, Figure 2.2) whereas the upper part of the section characterized by limestones of the Mantar Tepe Member (layers from sample TD-77 to TD-129, Figure 2.2).

The measured section starts with a major limestone bed consisting of benthic foraminifera and bioclasts (sample TD-51, Figure 2.2). Above this level, the investigated section displays a significant change in sedimentation and a 25 cm thick shale layer is recognized (TD-52, Figure 2.2). The shale layer is overlain by a 17 cm thick silty packstone layer consisting mainly of peloids and quartz grains. The silty peloidal packstone and shale alternation is observed in the interval from sample TD-52 to sample TD-59. In levels corresponding to samples TD-58 and TD-59, the peloidal limestones are dolomitized. Above these dolomitized limestone beds, a 4 cm thick mudstone layer is recognized which is overlain by a bioclastic wackestone-packstone bed including peloids (TD-61; Figure 2.2). The

bioclasts often include crinoids, fragments of brachiopod, bivalve and foraminifers. The bioclastic limestone bed continues upward with peloidal limestone beds (from sample TD-62 to TD-65, Figure 2.2). Above the level corresponding to sample TD-65, a 37 cm thick bioclastic limestone bed is recognized and it is capped by 2 cm thick shale layer. This thin shale layer is overlain by a 48 cm thick dolomitized peloidal mudstone bed (TD-67, Figure 2.2). The section follows upward with a 10 cm thick shale bed corresponding to sample TD-68 and then it overlain by a 27 cm thick silty peloidal limestone bed. A bioclastic limestone bed is recognized in the level corresponding to sample TD-69 and capped by a 15 cm thick shale bed (TD-70, Figure 2.2). Above this shale bed, a packstone-grainstone bed is observed (TD-71, Figure 2.2). This bed is rich in foraminiferal fauna and includes fragments of crinoids, brachiopods and bivalves. Above this foraminiferal limestone bed, two individual wackestone-packstone beds consisting mainly of fragments of bioclasts are recognized (TD-72 and TD-73, Figure 2.2). Above the level corresponding to sample TD-73, the succession continues with beds, measuring 12 cm and 9 cm in thickness and then by bioclastic packstone beds (TD-74 and TD-75, Figure 2.2). The level corresponding to sample TD-74 is characterized by the first appearance of *Siphonophyllia* within the measured section (Figure 2.3). This coral zone was first defined in the type section of Mantar Tepe Member by Özgül (1997). Above the level corresponding to sample TD-75, an unsampled 20 cm thick bioclastic limestone bed is capped by an unsampled 3 cm thick shale layer. This layer is the last level where the shale is recognized and followed upward with a 35 cm thick bioclastic limestone bed (TD-76, Figure 2.2). Above this bioclastic limestone bed, a 34 cm thick limestone consisting mainly of foraminifers and bioclasts is recognized (TD-77, Figure 2.2). The layers from sample TD-77 to sample TD-100 are characterized by foraminiferal limestone beds and the thickness of these limestone beds varies from 15 cm to 45 cm. Above the level corresponding to sample TD-100, a 38 cm thick silty peloidal packstone bed representing a significant change in sedimentation is recognized (TD-101, Figure 2.2). This level is overlain by a 38 cm thick bioclastic and foraminiferal packstone-grainstone bed (TD-102, Figure 2.2). Layers from sample TD-102 to sample TD-110, the

foraminiferal and bioclastic packstone and grainstone alternation is observed and the thickness of these beds varies from 12 cm to 70 cm. The level corresponding to the sample TD-107 is the last level where *Siphonophylla* is recognized. Above the level corresponding to sample TD-110, a silty limestone bed is observed and measures 16 cm in thickness. The measured section continues upwards with limestone beds including fragments of bioclasts and foraminifers (from sample TD-111 to sample TD-129). The thickness of beds corresponding to this interval varies from 30 cm to 110 cm and increases upwards within the measured section. Moreover, the layer corresponding to TD-117 is the thickest limestone bed along the measured section (Figure 2.2 and Figure 2.4).



Figure 2.3: Photograph of the level consisting of coral corresponding to the sample TD-74. (C: Coral).



Figure 2.4: The beds corresponding to the samples TD-53 and TD- 117 measure 17 cm and 110 cm respectively in the measured section.

2.2. Biostratigraphy

Many researchers have been studying the Upper Tournaisian to define the T- V boundary in recent years (e.g. Conil et al., 1991, Hance and Muchez, 1995; Hance et al., 1997; Kalvoda and Ondrackova, 1999; Devuyst and Hance, 2003; Kulagina *et al.*, 2003; Kalvoda *et al.*, 2005; Devuyst and Hance in Poty and others, 2006, Devuyst and Kalvoda, 2007). Since a careful examination of the evolutionary stages of foraminifer *Eoparastaffella* provides more accurate criteria for the definition of the Upper Tournaisian and the T-V boundary, *Eoparastaffella* is accepted to be a key taxon. Moreover *Eoparastaffella* also helps to understand the underpinning of the evolutionary relationships among certain foraminiferal groups during a time of significant environmental changes. Despite this, *Eoparastaffella* is a poorly known genus and only recently has it again attached the attention of researchers (Devuyst and Kalvoda, 2007). *Eoparastaffella* was first originally described by Vdovenko (1954) from the Donets Basin in the Ukraine. It firstly appears in the latest Tournaisian in studied stratigraphic sections. Vdovenko (1971) described the first representatives of the genus of the *rotunda* group. They are rapidly followed upsection by primitive *E. ovalis* and then the first representatives of the *interiacta* group (Devuyst and Kalvoda, 2007). Since range of *interiacta* group straddles the T-V boundary interval starting shortly above the *Eoparastaffella* and ending or becoming very rare at the appearance of *Eoparastaffella simplex* or shortly above, the *interiacta* group is useful biostratigraphically (Devuyst and Kalvoda, 2007).

Thin sections prepared from the samples of the measured section were analyzed under the microscope in detail for its foraminiferal fauna. *Earlandia* sp, *Lugtonia monilis*, *Granuliferella* sp., *Endothyra* sp. were the Upper Tournaisian foraminifers observed in the lower parts of the measured section. A diversification occurs in the middle part of the measured section with the entry of the first primitive *Eoparastaffella* M1 (Morphotype 1 of Hance and Muchez, 1995 and Hance, 1997). These primitive *Eoparastaffella* M1 including *Eoparastaffella* ex. gr. *interiacta* group are observed in samples TD-126, TD-127, TD-128 and TD-

129. The *interiacta* group is included in *Eoparastaffella* Morphotype 1 in this study (Figure 2.5).

In addition to this index taxon, the Upper Tournaisian foraminifers including *Earlandia* sp., *Lugtonia monilis*, *Tournayella* sp., *Tournayellina* sp., *Eoforschia moelleri*, *Septabrunkiina* sp., *Eblanaia* sp., *Eotextularia diversa*, *Palaeospiroplectamina meillina*, *Dainella* sp., *Granuliferella* sp., *Planoendothyra* sp., *Endothyra* sp., *Globoendothyra* sp., *Inflatoendothyra* sp., *Laxoendothyra* ex. gr. *laxa*, *Omphalotis* sp., *Latiendothyranopsis* sp., *Mediocris* sp., *Eoparastaffella* M1 are recognized towards the upper parts of the measured section. According to this foraminiferal fauna, the measured section is divided into two biozones as the Ut1 Zone and the Ut2 Zone (Figure 2.5 and Figure 2.6).

Ut1 Zone

Ut1 zone covers the lower part of the measured section corresponding to the uppermost part of the Çityayla Member. This interval consists of limestones intercalated with shale layers from sample TD-51 to TD-70 (Fig 2.2). Ut1 Zone is composed of Upper Tournaisian foraminifers including *Earlandia* sp., *Lugtonia monilis*, *Granuliferella* sp. and *Endothyra* sp. The content of this zone is similar respectively to that of upper part of Cf2, Cf3 and lower part of Cf4α1 Zone of Conil et al. (1991), Association A of Hance et al. (1997) and upper parts of MFZ5, MFZ6, MFZ7 Zone of Devuyt ad Hance in Poty and others (2006) (Table 2.1). The upper boundary of this zone is characterized by the the entry of the first primitive *Eoparastaffella* M1 (Morphotype 1 of Hance & Muchez, 1995 and Hance, 1997). The Upper boundary of Association A of Hance et al. (1997) and the MFZ7 Zone of Devuyt and Hance in Poty and others (2006) are also defined by the entry of the first primitive *Eoparastaffella* M1 (Morphotype 1 of Hance and Muchez, 1995 and Hance, 1997). The upper boundary of the Association A of Hance et al. (1997) is also characterized by the first occurrence of *Laxoendothyra* ex. gr. *laxa*, *Loeblichia* (?) ex. gr. *fragilis* in addition to the first appearance of *Eoparastaffella* M1. However, the *Laxoendothyra* ex. gr. *laxa* is observed in the upper parts of the Ut2 zone in this study.

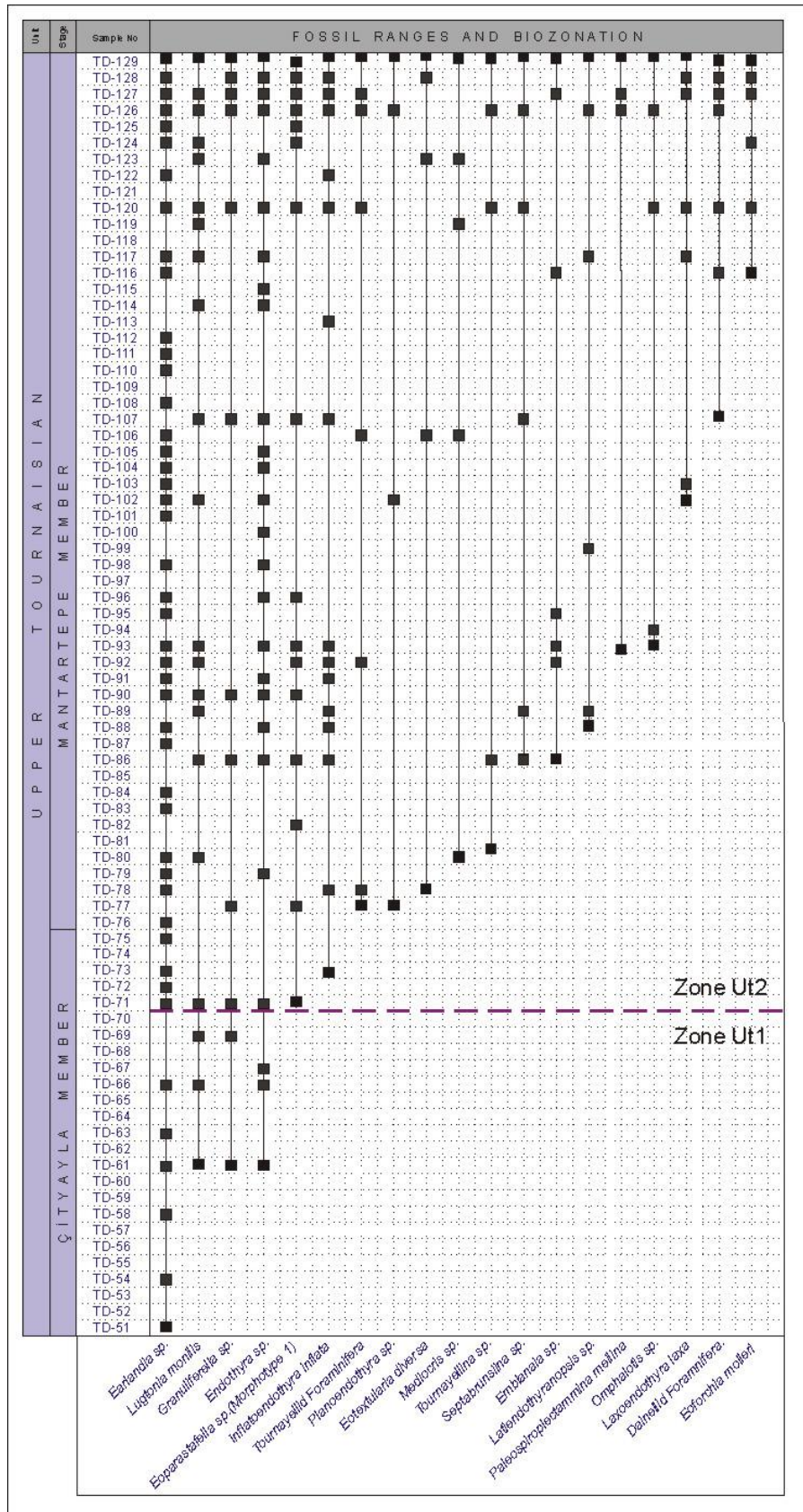


Figure 2.5: Fossil ranges and biozonation in the measured section.



Figure 2.6: The dashed line shows the boundary of the biozones Ut1 and Ut2 within the Upper Tournaisian.

Ut2 Zone

Ut2 Zone overlies the Ut1 Zone and comprises the interval from sample TD- 71 to TD-129 (Figure 2.2). Ut2 Zone is equivalent to Cf4α1 Zone of Conil et al. (1991), Association B of Hance et al. (1997), MFZ8 Zone of Devuyst and Hance in Poty and others (2006) (Table 2.1). Ut2 Zone is characterized by its diversity of Upper Tournaisian foraminifers. The base of the Ut2 Zone is defined by the entry of the first primitive *Eoparastaffella* M1 (Morphotype 1 of Hance and Muchez, 1995 and Hance, 1997). The taxa characterizing Ut1 Zone are still present in the Ut2 Zone characterized by the first appearances of *Eoparastaffella* M1 (Morphotype 1 of Hance and Muchez, 1995 and Hance, 1997). The zone consists of several taxa including *Earlandia* sp., *Lugtonia monilis*, *Tournayella* sp., *Tournayellina* sp., *Eoforschia moelleri*, *Septabrunkiina* sp., *Eblanaia* sp., *Eotextularia diversa*, *Palaeospiroplectamina meillina*, *Dainella* sp., *Granuliferella* sp., *Planoendothyra* sp., *Endothyra* sp., *Globoendothyra* sp., *Inflatoendothyra* sp., *Laxoendothyra* ex. gr. *laxa*, *Omphalotis* sp., *Latiendothyranopsis* sp., *Mediocris* sp.

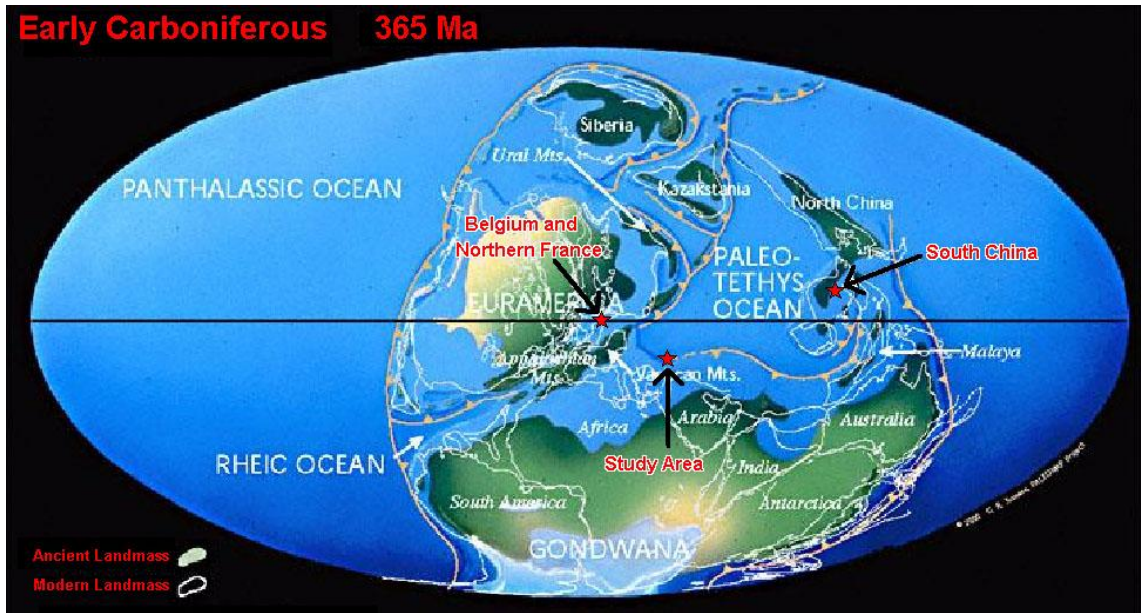


Figure 2.7: The study areas of Upper Tournaisian foraminiferal zones are shown on the Early Carboniferous World map (taken from www.scotese.com).

Table 2.1: Foraminiferal zones in different studies.

STAGE	UPPER TOURNAISIAN			
STUDY AREA	Hadim, Konya (SE Turkey)	Southern Belgium	South China (Guangxi)	Belgium and Northern France
REFERENCES	This Study	Conil, Groessens and Pirlet Conil et al. (1991)	Hance et al. (1997)	Devuyst and Hance in Poty and others (2006)
Foraminiferal Zones	Ut2		Association B	MFZ 8
	Ut1	Cf4 α 1	Association A	MFZ 7
		Cf3		MFZ 6
		Cf2		MFZ 5

Association B of Hance et al. (1997) differs from the Association A by the contemporaneous first occurrence of *Laxoendothyra* ex gr. *laxa*, *Loeblichia* (?) ex gr. *fragilis* and *Eoparastaffella* Morphotype 1, followed by the appearance of *Mediocris*. MFZ8 Zone of Devuyst and Hance in Poty and others (2006) is also characterized by the entry of the first primitive *Eoparastaffella* M1 (Morphotype 1 of Hance & Muechez, 1995 and Hance, 1997) including *E. ovalis* type1 (*E. ovalis sensu* Vdovenko, 1964), *E. rotunda* Vdoveko and *E. ex gr. interiacta* Vdovenko (Devuyst & Kalvoda). MFZ8 comprises also *Biseriella bristolensis* (Reichel), *Loeblichia fragilis* (Lipina), *Mediocris* sp. and *Lysella gadukensis* Bozorgnia with most of the taxa present in MFZ7. Therefore Ut2 Zone of Upper Tornaisian age can be considered a globally recognized biostratigraphic unit comprising the first occurrence of *Eoparastafella* M1 (Morphotype 1 of Hance and Muechez, 1995 and Hance, 1997).

CHAPTER 3

SEQUENCE STRATIGRAPHY

3.1. Microfacies Types

Microfacies studies aim for recognition of overall patterns that reflect the history of carbonate rocks, by means of a thorough examination of their sedimentological and paleontological characteristics. Microfacies characteristics may vary considerably within a limestone bed, both laterally and vertically. Vertical changes may indicate shallowing-up or deepening-up trends and reveal facies dynamics (e.g. regressive/ transgressive events). Lateral changes may indicate differences in water depths and hydrodynamics. Limestones are predominantly biogenetic sediments formed by biologically controlled processes. Especially, fossils are significant proxies for paleoenvironmental conditions. Since skeletal grains are highly sensitive to processes characterizing specific depositional environments, skeletal grains are of prime importance in defining microfacies types (Flügel, 2004).

To appreciate depositional environmental changes and ensure the facies control on biostratigraphy, microfacies studies are carried out. Study area mainly contains subtidal carbonates interclated with shales. Through the measured section, 7 microfacies types were identified according to Dunham (1962) classification. These are mudstone to siltstone microfacies (MS), silty peloidal mudstone microfacies (MS-P1), silty peloidal packstone microfacies (P1), peloidal and crinoidal wackestone-packstone microfacies (P1-P2), crinoidal wackestone-packstone microfacies (P2), crinoidal and foraminiferal packstone-grainstone microfacies (P2-P3) and foraminiferal grainstone-packstone microfacies (P3) (Table 3.1).

Table 3.1: Carbonate and siliciclastic facies and their depositional environments in the studied section.

Facies Type	Description	Grain types/fossils	Depositional Environment	SAMPLE NO
Mudstone to sandstone (MS)	It consists of fine sand to silt sized quartz grains embedded in an extremely fine-grained matrix partially calcium carbonate in composition.	Bioclasts are nearly absent.	Deepest deposits within the facies belt.	TD-52, TD-56, TD-58, TD-67, TD-68, TD-70
Silty peloidal mudstone (MS-P1)	It consists of fine grained, subangular silt-sized quartz grains and peloids.	It is unfossiliferous	Open Marine	TD-60, TD-64, TD-67
Silty peloidal packstone (P1)	It consists of subrounded to rounded quartz grains, peloids and dark clasts .	It is characterized by the presence of foraminifer, <i>Earlandia</i> and some minor amounts of macrofossil fragments such as bivalves and crinoids,	Open Marine to Shoal	TD-53, TD-54, TD-55, TD-56, TD-57, TD-58, TD-59, TD-62, TD-63, TD-65, TD-74, TD-101, TD-111
Peloidal and crinoidal wackestone-packstone (P1-P2)	It is transitional between the silty peloidal packstone microfacies and the crinoidal wackestone to packstone microfacies and it is poorly sorted.	It is characterized by skeloton grains such as foraminifers, fragments of crinoids, bivalves, brachiopods and abundant peloids.	Open Marine to Shoal	TD-61, TD-66, TD-69
Crinoidal wackestone-packstone (P2)	Micrite is observed between grains and matrix is usually dolomitized. This facies has very poorly sorted constituents.	It is composed of fragments of crinoids, echinoids, bryzoans, brachiopods, bivalves and foraminifers.	Shoal	TD-72, TD-73, TD-74, TD-75, TD-76, TD-81, TD-85, TD-94, TD-95, TD-102, TD-104, TD-105, TD-106, TD-108, TD-109, TD-110, TD-112, TD-115, TD-116, TD-118, TD-121, TD-122, TD-124
Crinoidal and foraminiferal packstone-grainstone (P2-P3)	It is transitional between the crinoidal wackestone-packstone microfacies and the foraminiferal grainstone-packstone microfacies.	It is composed of foraminifers and diverse assemblage of macrofossil fragments including crinoids, corals, brachiopods and bivalves.	Shoal	TD-71, TD-77, TD-78, TD-79, TD-80, TD-82, TD-83, TD-84, TD-91, TD-96, TD-97, TD-98, TD-99, TD-100, TD-103, TD-113, TD-117, TD-123, TD-125, TD-129
Foraminiferal grainstone-packstone (P3)	Sorting is relatively good and foraminifers are relatively more abundant than those in the other microfacies types.	The main components of this microfacies type are foraminifers. Bioclasts are also abundant.	Shoal to Restricted Platform	TD-51, TD-86, TD-87, TD-88, TD-89, TD-90, TD-92, TD-93, TD-107, TD-114, TD-119, TD-120, TD-126, TD-127, TD-128

3.1.1. Mudstone to Sandstone Microfacies (MS)

Mudstone to sandstone microfacies consists of fine sand to silt sized quartz grains embedded in an extremely fine-grained matrix partially calcium carbonate in composition. Bioclasts are nearly absent in this type of microfacies. This facies type is present at the base of the measured section, in samples TD-52, TD-56, TD-58, TD-67, TD-68, TD-70 (Table 3.1, Figure 3.1)

This type of microfacies corresponds approximately to the shale layers observed in the investigated part of the Huangjing Formation (lower 47 m) of Hance et al. (1997). The shale layers were recognized as the limestone-shale alternation by Hance et al. (1997). Hance et al. (1997) defined that the deepest water deposits were likely to be represented by the shale layers. The shale beds were deposited below wave base suggesting a quieter and deeper setting (Hance et al. 1997). We consider that the shale layers of this study were also deposited in low energy conditions below wave base indicating the deepest deposits within the facies belt. This type of microfacies, indicating the deposition in low energy shelf conditions below the wave base level, was also recognized in the type section of Özgül (1997) within the Çityayla Member.

3.1.2. Silty Peloidal Mudstone Microfacies (MS- P1)

Silty peloidal mudstone microfacies consists of fine grained, subangular silt-sized quartz grains and peloids. This microfacies is transitional between the mudstone to sandstone microfacies (MS) and silty peloidal packstone microfacies (P1). This type of microfacies is unfossiliferous and observed in the lower parts of the measured section, in samples TD-60, TD-64, TD-67 (Table 3.1, Figure 3.2). Silty peloidal mudstone microfacies differs from mudstone to siltstone microfacies by the presence of peloids.

This type of facies mainly occurs at the base of the measured section. It is equivalent of FZ7 of Wilson (1975) and Flugel (2004) defined for open-marine platform. It is deposited in moderate energy conditions close to or below wave base.

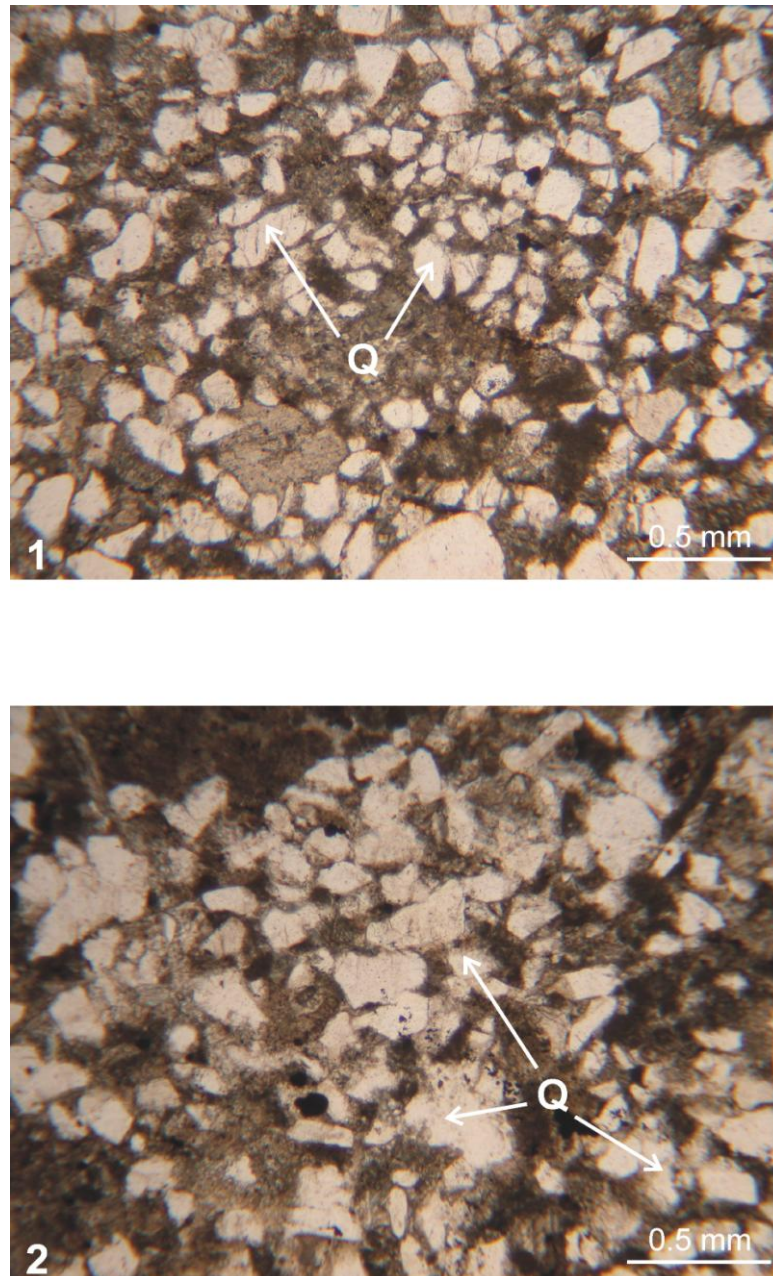


Figure 3.1: Photomicrographs of mudstone to sandstone lithofacies (MS). (Q: Quartz grain), (1: TD-68; 2: TD-70).

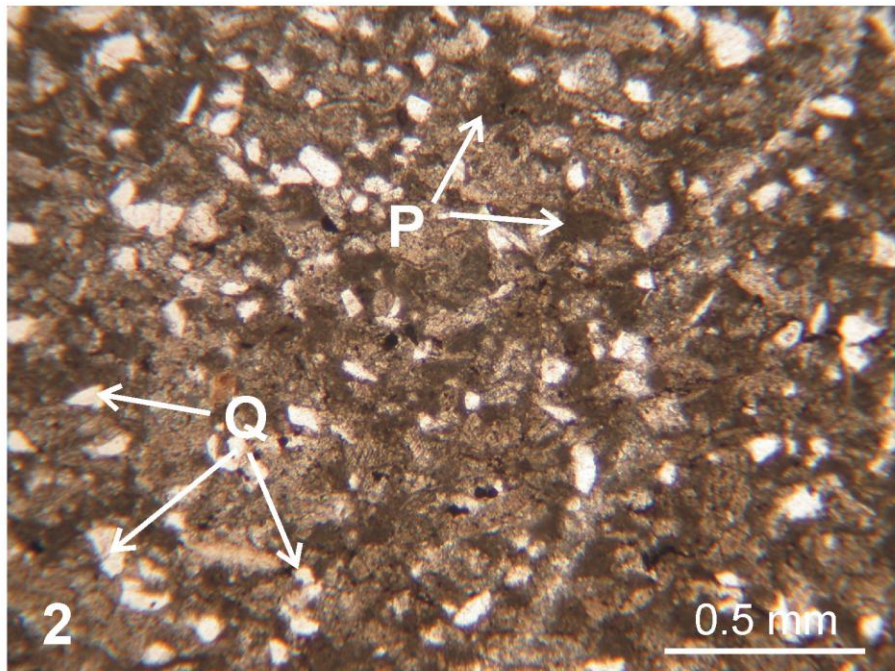
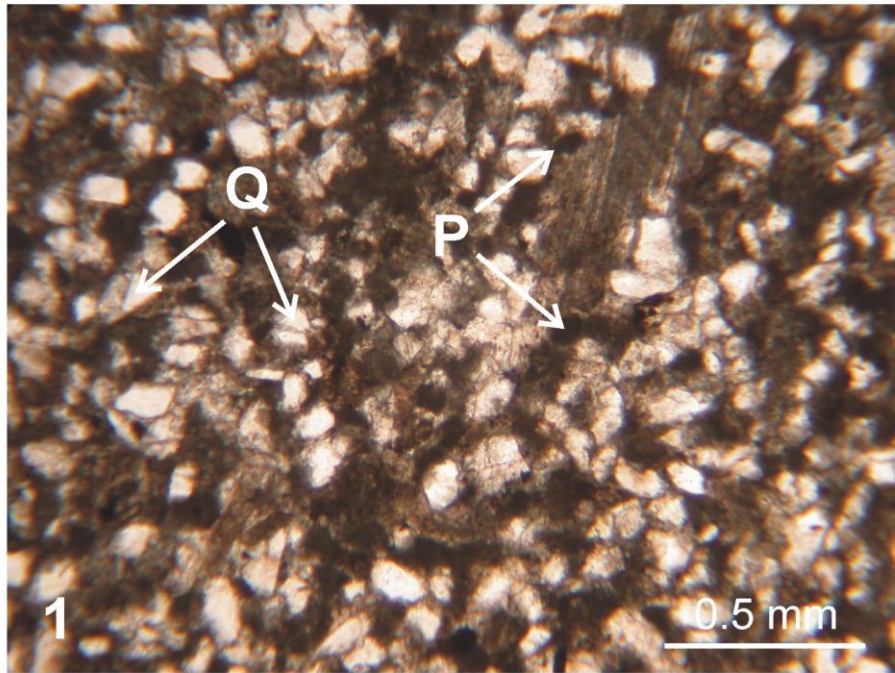


Figure 3.2: Photomicrographs of silty peloidal mudstone lithofacies (MS-P1). (Q: Quartz grain, P: Peloid), (1: TD-60; 2: TD-64).

3.1.3. Silty Peloidal Packstone Microfacies (P1)

Silty peloidal packstone microfacies mainly consists of subrounded to rounded quartz grains, peloids and dark clasts. This type of facies is also characterized by the presence of a foraminifer, *Earlandia* and some minor amounts of macrofossil fragment such as bivalves and crinoids. This facies type is present in the lower and middle parts of the measured section, in samples TD-53, TD-54, TD55, TD-56, TD-57, TD-58, TD-59, TD-62, TD-63, TD-65, TD-74, TD-101, TD-111 (Table 3.1, Figure 3.3). Peloids are the major constituents of this type of microfacies. Peloid is defined as a comprehensive term for polygenetic grains composed of micro and cryptocrystalline carbonate particles (McKee and Gutschick, 1969). Peloids are generally subrounded or rounded, but ovoid and rodlike shapes may also occur. In this type of facies, the peloids are observed as subrounded to rounded particles. Many peloidal limestones appear to have formed in shallow-warm-water environments (banks, shelf, and reef lagoons) and fine grained peloidal limestones are generally regarded as typical shallow, low energy environments (Flügel, 2004) which is the case in this facies.

This type of microfacies corresponds approximately to SMF16 of Flügel (2004). SMF 16 is defined by accumulations of peloids and is a constituent of shallow platform carbonates (Flügel, 2004). This packstone microfacies is also equivalent of FZ6 and FZ7 of Wilson (1975) and Flügel (2004) defined for shoals and open-marine platforms. This type of microfacies is deposited below or near wave base and landward direction of silty peloidal mudstone microfacies (MS-P1).

3.1.4. Peloidal and Crinoidal Wackestone-Packstone Microfacies (P1- P2)

Peloidal and crinoidal wackestone-packstone microfacies includes skeleton grains such as foraminifers, fragments of crinoids, bivalves, brachiopods and abundant peloids. This facies is poorly sorted and usually present in the lower parts of the

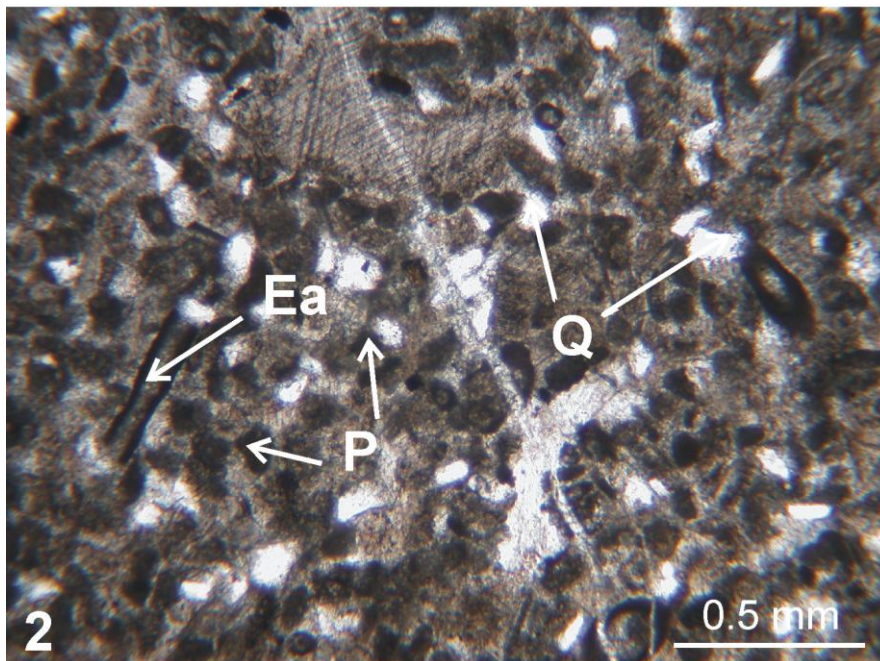
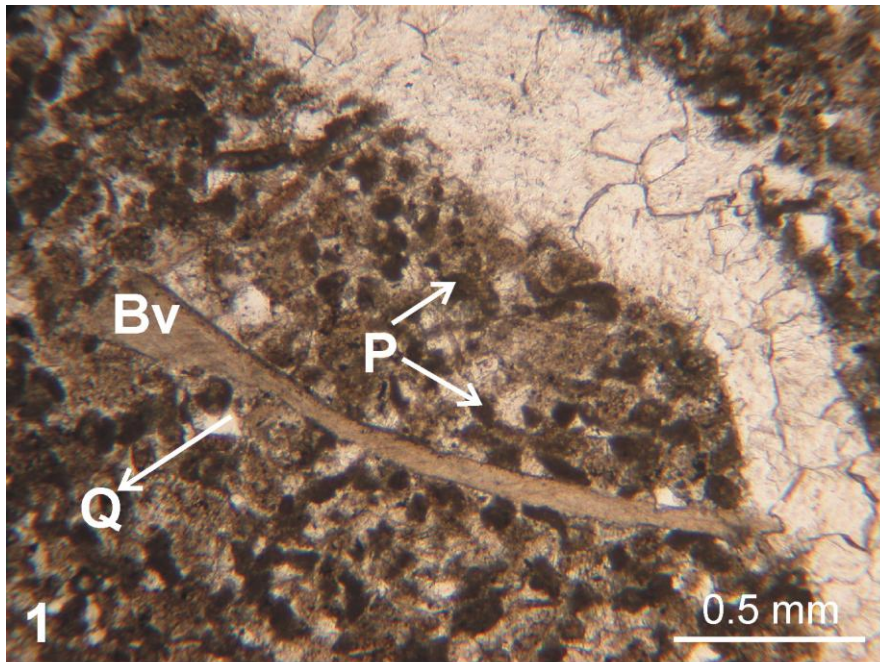


Figure 3.3: Photomicrographs of silty peloidal packstone lithofacies (P1). (Bv: Bivalve fragment, Ea: *Earlandia* sp., Q: Quartz grain, P: Peloid), (1: TD-59; 2: TD-62).

measured section, in samples TD-61, TD-66, TD-69 (Table 3.1, Figure 3.4). It differs from the silty peloidal packstone (P1) microfacies mainly by the presence of foraminifers and skeleton grains. However, foraminifers are never abundant whereas skeleton grains are abundant. The type and composition of skeleton grains are highly sensitive to the depositional environment and offer significant proxies for paleoenvironmental controls on carbonate deposition and paleoclimatic conditions. This type of facies indicates an open marine environment with moderate energy (Flügel, 2004). It is deposited below or near wave base and seaward direction of the crinoidal wackestone-packstone microfacies (P2).

This type of microfacies is equivalent of FZ6 and FZ7 of Wilson (1975) and Flügel (2004). It also corresponds to the peloidal and bioclastic packstone microfacies in the lower part of the Huaqiao Farm section and the peloidal and bioclastic wackestones in the upper part of the Yintang Formation of Hance et al. (1997).

3.1.5. Crinoidal Wackestone- Packstone Microfacies (P2)

Crinoidal wackestone-packstone microfacies mainly consists of fragments of crinoids, echinoids, bryozoans, brachiopods and bivalves. Micrite is observed between grains and matrix is usually dolomitized in this microfacies type. Foraminifers are present but never abundant. This microfacies differs from the other microfacies types in having very poorly sorted constituents. This facies type is present in the lower and middle parts of the measured section in samples TD-72, TD-73, TD-74, TD-75, TD-76, TD-81, TD-85, TD-94, TD-95, TD-102, TD-104, TD-105, TD-106, TD-108, TD-109, TD-110, TD-112, TD-115, TD-116, TD-118, TD-121, TD-122, TD-124 (Table 3.1, Figure 3.5).

Typical coral bearing levels corresponding to samples TD-74, TD-75 and TD-76 are characterized by the presence of the genera *Siphonopyllia*. This coral zone is

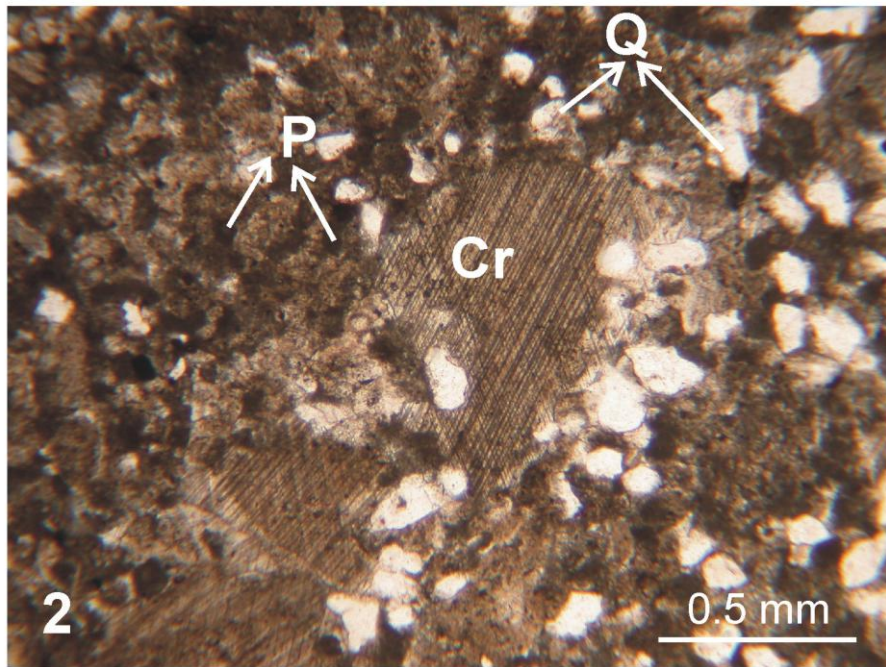
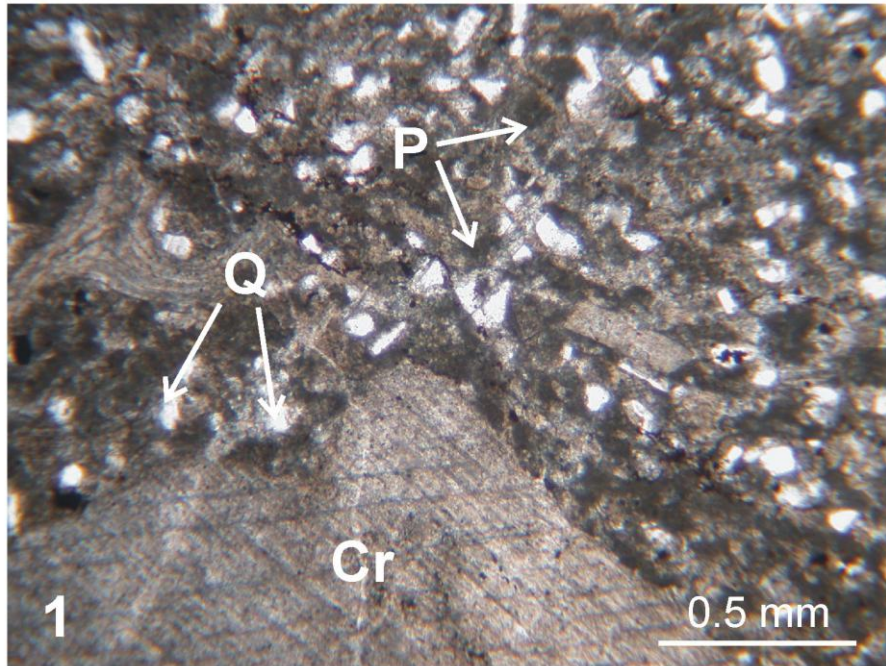


Figure 3.4: Photomicrographs of peloidal and crinoidal wackestone-packstone lithofacies (P1-P2). Note that fossil fragments are poorly sorted in this type of microfacies. (Cr: Crinoid fragment, Q: Quartz grain, P: Peloid), (1: TD-66; 2: TD-69).

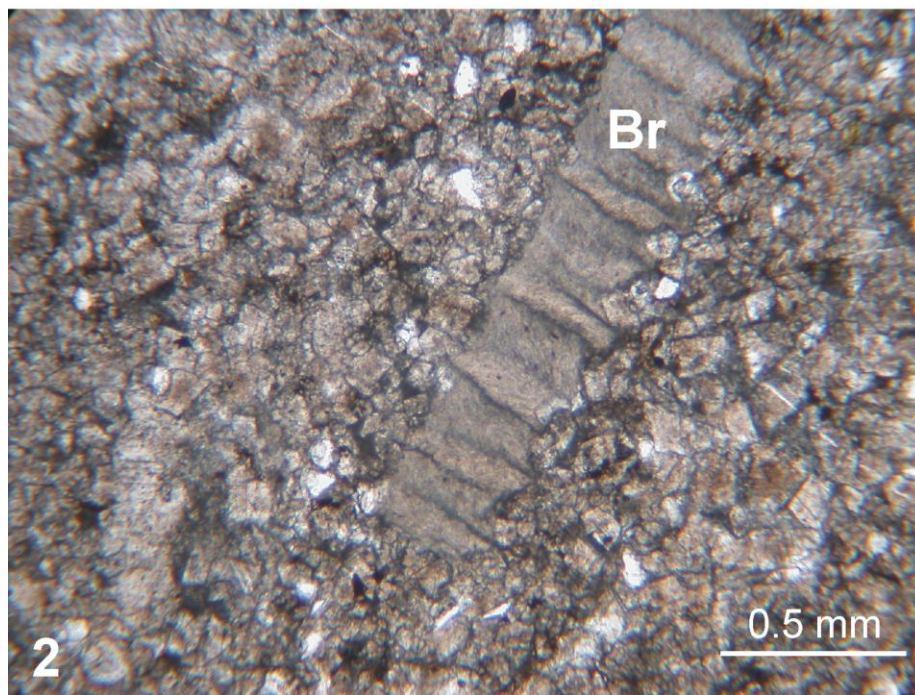
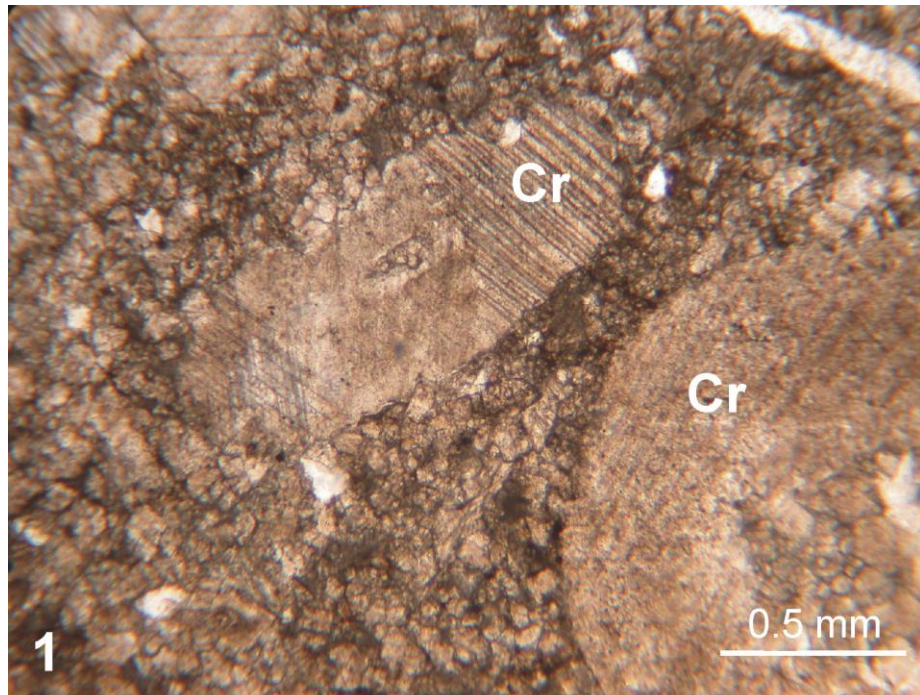


Figure 3.5: Photomicrographs of crinoidal wackestone-packstone lithofacies (P2). (Br: Bryzoa fragment; Cr: Crinoid fragment), (1: TD-74; 2: TD-75).

also defined in the type section of Mantar Tepe Member corresponding to the interval separating the Upper Tournaisian from the Lower Visean (Özgül, 1997).

Crinoidal wackestone-packstone microfacies correspond to bryzoan-echinoderm-wackestone/ packstone/ grainstone lithofacies of Algeo and Rich (1992). This type of lithofacies consists of bryzoan, echinoderms, brachiopods, corals and lesser amounts of microfossils. Like crinoidal wackestone-packstone microfacies (P2) of this study, sorting is poor in the bryzoan-echinoderm-wackestone/ packstone/ grainstone lithofacies of Rich et al. (1992). This microfacies also corresponds to the bioclastic wackestone-packstone microfacies in the Yajio River within the South China of Hance et al. (1997). It includes fragmented shells, foraminifers, crinoids, calcispheres, rare algae, echinoid spines, ostracods and bryzoa which are the similar constituents of the P2 in this study.

Crinoidal wackestone-packstone microfacies corresponds to FZ6 of Wilson (1975) and Flugel (2004) depositional environment model. This type of facies is deposited under high energy environments in shoals above wave base and influenced by tidal currents. This type of microfacies is also equivalent of SMF10 and SMF11 of Flugel (2004). The main constituents of both SMF10 and SMF11 are skeletal grains like the crinoidal wackestone-packstone microfacies of this study.

3.1.6. Crinoidal and Foraminiferal Packstone-Grainstone (P2-P3)

Crinoidal grainstone-packstone microfacies mainly consists of foraminifers and diverse assemblage of microfossil fragments including crinoids, corals, brachiopods and bivalves. This microfacies is transitional between the crinoidal wackestone-packstone microfacies and the foraminiferal grainstone-packstone microfacies. This facies type is present in samples TD-71, TD-77, TD-78, TD-79, TD-80, TD-82, TD-83, TD-84, TD-91, TD-96, TD-97, TD-98, TD-99, TD-100, TD-103, TD-113, TD-117, TD-123, TD-125, TD-129 (Table 3.1, Figure 3.6,

Figure 3.7). It differs from other types of facies basically by the richness in foraminiferal fauna.

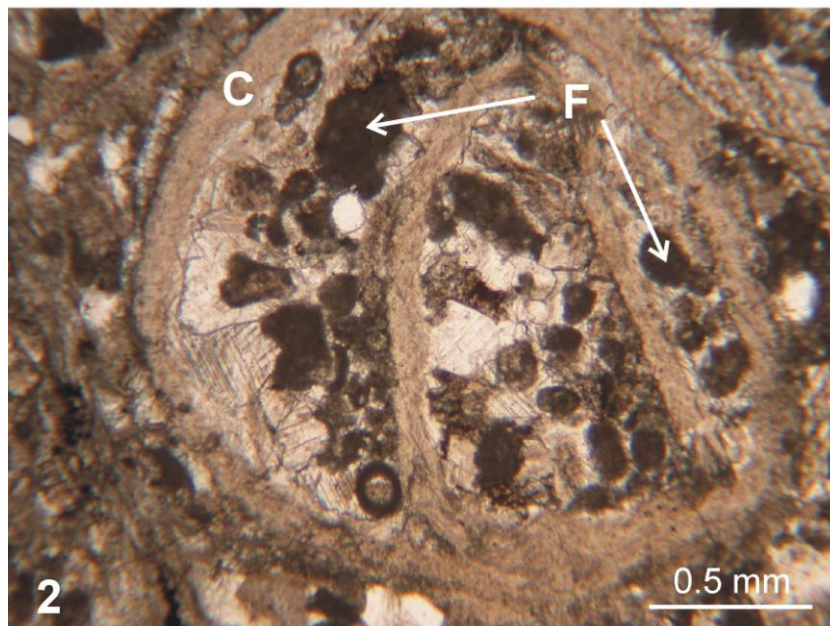
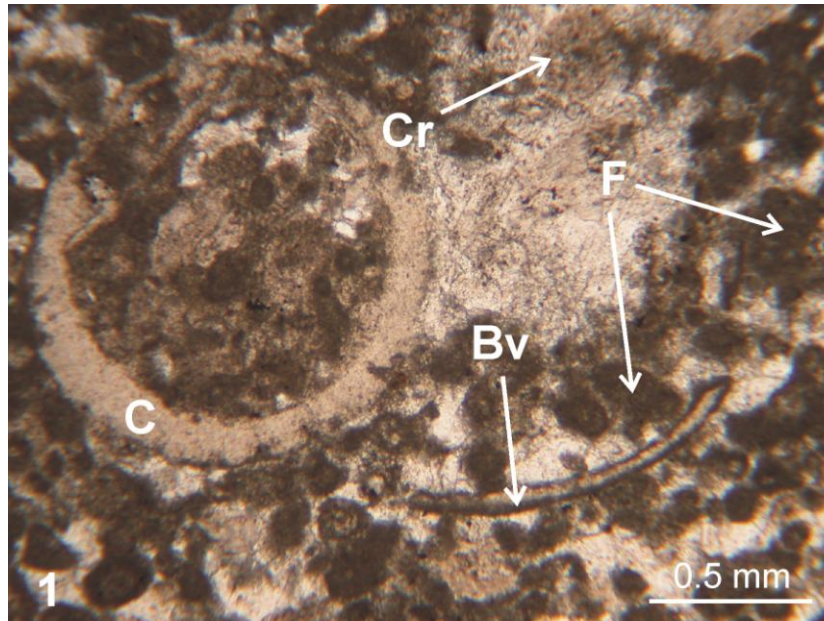


Figure 3.6: Photomicrographs of foraminiferal and crinoidal packstone-grainstone lithofacies (P2-P3). (Bv: Bivalve fragment, C: Coral, Cr: Crinoid fragment, F: Foraminifer), (1: TD-77; 2: TD-103).



Figure 3.7: The coral level (sample TD-77) in crinoidal and foraminiferal packstone-grainstone microfacies. The photomicrograph of the sample TD-77 is viewed in figure 3.6.

The coral level corresponding to samples TD-79, TD-80, TD-84, TD-91, TD-96, TD-98, TD-99, TD-102, TD-103 is also recognized within this microfacies.

Crinoidal and foraminiferal packstone-grainstone microfacies corresponds to FZ7 and FZ8 of Wilson (1975) and Flugel (2004) defined for open marine platforms and restricted shallow platforms. This type of microfacies is also equivalent of SMF10 and SMF11 of Flugel (2004). This packstone-grainstone facies predominantly consisting of bioclasts are characteristic parts of platforms formed during sea level highstands (Flugel, 2004). This type of facies is deposited in high energy environments above wave base.

3.1.7. Foraminiferal Grainstone-Packstone Microfacies (P3)

The main components of the foraminiferal grainstone-packstone microfacies are foraminifers. In this kind of microfacies, sorting is relatively good and foraminifers are relatively more abundant than in the other microfacies types. This microfacies is present in samples TD-51, TD-86, TD-87, TD-88, TD-89, TD-90, TD-92, TD-93, TD-107, TD-114, TD-119, TD-120, TD-126, TD-127, TD-128 (Table 3.1, Figure 3.8). It is observed towards the upper part of the section. The coral level corresponding to samples TD-89, TD-90 and TD-93 is also recognized within this microfacies.

This type of microfacies is equivalent to FZ7 and FZ8 of Wilson (1975) and Flugel (2004). This facies also corresponds to SMF18 of Flugel (2004) characterized by the high abundance of benthic foraminifera. Common textures of this standard microfacies are grainstones and packstones. The P3 of this study is most probably deposited in shelf lagoons with open circulation during sea level highstand phases (FZ7 of Flugel, 2004).

3.2. Meter Scale Cycles through the Upper Tournaisian

This study documents a detailed study of cyclic sedimentation in the subtidal carbonate deposits of Upper-Tournaisian deposits within the Yarıcağ Formation. Cyclicality is defined as stratal repetition of physical and chemical characters of sedimentary rocks, such as, lithofacies and biofacies (Flügel, 2004). Thus both biostratigraphy and sedimentological evolution through the measured section have been investigated to define the shallowing-upward cycles. Shallowing-upward cycles were also named as parasequences. Van Wagoner et al. (1988) defined the parasequence as a relatively conformable succession of beds or bedsets bounded by marine flooding surfaces and their correlative surfaces.

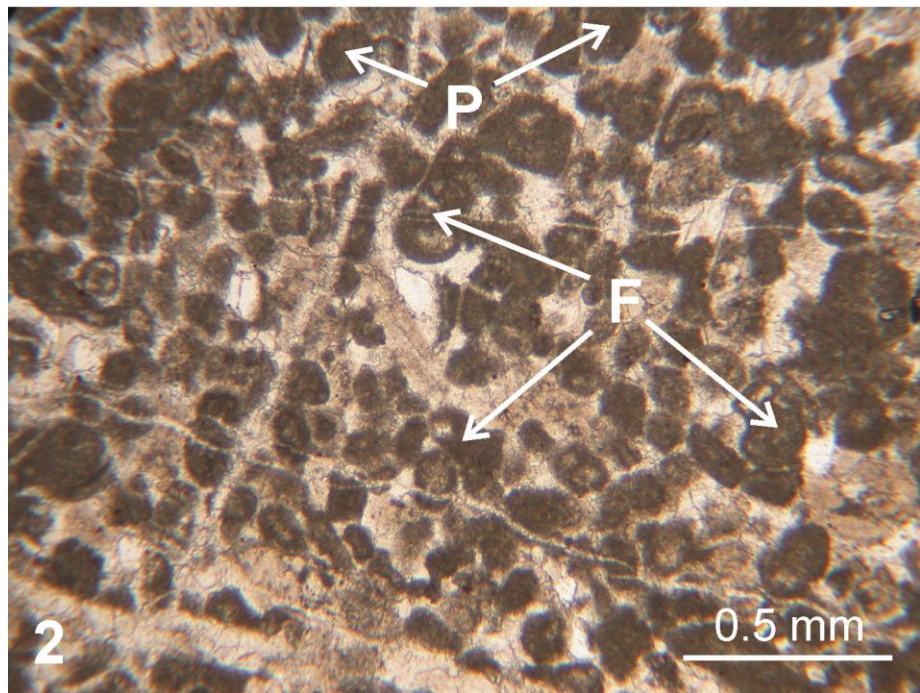
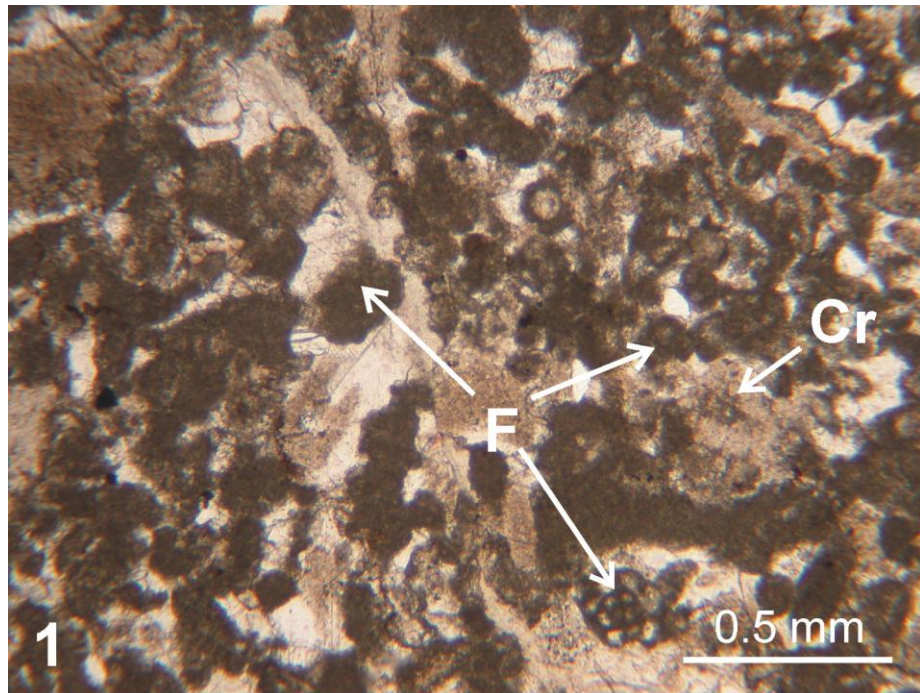


Figure 3.8: Photomicrographs of foraminiferal grainstone-packstone lithofacies (P3). (Cr: Crinoid fragment; F: Foraminifer; P: Peloid), (1-2: TD-107).

The measured section contains 25 shallowing-upward meter-scale cycles through the Upper Tournaisian in the Hadim Region (Figure 3.9). Individual cycles show a range of thickness from 18 to 261 cm. Shallowing upward meter scale cycles (paracycles) tend to be systematically arranged within larger scale successions that is parasequence sets. Osleger and Read (1991) and Goldhammer et. al. (1990) defined that stacking patterns of the meter-scale cycles can be used to define large scale sequences, system tracts and long term relative sea-level fluctuations. System tracts are defined by stacking patterns of parasequence sets or cycles (Van Wagoner et. al., (1988). The 25 shallowing upward-meter scale cycles show low and high energy facies according to their microfacies texture. Variations in microfacies criteria within a sedimentary succession (e.g. a cycle or a parasequence) indicate changes in environmental controls and depositional rates. Changes in depositional rates influenced by sea-level fluctuations may led to the formation of boundries between depositional units (sequences). Sea level fluctuations can be identified very well by the help of shallow marine carbonates (Goldhammer et al., 1990). Thus, changes in sea level fluctuations within the study area can be identified. Depending on the stacking patterns of microfacies, two fundamental types, A and B, were recognized in this study (Figure 3.9 and Figure 3.10).

A type Cycles

A-type cycles are characterized by different stacking patterns of mudstone to sandstone microfacies (MS), silty peloidal mudstone microfacies (MS-P1), silty peloidal packstone microfacies (P1), peloidal and crinoidal wackestone-packstone microfacies (P1-P2), crinoidal wackestone-packstone microfacies (P2), crinoidal and foraminiferal packstone-grainstone microfacies (P2-P3) (Figure 3.9 and Figure 3.10). Basically 4 subtypes, namely A1, A2, A3, A4 are recognized (Figure 3.10). These type of cycles are presented by low energy facies.

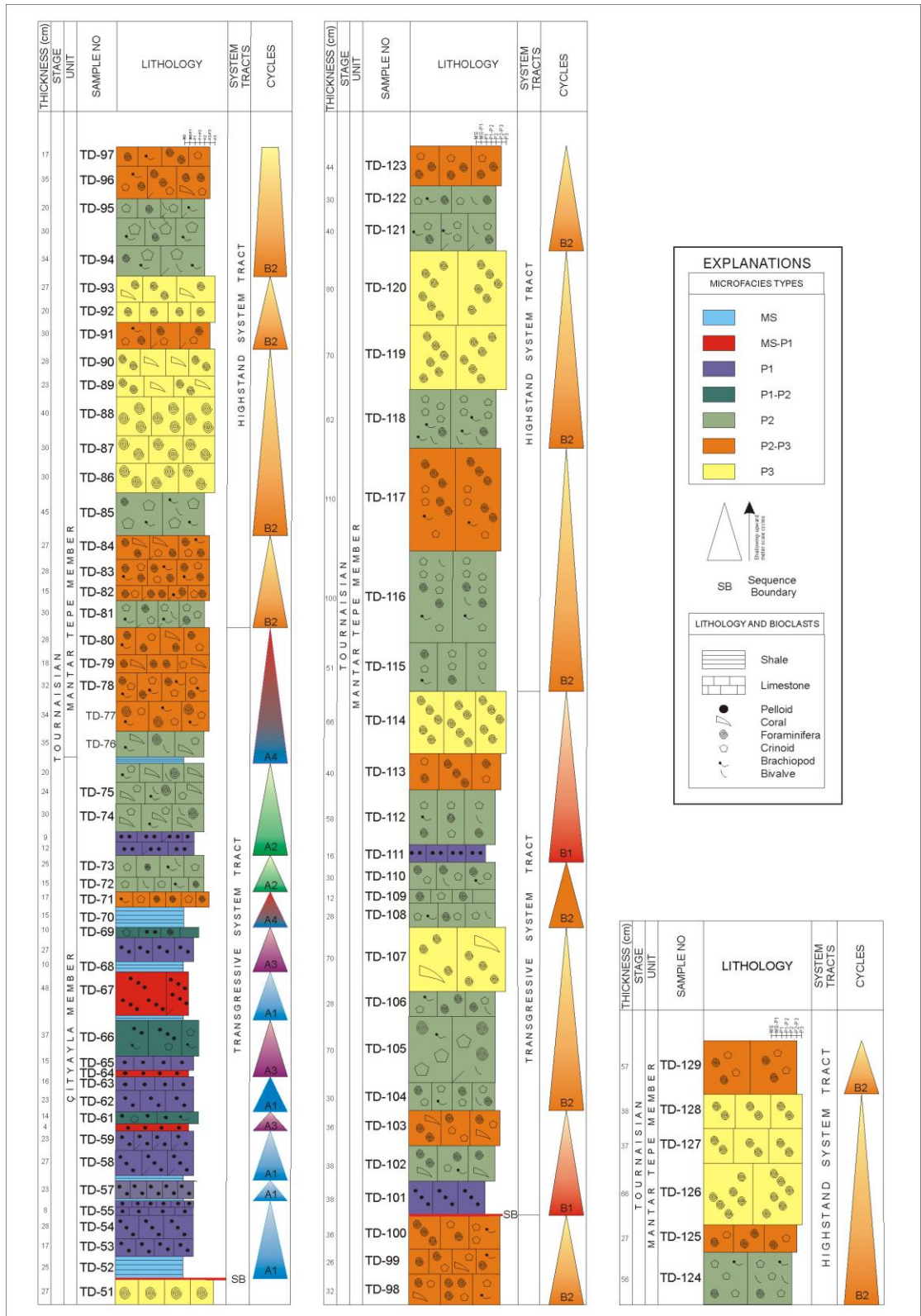


Figure 3.9: Meter-scale cycles derived from microfacies analysis in the measured section.

A1-type cycles generally start at the base with mudstone to sandstone microfacies (MS) and are capped by the silty peloidal packstone microfacies (P1) (Figure 3.10). In some levels the stacking pattern varies since the variations occur within the same cycle type due to higher order sea level oscillations. For instance, A1-type cycle recognized in level from TD-62 to TD-63 is only characterized by silty peloidal packstone microfacies and it is defined as A1-type cycle (Figure 3.9). Moreover, A1-type cycle recognized in the level corresponding to top of sample TD-66 to sample TD-67 is characterized by shale layer overlain by silty peloidal mudstone microfacies (Figure 3.9). This cycle is defined as A1-type cycle since the silty peloidal mudstone microfacies (MS-P1) is generally recognized between mudstone to sandstone microfacies (MS) and peloidal siltstone packstone microfacies (P1) like a transitional microfacies. A1-type cycles are observed in the lower part of the measured section. A1-type cycles are generally unfossiliferous and include sometimes some sections of foraminifera mostly belonging to the genus *Earlandia*. 5 individual cycles of A1-type are recognized in levels corresponding to the samples TD-52, TD-53, TD-54, TD-55, TD-56, TD-57, TD-58, TD-59, TD-62, TD-63, TD-67 (Figure 3.9). The thickness of A1-type cycles varies from 26 cm to 78 cm. A1-type cycles are the dominant cycle type in A-type cycles.

A2-type cycles are composed of silty peloidal packstone microfacies (P1) overlain by the crinoidal wackestone-packstone microfacies (P2) (Figure 3.10). A2-type cycle recognized in level from TD-72 to TD-73 is only characterized by crinoidal wackestone-packstone microfacies (P2) and it is defined as A2-type cycle since the variations occur within this cycle due to higher order sea level oscillations. A2 type cycles are usually observed in the middle part of the measured section. A2-type cycles are recognized in levels corresponding to the samples TD-72, TD-73, TD-74, TD-75 in the measured section. The thickness of A2-type cycles varies from 40 cm to 95 cm. (Figure 3.9).

A3 type cycles generally start with the mudstone to sandstone microfacies (MS) at the base. This facies is followed upwards by the silty peloidal packstone microfacies (P1). The cycle ends with the peloidal and crinoidal wackestone-packstone microfacies (P1-P2) (Figure 3.10). Because of sea level oscillations, in cycles corresponding to samples from TD-60 to TD-61 and from TD-64 to TD-66, mudstone to sandstone microfacies (MS) is not recognized (Figure 3.9). Moreover, silty peloidal mudstone facies (MS-P1), which is a transitional microfacies between mudstone to sandstone microfacies (MS) and silty peloidal packstone microfacies (P1), can be recognized within these A3-type cycles. The third A3-type cycle corresponds to samples from TD-68 to TD-69 (Figure 3.9). The thickness of A3-type cycles varies from 18 cm to 53 cm.

A4 type cycles generally start with mudstone to sandstone microfacies (MS) and ends with crinoidal and foraminiferal packstone-grainstone microfacies (P2-P3) (Figure 3.10). However, the other microfacies might be observed between these two microfacies (MS and P2-P3). For example, in A4 type cycles corresponding to samples from TD-76 to TD-80, mudstone to sandstone microfacies (MS) is followed by crinoidal wackestone-packstone microfacies (P2) and ended with crinoidal and foraminiferal packstone-grainstone microfacies (P2-P3) (Figure 3.9). A4 type cycles are observed in the middle of the section and the thickness of these cycles varies from 32 cm to 167 cm.

B Type Cycles

B type cycles are characterized by the stacking patterns of silty peloidal packstone microfacies (P1), crinoidal wackestone-packstone microfacies (P2), crinoidal and foraminiferal packstone- grainstone (P2-P3), foraminiferal grainstone- packstone microfacies (P3). B type cycles are subdivided into 2 subtypes, as B1 and B2. These types of cycles are generally characterized by relatively higher energy facies (Figure 3.9 and Figure 3.10).

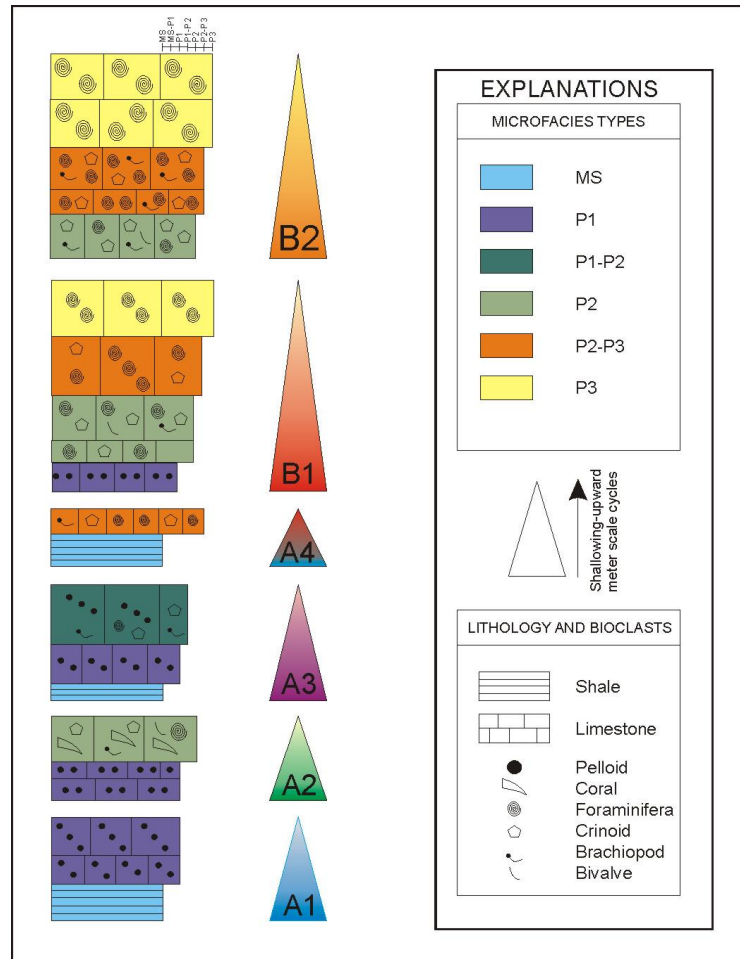


Figure 3.10: Types of cycles based on microfacies stacking patterns.

B1 type cycles are usually composed of silty peloidal packstone microfacies (P1) at the bottom. This microfacies is generally followed upwards by the crinoidal wackestone-packstone microfacies (P2). These two microfacies are capped by crinoidal and foraminiferal packstone-grainstone facies (P2-P3) and the cycle ends generally with the foraminiferal grainstone-packstone facies (P3) (Figure 3.9 and Figure 3.10). The B1-type was recognized in levels corresponding to the samples from TD-101 to TD-102 and from TD-111 to TD-115. The thickness of these cycles varies from 112 cm to 179 cm (Figure 3.9).

B2 type cycle generally starts with crinoidal wackestone-packstone microfacies (P2) at its base. This facies is followed upwards by the crinoidal and foraminiferal packstone-grainstone facies (P2-P3). The cycle generally ends with the foraminiferal grainstone-packstone facies (P3) (Figure 3.9 and Figure 3.10). B

type cycles are seen in the uppermost part of the measured section (Figure 3.9). B2-type cycles are the dominant cycle type in B-type cycles. 12 individual cycles of B2-type are recognized in levels corresponding to the samples TD-81, TD-82, TD-83, TD-84, TD-85, TD-86, TD-87, TD-88, TD-89, TD-90, TD-91, TD-92, TD-93, TD-94, TD-95, TD-96, TD-97, TD-98, TD-99, TD-100, TD-104, TD-105, TD-106, TD-107, TD-108, TD-109, TD-110, TD-116, TD-117, TD-118, TD-119, TD-120, TD-121, TD-122, TD-123, TD-124, TD-125, TD-126, TD-127, TD-128, TD-129 in the measured section (Figure 3.9). The thickness of B2-type cycles varies from 57 cm to 230 cm.

3.3. Lateral Relationship of Meter-Scale Cycles

In order to understand the lateral relationship of meter scale cycles, a composite model illustrating the microfacies distribution of Upper Tournaisian beds in the investigated section is constructed based on microfacies evolution through the carbonate platform. Microfacies characteristics may vary considerably within a limestone bed, both vertically and laterally. According to vertical evolution of microfacies, 25 shallowing-upward cycles have been identified as mentioned in section 3.2. The microfacies types defined within the measured section also have lateral relationships with each other. Since the types of cycles are defined based on the stacking patterns of microfacies, the cycle types are considered as major criteria while constructing the facies model. A1, A2, A3, B1, B2 types parasequences illustrated in Figure 3.10 fit well to the lateral facies change illustrated in the Figure 3.11. As can be seen in the figure, A-type cycles are located in a more basinward setting while on the other hand B type cycles take place in the landward direction of the carbonate platform. However, the A4-type parasequence which requires a rather abrupt facies change model can be viewed within the composite model.

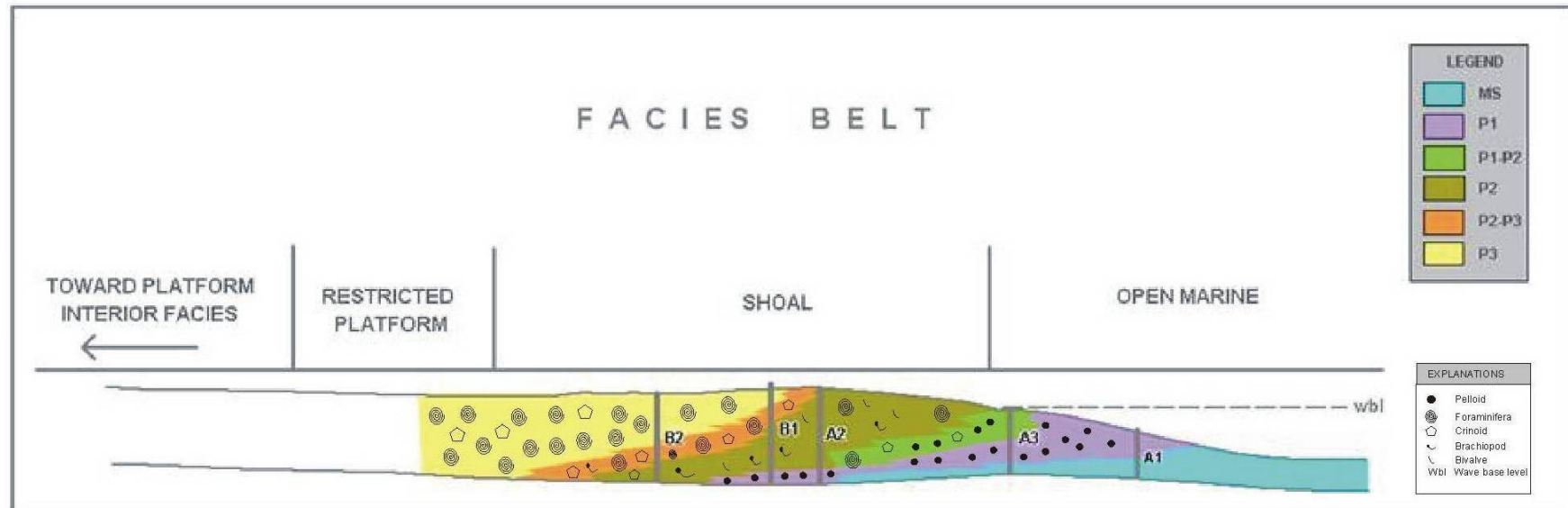


Figure 3.11: Composite model illustrating the microfacies distribution of Upper-Tournaisian beds in the investigated section (A1, A2, A3, B1, B2 are parasequence type illustrated in Figure 3.10). Note that parasequence organization illustrated in Figure 3.10 fit well to the lateral facies change illustrated in the figure with the exception of A4 type parasequence which requires a rather abrupt facies change model.

Consequently, all types of cycles can be recognized within the composite model illustrating the microfacies distribution of Tournaisian beds in the investigated section with the exception of A4-type cycle. This composited model is a summary of the depositional environment model in which our stratigraphic section formed. This facies belt model can act as norms for purposes of comparison, as a framework and guideline for future observations, as a predictor of new geological situations, and as an integrated basis for the system that it represents.

3.4. Sequence Stratigraphic Interpretation

Sequence stratigraphic analysis is based on the subdivision of sedimentary sequences into units (sequences) that are bounded by surfaces of stratal discontinuities or their correlative conformities. Since there is no exposure surface and erosional boundary, the vertical evolution of microfacies and the interaction of the cycle types within the measured section is investigated to define the system tracts. The system tracts are defined mainly on the basis of their stratal geometries, using terminations on the basis of their stratal geometries, using terminations of seismic reflectors of onlap, downlap, and offlap, but must be also defined in terms of facies and microfacies (Flugel, 2004).

The measured section starts with a foraminiferal grainstone-packstone facies corresponding to sample TD-51 and it is overlain by a mudstone to sandstone facies (TD-52) indicating a significant change in sedimentation pattern. Although the most important criteria for recognizing sequence boundaries are incised valleys and related unconformities (Flugel, 2004), these criteria are difficult to trace on carbonate platforms. Consequently, sequence boundaries of platforms are often characterized by increasing terrigenous input, abundant allochthonous sediment and coarse microfacies. The first sequence boundary is interpreted in the level corresponding to the top of sample TD-51 (Figure 3.9). Since the facies underlying sample TD-51 can not be considered, the level corresponding to sample TD-51 is not identified as a cycle.

The first types of cycles identified in the measured section are A-type cycles. These A-type cycles start at the base through the levels corresponding to samples from TD-52 to TD-80 and continue upward with B-type cycles through the levels corresponding to samples from TD-81 to TD-129 (Figure 3.9). The first A-type cycle recognized as A1-type cycle corresponds to the samples from TD-52 to TD-56. It is the thickest A1-type cycle measuring 78 cm in thickness. Above this first A1-type cycle, overlying two A1-type cycles are recognized in the interval corresponding to samples from TD-57 to TD-59. The section follows upwards with an A3-type cycle measuring 18 cm in thickness. From the level corresponding to sample TD-60 to the level corresponding to sample TD-69, an alternation of A3-type and A1-type cycles is recognized. Above the level corresponding to the sample TD-69, a 32 cm thick A4-type cycle is followed upwards by a 40 cm thick A2-type cycle. This A2-type cycle is capped by a 95 cm thick A2-type cycle in the level corresponding to the samples from TD-74 to TD-75. The A-type cycles are ended with an A4 type cycle in the level corresponding to samples from TD-76 to TD-80 in the measured section. This A4-type cycle is the thickest cycle within the A-type cycles and measures 167 cm in thickness.

A-type cycles (levels corresponding to samples from TD-52 to TD-80) dominated by siltstone and peloidal-crinoidal packstone facies are usually interpreted as transgressive system tracts since the vertical evolution of these cycles implies a change to higher energy conditions (Figure 3.9). Transgressive system tract generally comprises the deposits accumulated from the onset of coastal transgression until the time of the maximum transgression of the coast (maximum flooding surface), just prior to renewed regression. The possible maximum flooding surface is observed in the level corresponding to the sample TD-80 where the transgressive system tract ends (Figure 3.10). If rise is rapid, carbonate platforms will drown, producing drowning unconformity surface (characterized by a rapid lithological change from shallow-marine carbonates to deep shelf, slope or basin deposits) (Flügel, 2004). Therefore the unconformity surface is not recognized in the measured section. Moreover, characteristic features of transgressive system tract are deepening-upward and increasingly open marine

conditions indicated by the composition of the microfossils, the increase in bioclastic carbonates and as well as the relatively small thickness of thin-bedded deposits (Flügel, 2004). The abundance of benthic foraminifera increases along the transgressive system tract. The bedsets corresponding to transgressive system tract in the measured section show these characteristic features. For instance, the number of benthic foraminifera increases towards upper parts of the transgressive system tract (see cycles from 1 to 12, Figure 3.15). Moreover, the thickness of the beds increases towards upper parts of the transgressive system tract. The thickness of the bed corresponding to sample TD-56 is 2 cm whereas the thickness of the bed corresponding to sample TD-67 reaches 48 cm (Figure 3.10)

A-type cycles continue upward with B-type cycles. The first B-type cycle observed in the measured section is 100 cm thick (Figure 3.10). From the level corresponding to sample TD-81 to the level corresponding to the sample TD-100, four B2-type cycles are recognized (Figure 3.10). The thickness of these B2-type cycles varies from 77 cm to 230 cm (Figure 3.10). The level corresponding to sample TD-100 consisting of crinoidal and foraminiferal packstone-grainstone facies is overlain by a silty peloidal packstone facies. A significant change in sedimentation takes place in this level and it is interpreted as a sequence boundary. A highstand system tract is defined from the level where the B-type cycles start (TD-81) to the level where the second sequence boundary is interpreted (TD-100, Figure 3.10). Above the second sequence boundary corresponding to top of sample TD-100, a 112 cm thick B1-type cycle is observed and capped by two successive B2-type cycles (Figure 3.10). The thickness of B2-type cycles corresponding to the samples from TD-104 to TD-110 varies from 70 cm to 198 cm (Figure 3.10). Above these two B2-type cycles, a 180 cm B1-type cycle is observed. Between the B1-type cycles in the level corresponding to samples from TD-101 to TD-114 are defined as transgressive system tract. Above the transgressive system tract (from TD-101 to TD-114), A 161 cm B2-type cycle is recognized and continues upward with successive B2-type cycles (from TD-115 to TD-129). These B2-type cycles are generally interpreted as highstand system tract where the environment changed into higher energy conditions (Figure 3.10).

Highstand system tracts are formed by the regressive deposits when the sedimentation rates exceed the rate of relative sea-level-rise.

Within this anatomical organization of depositional sequences, sequence boundaries are located at the levels corresponding to base of sample TD-52 and TD-101 according to abrupt changes in sedimentation patterns (Figure 3.10 and Figure 3.12). Unexpectedly, a similar change in sedimentation takes place in level corresponding to sample TD-111. Since this significant change in sedimentation pattern starts at first in level corresponding to TD-101, the level corresponding to sample TD-101 is interpreted as a sequence boundary (Figure 3.10 and Figure 3.12). The abrupt change in sedimentation might be caused due to basin morphology of the studied area.

3.5. Sequence Stratigraphic Correlations with Well-Known Tournaisian Sections of the World

In order to apply a worldwide sequence stratigraphic correlation, the meter scale cycles of this study was compared with the relative sea-level fluctuations of South China and Western European Platform and Moscow Syncline. To construct a sequence stratigraphical approach in this study, microfacies studies have been carried out. Based on the vertical evolution of the microfacies, 25 shallowing upward cycles have been identified in the measured section. Stacking pattern of these meter scale cycles has been used to define large scale sequences, system tracts and long term sea-level fluctuations. Within the measured section, two main sequences and two sequence boundaries have been interpreted. The level corresponding to the bottom of sample TD-52 is identified as the first sequence boundary (SB1) and the level corresponding to the top of sample TD-100 is defined as second sequence boundary (SB2) where the investigated section represents significant changes in sedimentation patterns (Figure 3.9). The first

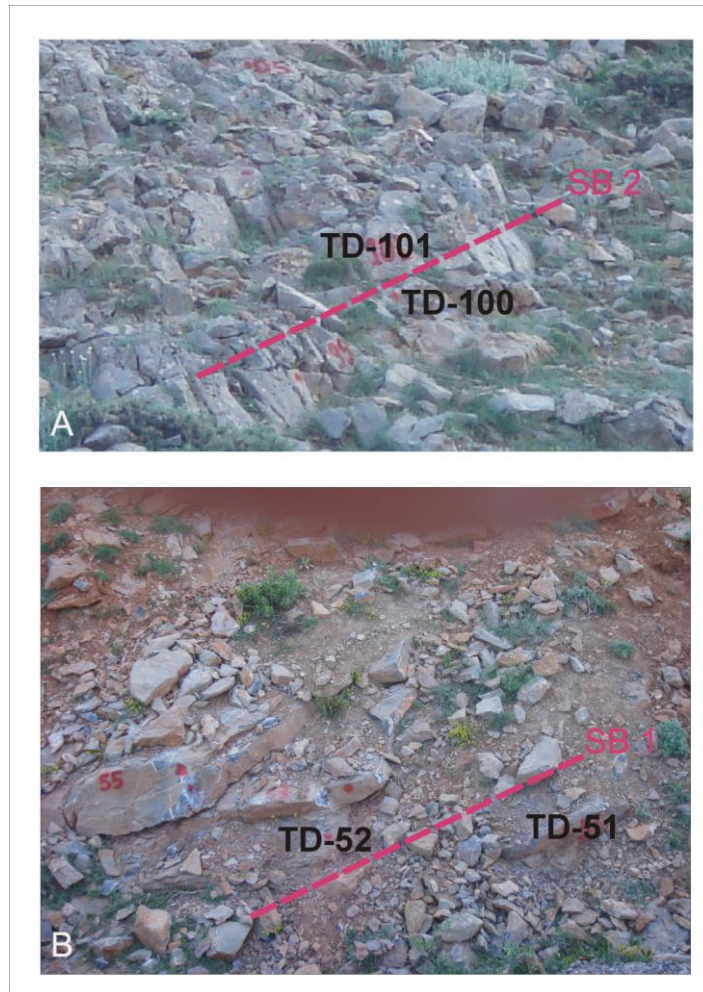


Figure 3.12: The levels of sequence boundaries, namely SB1 and SB2, are interpreted as top of the layers corresponding to sample TD-51 and TD-100.

transgressive system tract is defined in the level corresponding to samples from TD-52 to TD-80 and the second one is defined in the level corresponding to samples from TD-101 to TD-114 (Figure 3.9). Above TD-80, the first highstand system tract is defined in the level corresponding to samples from TD-81 to TD-100 (Figure 3.9). The second highstand system tract is interpreted in the level corresponding to samples from TD-114 to TD-129 (Figure 3.9). The general trend of the meter scale cycles of this study displays similar sea level fluctuations took place in all carbonate platforms of South China and Western European Platform and Moscow Syncline.

The sequence stratigraphy of the Tournaisian-Visean strata in South China was constructed by Hance et al. (1997). South China was located in a subaequatorial position on the northern border of Tethys realm during the Early Carboniferous. Four sections, namely Huaqiao Farm, Mopanshan, Yajiao River, Pengchong, were investigated by Hance et al. (1997) in South China. Both the biostratigraphical and the sedimentological data of these studied sections were used to construct the sequence stratigraphical framework in South China by Hance et al. (1997). To apply a sequence stratigraphical correlation between the investigated sections in the Early Carboniferous carbonate platform of South China (Hance et al., 1997) and the studied Upper-Tournaisian carbonate succession within the measured section, a major key surface has been identified. This key surface is interpreted as the sequence boundary that is defined in the level corresponding to unit 30 within the Yajiao River section of Hance et al. (1997) where a significant change in sedimentation pattern was observed (Figure 3.13). This sequence boundary is interpreted in the Association B of Hance et al. (1997) (Figure 3.13) which is the equivalent of Ut2 zone in our study (Table 2.1). In the Ut2 zone of this study, a sequence boundary (SB2) has also been interpreted (TD-100). These two sequence boundaries most probably are equivalent to each other. The sequence boundary of Hance et al. (1997) was also interpreted as a paleokarst in Huaqiao Farm and Mopanshan sections and was characterized by a stratigraphic hiatus, since the Association C of Hance et al. (1997) was absent (Figure 3.13). Moreover, a highstand system tract is interpreted below the sequence boundary in Yajiao section of Hance et al (1997) and the equivalent highstand system tract under the SB2 has also been interpreted in our study (Figure 3.9). Hance et al. (1997) defined that the most striking evidence was a major fall in relative sea-level that occurred during Late Tournaisian time and the inprints of this sea level fall are also recognized in the studied Upper-Tournaisian carbonate succession. Moreover, both sequence boundaries of Hance et al (1997) and this study were interpreted very close to Tournaisian-Visean boundary. Therefore, the sequence boundary of both Hance et al. (1997) and this study have the potential to be used in worldwide correlation.

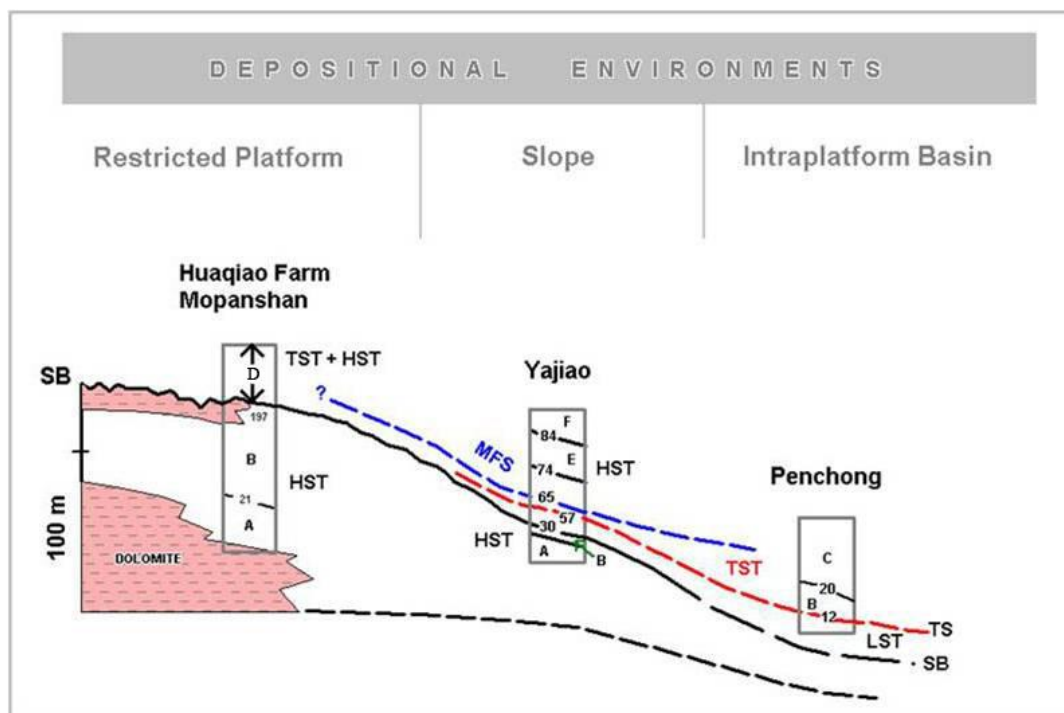


Figure 3.13: Sequence stratigraphic correlation scheme for the Upper Tournaisian and Lower-Visean strata in the Guangxi region (South China). LST: Lowstand system tract, TST: Transgressive system tract, HST: Highstand system tract, SB: Sequence Boundary, MFS: Maximum flooding surface, A-F: Foraminiferal associations (modified from Hance et al., 1997)

The Carboniferous Namur-Dinant Basin has been studied extensively since it is the type area for the Tournaisian and Visean stages. Consequently, outcrops in Western European Platform have been used as worldwide references for Mississippian subsystem (Lower Carboniferous). Poty et al. (2006) carried out a detailed study in Belgium and Northern France. They used both biostratigraphical and sedimentological data to construct a sequence stratigraphical approach. The biostratigraphical data of Poty et al. (2006) is based on mainly on foraminifer associations. They used the radiations of Early Carboniferous foraminifers following the Devonian-Carboniferous crisis as a tool for high-resolution correlation in Mississippian. However, some of these guides were facies controlled and they found critical to perform an integrated approach combining the biostratigraphy, sedimentology and sequence stratigraphy to identify delayed entries, potential stratigraphic gaps and to avoid diachronous correlations. The

main difficulty for them was correlating shallow and deeper water facies at any given time. When they considered the existing biozonations, they realized that the Viséan part of the scheme was always more detailed reflecting the widespread development of shallow-water platforms in Early Viséan which created conditions more suitable for foraminifers and the Tournaisian biozones, less well documented, reflect unfavourable environmental conditions in the lower ramp (Dinant Sedimentation Area) and pervasive dolomitization in the inner ramp (Condruz and Namur Sedimentation Area). Based on foraminiferal assemblage and diversity of foraminifers, they identified sixteen Mississippian Foraminiferal Zones (MFZ1-MFZ16). The Mississippian Foraminiferal Zones including MFZ5, MFZ6, MFZ7 and MFZ8 were identified within the Upper-Tournaisian substage. In order to apply a biostratigraphical correlation within the Upper Tournaisian substage between SE Turkey and Belgium and Northern France, the biozones Ut1 and Ut2 of this study was compared with the MFZ5, MFZ6, MFZ7 and MFZ8 of Poty et al. (2006) (Table 2.1).

Poty et al. (2006) reconstruct a sketch combining the foraminiferal zones of Poty et al (2006) and third-order sequences of Hance, Poty and Devuyt (2001). According to this correlation, Poty et al. (2006) observed a sequence boundary within the MFZ5 which is equivalent of Ut1 zone of this study and a second sequence boundary within the MFZ8 which is the equivalent of Ut2 zone of this study (Table 3.2). Within Upper Tournaisian we recognized two sequence boundary named as SB1 and SB2 (Table 3.2). SB1 is identified in Ut1 zone whereas SB2 is identified within Ut2 zone. Therefore, the SB1 of this study corresponds to the sequence boundary observed at the bottom of the sequence named 4 of Poty et al. (2006) and the SB2 is equivalent of the sequence boundary observed at the top of the sequence named 4 of Poty et al. (2006) (Table 3.2).

The Moscow Syncline is a vast sedimentary basin located in the centre of the East-European Platform which is one of the largest Precambrian cratons of the world. The main part of the sedimentary platform consists mainly of Carboniferous shallow-marine carbonates including several subordinate

terrigenous intervals (Alekseev et al., 1996). Especially, the southern limb of the Moscow Syncline is a classic area where mainly shallow-marine Carboniferous deposits are exposed as a wide belt. Since Paleozoic sequence of this syncline is suitable for sea-level fluctuations, Devonian and Carboniferous relative sea level curves of Moscow Syncline were calibrated by Alekseev et al., 1996. Carboniferous sea-level changes were previously described for the Donets Basin, the Voronezh Anticline, the Volga-Ural Region the Moscow Syncline by Aisenverg et al. (1985, 1986). Since the principles of construction and design of

Table 3.2: Sequence stratigraphic correlation with biozones and sequence boundaries between the Western European Platform (Belgium and Northern France) and this study.

STAGES	Belgium and Northern France		Hadim, Konya (SE Turkey)		
	Devuyst and Hance in Poty and other (2006)		THIS STUDY		
	3-ord seq.	Foraminiferal Zones	Foraminiferal Zones	3-ord Seq Boundary	Sample No
UPPER TOURNAISIAN	5	MFZ8	Ut2	SB 2	TD-101
	4	MFZ7	Ut1		
		MFZ6			
	3	MFZ5	SB 1	TD-52	

the curves of Aisenverg et al. (1985, 1986) are not compatible with modern sea-level curves, Alekseev et al. (1996) developed a new relative sea level curve for the Devonian and Carboniferous of Moscow Syncline, using the Harland et al. (1990) geological time scale (Figure 3.14). The calibrated Carboniferous sea level curves of the Moscow Syncline reflect early Tournaisian transgression covered

almost the entire area with normal-marine waters. During Early Visean, a prominent regression induced and the Moscow syncline was uplifted. Tournaisian rocks were eroded by numerous river systems. Thus, Late Tournaisian-Early Visean sedimentation did not take place due to subaerial exposure in the Moscow syncline. The Carboniferous sea-level curves for the Moscow Syncline of Alekseev et al. (1996) is very similar to the marine onlap curve of Ross and Ross (1988) (Fig 3.14). The comparison of the general trend of

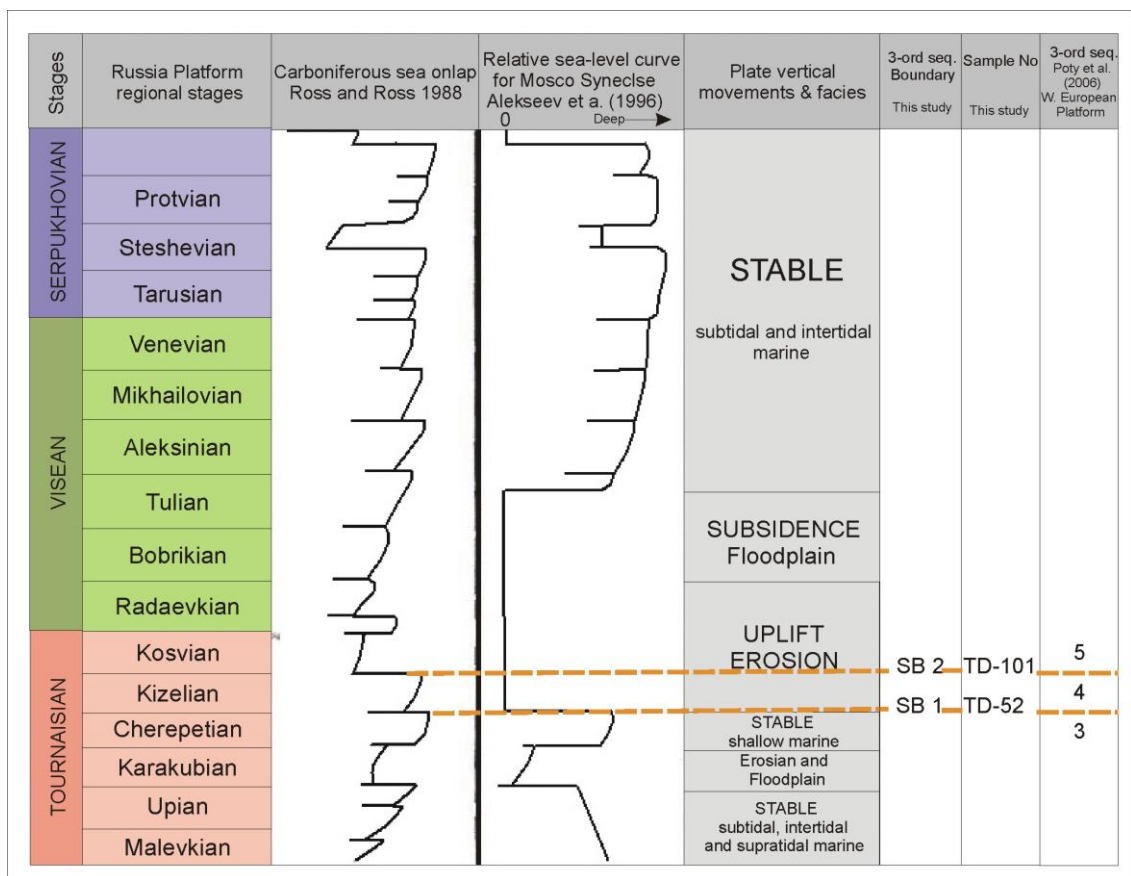


Figure 3.14: Carboniferous sea-level changes in the Moscow Syncline and comparison with the Carboniferous sea level curves of Ross and Ross (1988) and this study (modified from Alekseev et al. (1996)).

cyclicality of this study with both the relative sea level curve for the Carboniferous of Moscow Syncline of Alekseev et al. (1996) and marine onlap curve of Ross and Ross (1988) shows that a rise of relative sea level takes place during

Tournaisian. Moreover, the sequence boundary SB 1 of this study corresponding to sample TD-52 is approximately equivalent to sequence boundary recognized in the Early Kizelian of Alekseev et al. (1996) and the second sequence boundary SB2 of this study corresponding to sample TD-101 is approximately equivalent to sequence boundary recognized in the early Kosvian of Alekseev et al. (1996) (Figure 3.14). Since the SB1 of this study corresponds to the sequence boundary observed bottom of sequence named 4 of Poty et al. (2006) and SB2 of this study is equivalent to the sequence boundary observed top of sequence named 4 of Poty et al. (2006) (Figure 3.14), the Tournaisian transgression is also recognized in Western European Platform like in the Central Taurides with indicating a global sense when compared with the sea level curve for the Carboniferous of Moscow Syncline of Alekseev et al. (1996) and marine onlap curve of Ross and Ross (1988).

A sequence stratigraphic approach allowed the correlation of the measured section of this study in Hadim-Taşkent region (Central Taurides) with the other Upper Tournaisian data illustrated in Hance et al. (1997) from South China in Poty et al. (2006) from Belgium and Northern France and the Carboniferous sea level curves for the Moscow Syncline of Alekseev et al (1996). Since the sea level changes observed within the studied section is correlative with those illustrated in these regions, the records of sequence stratigraphy in the Hadim-Taşkent region can be considered a global event.

3.6. Interpretation of Response of Benthic Foraminifers

Biological response of benthic foraminifera to carbonate cyclicity in shallow subtidal carbonate deposit is investigated within the measured section. Microfossil data provides useful tools for studying the response of cycles. The measured section is composed mainly of limestones containing benthic foraminifers and bioclasts. The abundance of counted benthic foraminifera points out a good response to shallowing responses in the parasequences of the studied section. In

general, the abundance of foraminifera increases in bioclastic and foraminiferal grainstone facies and decreases in silty peloidal packstone facies. The abundance of benthic foraminifera generally displays a good response to sedimentary cyclicity in both A and B type cycles. A1-type cycles generally consist of mudstone to sandstone (MS) facies. In this type of cycles, foraminifers are present but very rare. Thus, their abundance does not give good response to the cyclic phenomena in this type of cycles (see cycle 1, 2, 3, 5, 7, Figure 3.15). In A2-type cycles, which are generally characterized by sandy peloidal packstone facies at the base and the crinoidal wackestone-packstone facies at the top, foraminifers do not give good response because of dolomitization of the samples TD-72, TD-73, TD-74 and TD-75 (see cycle 10, 11, Figure 3.15). In A3-type cycles, which are generally characterized by mudstone to sandstone facies at the bottom and peloidal and crinoidal packstone facies at the top, foraminifers give quite good response to cyclicity (see cycle 4, 6, 8, Figure 3.15). For instance, in the A3-type cycle corresponding to samples from TD-60 to TD-61, benthic foraminifers display a good response to cyclicity. The number of foraminifera is zero in sample TD-60 whereas it increases up to 61 in sample TD-61. In the A4-type cycles, which are generally composed of siltstone to mudstone facies at the bottom and crinoidal and foraminiferal packstone-grainstone facies at the top, foraminifers give good response to cyclicity. The bottom of A4-type cycles consist of less benthic foraminifera whereas the top of the cycles contain abundant benthic foraminifera (see cycle 9, 12, Figure 3.15).

In B type cycles, which are characterized by a good foraminiferal diversity, benthic foraminifers give a good response to cyclicity. In B1-type cycles, which are recognized in the level corresponding to the samples from TD-101 to TD-103 and from TD-111 to TD-114, number of foraminifera increases from cycle bottoms to cycle tops. For example, the benthic foraminifers are counted 24 in sample TD-101 whereas it exceeds 340 in sample TD-103. Therefore, the abundance of benthic foraminifera displays a good response to sedimentary cyclicity in B1-type cycles (see cycle 17, 20 Figure 3.15). Like in B1-type cycles,

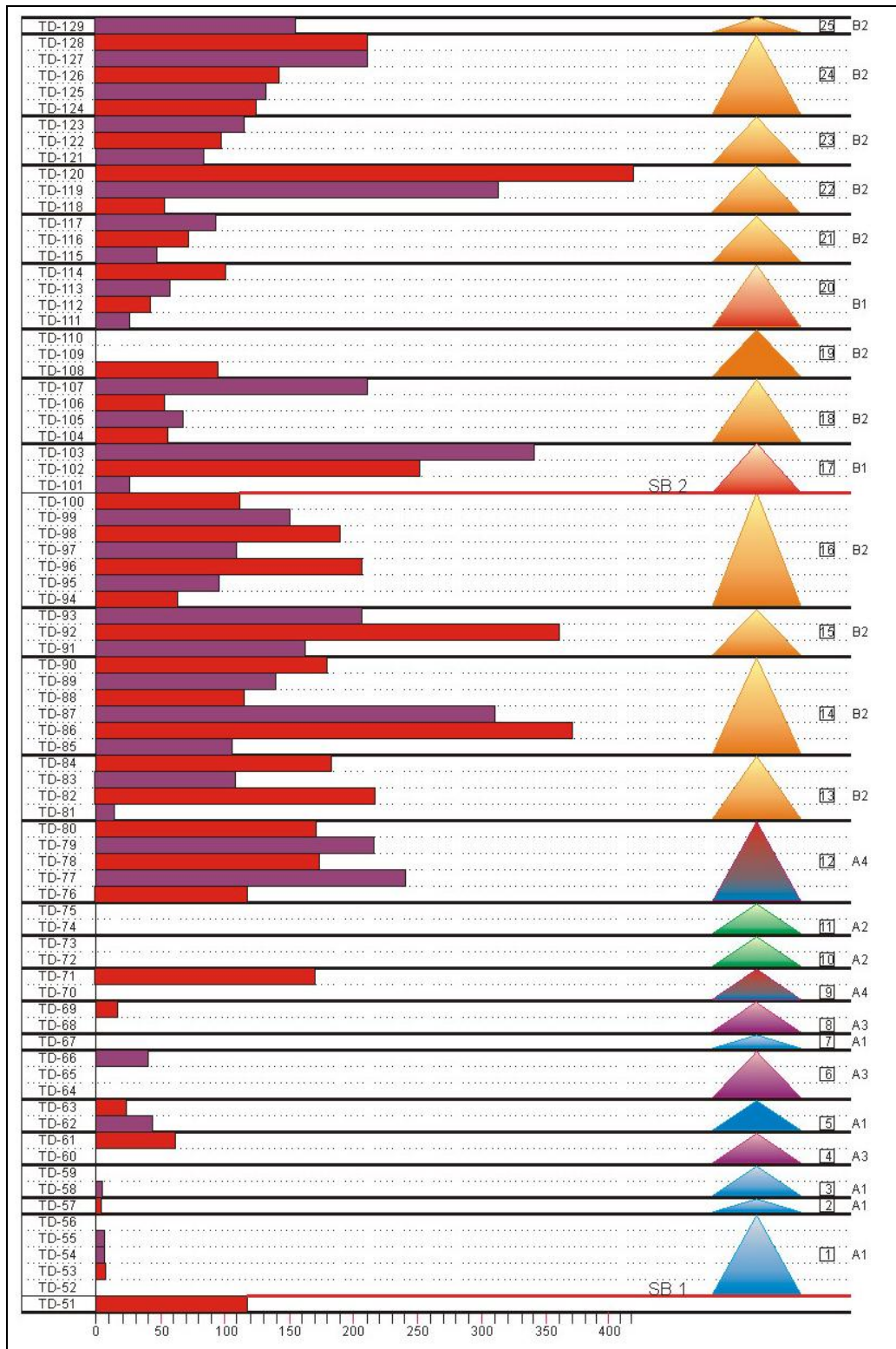


Figure 3.15: Benthic foraminiferal countings and response of foraminiferal abundance to meter-scale cycles (SB1: sequence boundary 1, SB2: sequence boundary 2).

foraminifers give a good response to cyclicity in B2-type cycles. The number of benthic foraminifera increases from bottom to the top of the B2-type cycles. The cycle tops are characterized by the abundance of foraminifers with respect to the bottom of the following cycles which show a decrease in abundance (see cycle 13, 14, 15, 16, 18, 19, 21, 22, 23, 24, 25 Figure 3.15).

The sequence boundaries within the measured section can easily be recognized by the evidence of a decrease in foraminiferal assemblages. The number of foraminifera decreases abruptly at the levels corresponding to the sequence boundaries. The number of benthic foraminifera is 118 in sample TD-51 whereas the number of benthic foraminifera is 0 in sample TD-52. Since the SB1 is interpreted between the samples TD-51 and TD-52, response of benthic foraminifera gives a good response at this sequence boundary. Like SB1, the second sequence boundary SB2 can easily be interpreted by the evidence decreasing in foraminiferal assemblages. The number of benthic foraminifera is 96 in sample TD-100 while the number of benthic foraminifera is 24 in sample TD-101 (Figure 3.15). Consequently, the response of benthic foraminifera also gives a good response in the level corresponding to the second sequence boundary (Figure 3.15). Since foraminifers are very sensitive to sea level changes, response of foraminiferal abundance to sea level fluctuations gives a good response to cyclicity.

CHAPTER 4

SYSTEMATIC PALEONTOLOGY

Based on thin sections of benthic foraminifera obtained from the collected samples of the measured section, a systematic micropaleontological study was carried out. Benthic foraminiferal species has been identified from 89 thin sections based on the taxonomic parameters including wall structure, wall composition, manner of coiling, number of volutions, number of chambers, peripheral shape, position of septa and secondary deposits.

In this study, based on the criteria mentioned above, 21 different species were identified. The taxonomic classification of the benthic foraminifera is carried out according to the descriptions of Ellis and Messina (1940), and Loeblich and Tappan (1988). Moreover, a synonym list is presented by the use of recent publications and manuals. The description, remarks and stratigraphic distribution for each identified species are given below, respectively. Although Calcispharidae is recognized in thin sections and illustrated in Plate-1, the systematic paleontology of this family is not considered since it is easily differentiated from the other benthic foraminifers illustrated in this study.

SUPERFAMILY EARLANDIACEA CUMMINGS, 1955

Family Earlandiidae Cummings, 1955

Genus *Earlandia* Plummer, 1930

Type species: *Earlandia perparva* Plummer, 1930

Earlandia sp.

Pl. 1, figs. 10-12

Description:

Test is free and elongate. This species is characterized by globular proloculus followed by a long, straight, undivided tubular chamber. Wall is calcareous and microgranular.

Dimensions (mm):

Diameter of proloculus: 0.067-0.088

Width of the test: 0.033-0.056

Length of the test: 0.311-0.367

Thickness of wall: 0.009-0.012

Remarks:

The distinguishing character of *Earlandia* is the composition of the microgranular shell wall and its undivided rectilinear tubular chamber. Among Paleozoic foraminifera, the genus *Syzrania* is the closest form to *Earlandia*. However the populations belonging to *Earlandia* are easily distinguished from the species of *Syzrania* by the absence of outer hyaline layer. Our specimens illustrated in this study are quite close to *Earlandia* illustrated by Gallagher (1998) in terms of its globular chamber followed by long, straight, tubular second chamber and its calcareous wall.

Stratigraphic Distribution:

Specimens were recovered from Silurian (Ludlovian) to Permian (Loeblich and Tappan, 1988). Our specimens were recovered through the Upper Tournaisian. According to Poty et al. (2006), Carboniferous *Earlandia* species appeared very close to Devonian-Carboniferous boundary and survived into the Mississippian stages of Carboniferous.

SUPERFAMILY NODOSINELLACEA RHUMBLER, 1895

Family Earlandinitidae Loeblich and Tappan, 1984

Genus *Lugtonia* Cummings, 1955
Type species: *Nodosinella concinna* Brady, 1876

Lugtonia monilis Malakhova, 1963

Pl. 1, figs. 6-9

1963. *Darjella monilis* Malakhova, pp. 111-112.

1968. *Darjella monilis* Malakhova, Conil and Lys, p. 539, pl.2, fig. 22

1876. *Nodosinella concinna* Brady, p. 106

1988. *Lugtonia monilis*, Loeblich and Tappan, pl. 221, figs. 11-13.

Description:

Test is free, small and slightly curved. This species is composed of a series of globular, inflated chambers arranged in a uniserial pattern. It is characterized by its chamber form and arrangement. Chambers are separated by depressed and distinct sutures creating lobulate lateral margins. Wall is originally calcareous but a secondary origin material is preserved in crystalline silica.

Dimensions (mm):

Chamber height: 0.067-0.075

Chamber width: 0.091-0.108

Thickness of wall: 0.012-0.016

Remarks:

Although observed specimens are incomplete, *Lugtonia monilis* observed can easily be distinguished among several foraminifers by its globular chambers arranged in a uniserial pattern and distinct sutures creating lobulate lateral margins. The incomplete sections composed of two chambers of this species are quite frequent in the studied sections.

Stratigraphic Distribution:

The stratigraphic range of *Lugtonia monilis* is from Lower Carboniferous (Tournaisian) to Upper Carboniferous (Namurian) (Loeblich and Tappan, 1988). Our specimens were also recovered through Upper Tournaisian. In Poty et al. (2006), *Lugtonia monilis*, reported as *Darjella monilis*, is given as one of the marker species of the Upper Ivorian corresponding to their foraminiferal zones, MFZ7 and MFZ8.

SUPERFAMILY TOURNAYELLACEA DAIN, 1953

Family Tournayellidae Dain, 1953

Subfamily Tournayellinae Dain, 1953

Genus *Tournayella* Dain, 1953

Type species: *Tournayella discoidea* Dain, 1953

Tournayella sp.

Pl. 2, figs. 15, 16

Description:

Test is free and evolute. This species consists of a round proloculus and a second pseudotubular chamber. Coiling is planispiral. Wall is calcareous and microgranular.

Dimensions (mm):

Diameter of test: 0.385-0.471

Thickness of wall: 0.011-0.013

Remarks:

Tournayella is differentiated from *Forchia* by the appearance of pinches in earlier whorls and its wall structure. The wall of *Forchia* is coarsely granular, thick, usually with a finely granular inner layer and a more coarsely granular outer

one whereas in *Tournayella* the wall is homogenous. The wall of this species is also recognized as homogenous in the studied sections. The specimens illustrated in our study are close to the type species of *Tournayella*, *T. discoidea*. The specimens illustrated in this study are quite close to *Tournayella* illustrated by Malpica (1973) in terms of its planispiral coiling and its calcareous wall. *Tournayella* illustrated by Marchant (1974) also resembles the specimens illustrated in this study with its planispiral coiling and microgranular calcareous wall.

Stratigraphic Distribution:

The stratigraphic range of *Tournayella* sp. is Lower Carboniferous (Tournaisian to Visean) (Loeblich and Tappan, 1988). Our specimens were also recovered through Upper Tournaisian. According to Poty et al. (2006), *Tournayella* appeared in Ivorian (MFZ5).

Genus *Tournayellina* Lipina, 1955

Type species: *Tournayellina vulgaris* Lipina, 1955

Tournayellina ? sp.

Pl. 2, figs. 13, 14

Description:

Test consists of a small number of high whorls and a few pseudochambers. The coiling occurs in one plane. Wall is calcareous and microgranular.

Dimensions (mm):

Diameter of test: 0.230-0.240

Thickness of wall: 0.011-0.013

Remarks:

This species is characterized by its smaller number of whorls. The identification of our specimens is problematic. Although we report these sections as *Tournayellina* ? sp., these forms might be atypical sections of the genus *Endothyra*. The specimens illustrated in this study are quite close to *Tournayellina* illustrated by Conil et al. (1989) in terms of its small numbers of high whorls, its planispiral coiling and its calcareous wall.

Stratigraphic Distribution:

The stratigraphic range of *Tournayellina* sp. is Lower Carboniferous (Tournaisian) (Loeblich and Tappan, 1988). Our specimens were also recovered through Upper Tournaisian. According to Poty et al. (2006), *Tournayellina* is recognized in Hastarian and Ivorian (MFZ3-MFZ5).

Subfamily *Forschiinae* Dain, 1953

Genus *Eoforschia* Mamet, 1970

Type species: *Tournayella moelleri* Malakhova, in Dain and Grozdilova, 1953

Eoforschia moelleri Malakhova, 1953

Pl. 1, figs. 13-15

1953. *Eoforschia moelleri* Malakhova, p. 33

1988. *Eoforschia moelleri*, Loeblich and Tappan, pl. 233, figs. 3-4

Description:

Test is enrolled. Proloculus is followed by planispirally coiled tabular chamber. Wall is calcareous and composed of a well developed microgranular inner layer and a thin microgranular outer layer.

Dimensions (mm):

Diameter of test: 0.260-0.320

Thickness of wall: 0.011-0.013

Remarks:

This species can be differentiated by its planispirally coiled tabular chamber around the proloculus and two layered wall with a thin microgranular outer layer and a microgranular inner layer.

The coiling of *Eoforschia moelleri* is similar to *Tournayella*. However, an important difference from *Tournayella*, is the structure of the wall. The wall of this species is two layered, while in *Tournayella* the wall is homogenous and single layered. Our specimens illustrated in this study are not perfectly oriented sections. They are rather tangential or tangential oblique sections. However, the measured parameters and the wall composition fit well to the original description of the species.

Stratigraphic Distribution:

The stratigraphic range of *Eoforschia moelleri* is from Upper Tournaisian to Viséan (Loeblich and Tappan, 1988). Our specimens were recovered also through Upper Tournaisian. According to Hance et al. (1997), *Eoforchia* is recognized in the Association A of Hance et al. (1997) in Ivorian. In Poty et al. (2006), *Eoforchia moelleri* is a typical marker of Ivorian (Upper Tournaisian) corresponding to MFZ5 to MFZ8 Zones in Western European.

Subfamily Septabrunsiinae, Conil and Lys, 1977

Genus *Septabrunsiina* Lipina, 1955

Type species: *Endothyra? krainica* Lipina, 1948

Septabrunsiina sp.

Pl. 5, figs. 11, 12

Description:

Test is enrolled and circular in outline. The coiling is initially streptospiral but the last whorls are planispiral. The inner whorls are not subdivided but have constrictions. The final whorl has septa and distinct chambers. Wall is calcareous and microgranular.

Dimensions (mm):

Diameter of test: 0.378-0.422

Width of test: 0.167-0.178

Thickness of wall: 0.006-0.007

Remarks:

The specimens in this study are quite close to *Septabrunsiina* illustrated by Dil (1976) in terms of nonseptate early stage with pseudochambers and septate later stages with true chambers. *Septabrunsiina* illustrated by Conil et al. (1989) also resembles to our specimens in this study with its manner of coiling and its constrictions in inner whorls and distinct chambers in outer whorls.

Stratigraphic Distribution:

The stratigraphic range of *Septabrunsiina* sp. is Lower Carboniferous (Loeblich and Tappan, 1988). Our specimens were recovered through Upper Tournaisian.

Subfamily Chernyshinellinae, Reytlinger, 1958

Genus *Eblanaia* Conil and Marchant, in Conil, 1977

Type species: *Plectogyra michoti* Conil and Lys, 1964

Eblanaia sp.

Pl. 5, fig. 1, 2

Description:

Test is enrolled, evolute and biconcave. Chamber arrangement is streptospiral. Wall is calcareous and microgranular. Main layer is recognized thick and irregularly granular and the inner layer is observed as microgranular. Supplementary deposits form thickenings at the ends of the septa and infillings at the corners.

Dimensions (mm):

Diameter: 0.378-0.398

Thickness of wall: 0.009

Remarks: The specimens illustrated in this study are quite close to the *Eblanaia* illustrated by Michelsen (1971) in terms of its streptospiral coiling, calcareous wall and supplementary deposits. *Eblanaia* illustrated by Conil and Lees (1974) resembles the specimens illustrated in this study with its manner of coiling, thick septa and its thick, microgranular wall. The specimens in this study are also quite close to *Eblanaia* illustrated by Conil et al. (1989) in terms of its thick septa, secondary deposits and streptospiral coiling.

Stratigraphic Distribution:

The stratigraphic range of *Eblanaia* sp. is Lower Carboniferous (Upper Tournaisian to Upper Viséan) (Loeblich and Tappan, 1988). Our specimens were recovered through Upper Tournaisian. According to Poty et al. (2006), *Eblanaia* appeared in Ivorian (MZ5-MFZ8).

Family Palaeospiroplectamminidae Loeblich and Tappan, 1984

Subfamily Palaeospiroplectammininae Loeblich and Tappan, 1984

Genus *Eotextularia* Mamet, 1970

Type species: *Palaeotextularia diversa* Chernysheva, 1948

Eotextularia diversa Chernysheva, 1948

Pl. 5, fig 13

1948. *Eotextularia diversa* Chernysheva, p.248

1988. *Eotextularia diversa*, Loeblich and Tappan, pl. 239, fig. 6-8

Description:

The proloculus is followed by irregularly coiled whorls, later uncoiled with a few pair of biserial chambers. Wall is double layered with a thin dark microgranular inner layer and a thick coarsely granular outer layer.

Dimensions (mm):

Height of test: 0.59

Thickness of wall: 0.045

Remarks:

Mamet (1970) described the wall of this species as having a single layer. However, Conil and Lys (1977) described the wall as differentiated into an outer coarsely granular layer and a thin dark microgranular inner layer. The wall of the illustrated specimens in this study also consists of a microgranular inner layer and a coarsely granular outer layer.

Stratigraphic Distribution:

The stratigraphic range of *Eotextularia diversa* is Lower Carboniferous (Upper Tournaisian to Middle Viséan) (Loeblich and Tappan, 1988). Our specimens were also recovered through Upper Tournaisian. According to Poty et al. (2006), *Eotextularia diversa* appeared in Ivorian (MFZ6) and survived into the Viséan.

Genus *Palaeospiroplectammina* Lipina, 1965

Type species: *Spiroplectammina tchernyshinensis* Lipina, 1948

Palaeospiroplectamina mellina Malakhova, 1956

Pl. 2, figs. 1-3

1956. *Palaeospiroplectamina mellina* Malakhova, p. 151

1968. *Palaeospiroplectamina mellina*, Conil and Lys, p. 540, pl. 3, fig. 36

1974. *Palaeospiroplectamina mellina*, Conil et al., p. 471, pl. 3, fig. 26

1975. *Palaeospiroplectamina mellina*, Dil, p. 224, pl. 3, fig. 33

1976. *Palaeospiroplectamina mellina*, Dil, p. 386, pl. 3, fig. 48, 49

1976. *Palaeospiroplectamina mellina*, Conil, p. 475, pl. 2. Fig. 15

Description:

Small streptospirally enrolled early stage is followed by uncoiled, biserial later stage. Test is elongate in shape. Wall is calcareous and microgranular.

Dimensions (mm):

Height of test: 0.32-0.38

Thickness of wall: 0.015- 0.017

Remarks:

The most characteristic feature of this species is its small streptospiral early stage and uncoiled, biserial later stage. This species resembles to genus *Eotextularia diversa* but it is differentiated from it by having a microgranular single layer and smaller streptospiral enrolled early stage. In our material most sections of this species are incomplete due to the orientation of thin sections.

Stratigraphic Distribution:

The stratigraphic range of *Palaeospiroplectamina mellina* is Upper Devonian (Fammenian) to Lower Carboniferous (Late Visean) (Loeblich and Tappan, 1988). Our specimens were recovered through Upper Tournaisian.

SUPERFAMILY ENDOTHYRACEA BRADY, 1884

Family Endothyridae Brady, 1884

Subfamily Endostaffellinae Loeblich and Tappan, 1984

Genus *Dainella* Brazhnikova, 1962

Type species: *Endothyra? chomatica* Dain, in Brazhnikova, 1962

Dainella sp.

Pl. 2, figs. 11-12

Description:

Test is small, axially compressed involute, sometimes evolute. Coiling is streptospiral and axis of coiling varies sharply. Chambers per whorl increase gradually in size. This species is characterized by its secondary deposits in the form of massive chomata. Wall is single layered and calcareous.

Dimensions (mm):

Diameter of test: 0.278-0.311

Thickness of wall: 0.015-0.017

Remarks:

The characteristic features of this genus are sharp changes in the axis of coiling, great number of slowly enlarging chambers and its massive chomata. The specimens illustrated in this study are quite close to the *Dainella* illustrated by Conil and Lys (1967) in terms of its number of slowly enlarging chambers, massive chomata and structure of wall. *Dainella* sp. illustrated in this study resembles the *Dainella* illustrated by Segura (1973) with its secondary deposits and manner of coiling. This species in this study is also quite close to the *Dainella* illustrated by Cozar and Vachard (2001) in terms of its type of coiling, structure of wall and type of chomata.

Stratigraphic Distribution:

The stratigraphic range of *Dainella* sp. is Lower Carboniferous (Loeblich and Tappan, 1988). Our specimens were recovered through Upper Tournaisian. According to Poty et al. (2006), *Dainella* appeared in Ivorian (MFZ6) and survived into the Viséan.

Genus *Granuliferella* E. J. Zeller, 1957

Type species: *Granuliferella granulosa* E. J. Zeller, 1957

Granuliferella sp.

Pl. 2, figs. 1-3

Description:

Test is discoidal and involute. Coiling in the initial stage is streptospiral, later becoming nearly planispiral. Septa are short and slightly oblique and showing little anterior direction. Wall is very thick, coarsely granular and single layered.

Dimensions (mm):

Diameter of test: 0.26-0.31

Width of test: 0.16-0.18

Thickness of wall: 0.017-0.019

Remarks:

This species is differentiated from the other members of endothyroid foraminifera by its thicker and coarsely granular wall. In general, this species shows many affinities to some of the primitive species of *Plectogyra* (E. J. Zeller, 1950). It differs from *Plectogyra* in having a coarsely granular nature of its wall. This species illustrated in this study are quite close to the *Granuliferealla* illustrated by Conil et al. (1989) in terms of its thick, coarsely granular wall, its manner of coiling and its position of septa.

Stratigraphic Distribution:

The stratigraphic range of *Granuliferella* sp. is Upper Devonian (Fammenian) to Lower Carboniferous (Tournaisian to Late Viséan) (Loeblich and Tappan, 1988). Our specimens were recovered through Upper Tournaisian. According to Hance et al. (1997), *Granuliferella* is one of the most common the Upper Tournaisian elements within Association A of Hance et al. (1997) in South China. In Poty et al. (2006), *Granuliferella* appeared in Ivorian (MFZ5) and survived into the Viséan.

Genus *Planoendothyra* Reitlinger, 1959

Type species: *Endothyra aljutovica* Reitlinger, 1950

Planoendothyra sp.

Pl. 4, figs. 15, 16

Description:

Test is slightly compressed and biumbilicate. Coiling is initially streptospiral and the final volutation is planispiral and evolute. Septa are radial to slightly oblique. Wall is calcareous and microgranular. Well developed secondary deposits in the form of pseudochomata are present.

Dimensions (mm):

Diameter of test: 0.37-0.38

Width of test: 0.14-0.17

Thickness of wall: 0.015-0.017

Remarks:

The distinguishing features of this species are slightly compressed test, its initially streptospiral volutions and final planispiral volutation and its secondary deposits as pseudochomata. This species differs from the species of

Quasiendothyra by the different character of supplementary deposits. Secondary deposits in this species fill the lateral parts of the chambers, line the base of the chambers and form infrequent pseudochomata. The specimens illustrated in this study are quite close to the *Planoendothyra* illustrated by Dil (1976) in terms of its coiling pattern, the character of secondary deposits and structure of the wall.

Stratigraphic Distribution:

The stratigraphic range of this species is from Lower Carboniferous to Upper Carboniferous (Loeblich and Tappan, 1988). Our specimens were recovered through Upper Tournaisian.

Subfamily Endothyrinae Brady, 1884

Genus *Endothyra* Phillips, 1846

Type species: *Endothyra bowmani* Phillips, 1846

Endothyra sp.

Pl. 5, figs. 3-9, 10?

Description:

Test is enrolled and partially involute. Periphery is broadly rounded and discoidal. The plane of coiling changes abruptly during growth. Coiling is streptospiral and the final volutation is nearly planispiral. Chambers are inflated. Septa are thin and weakly oblique opposite to the coiling. Wall is calcareous and microgranular.

Dimensions (mm):

Diameter of test: 0.325-0.388

Width of test: 0.225-0.242

Thickness of wall: 0.019-0.021

Remarks:

The characteristic features of this species are its streptospiral coiling and calcareous microgranular wall. The species illustrated in this study are close to the species of Conil and Lys (1968) in terms of its pattern of coiling, septa and wall structure. Our species are also quite close to *Endothyra* sp. illustrated in Segura (1973). The forms illustrated by Segura (1973) resemble to our species with their character of coiling and wall structure. *Endothyra* sp. illustrated by Marchant (1974) is close to our species in terms of type of its coiling, septa and structure of wall. The main characteristic features of *Endothyra* sp. illustrated in this study are also quite close to the *Endothyra* sp. illustrated by Dil (1975) and Conil (1976).

Stratigraphic Distribution:

The stratigraphic range of this species is from Lower Carboniferous to Upper Carboniferous. Our specimens were recovered through Upper Tournaisian (Loeblich and Tappan, 1988). According to Poty et al. (2006), *Endothyra* appeared in Ivorian (MFZ6) and survived into the Viséan.

Genus *Globoendothyra* Bogush and Yuferev, 1962

Type species: *Globoendothyra pseudoglobulus* Bogush and Yuferev, 1962

Globoendothyra sp.

Pl. 2, fig. 4

Description:

Test is enrolled. Coiling in the initial stage is streptospiral, later becoming nearly planispiral. Septa are oblique. The wall is calcareous and three layered. It has a distinct dark tectum, clear diaphanotheca and a dark inner layer. There are secondary deposits on the chamber floors and these secondary deposits forms thickenings in the chamber corners.

Dimensions (mm):

Diameter of test: 0.314

Thickness of wall: 0.011

Remarks:

This species is characterized by its type of coiling, three layered calcareous wall and secondary deposits forming thickenings in the chamber corners.

Stratigraphic Distribution:

The stratigraphic range of this species is Lower Carboniferous (Loeblich and Tappan, 1988). Our specimens were recovered also through Upper Tournaisian. According to Hance et al (1997), *Globoendothyra* is recognized in Association A of Hance et al (1997) in Ivorian and survived into the Viséan.

Genus *Inflatoendothyra* Lipina, 1955

Type species: *Endothyra inflata* Lipina, 1955

Inflatoendothyra inflata Lipina, 1955

Pl. 3, figs. 1-12

1955. *Inflatoendothyra inflata* Lipina, p. 55

1981. *Inflatoendothyra inflata*, Işık, p.18, pl. 1, fig. 2

Description:

Test is semi-involute and compressed laterally. Pheriphery is rounded and lobate. Coiling is streptospiral in early stage, later one or two whorls coil in one plane. Number of chambers in last whorl varies from seven to nine. Septa are straight, slightly oblique to the coiling. Wall is single layered, dark and granular.

Dimensions (mm):

Diameter of test: 0.227-0.291

Width of test: 0.154-0.172

Thickness of wall: 0.011-0.014

Remarks:

This species is named by Lipina (1955) but it was first described and illustrated by Lebedeva in 1954.

This species consists of three to five whorls and there are usually eight chambers in the final whorl in the studied sections. In our material, we have met several sections of this species. Some sections are nearly identical to the type specimens.

Stratigraphic Distribution:

The stratigraphic range of this species is Lower Carboniferous (Tournaisian-Visean) (Loeblich and Tappan, 1988). Our specimens were recovered also through Upper Tournaisian. According to Poty et al. (2006), this species appeared in Ivorian (MFZ5) and survived into the Visean.

Genus *Laxoendothyra* Brazhnikova and Vdovenko, 1972

Type species: *Endothyra parakonvensis* Lipina, 1955

Laxoendothyra ex. gr. *laxa* Conil and Lys, 1964

Pl. 4, figs. 1-4

1964. *Laxoendothyra* ex. gr. *laxa* Conil and Lys, p. 290

1972. *Endothyra* (*Laxoendothyra*) Brazhnikova and Vdovenko in Vdovenko; p. 106

1988. *Laxoendothyra* Brazhnikova and Vdovenko; Loeblich and Tappan, pl. 245, figs. 10-12

Description:

Test is small and enrolled. Initial volutions are streptospiral, later volutions are nearly planispiral. Axis of coiling changes abruptly in the inner volutions. Septa are short. Wall is calcareous, microgranular and double layered.

Dimensions (mm):

Diameter of test: 0.244-0.289

Thickness of wall: 0.012-0.015

Remarks:

This species illustrated in this study are mainly characterized by its type of coiling and its double layered calcareous wall. The axis of coiling changes abruptly in the inner volutions and followed with planispiral final volution.

Stratigraphic Distribution:

The stratigraphic range of *Laxoendothyra* ex gr. *laxa* is Lower Carboniferous (Tournaisian to Visean) (Loeblich and Tappan, 1988). According to Hance et al. (1997), Association B of Hance et al (1997) differs from Association A of Hance et al (1997) by the contemporaneous first occurrence of *Laxoendothyra* ex gr. *laxa* in Moliniacian. Moreover, *Laxoendothyra* ex gr. *laxa* becomes one of the most abundant species within the Association C of Hance et al. (1997) in the Visean. In Poty et al. (2006), *Laxoendothyra* ex gr. *laxa* appeared in Ivorian (MFZ7) and survived into the Visean (up to MFZ11).

Genus *Omphalotis* Shlykova, 1969

Type species: *Endothyra omphalota* Rauzer-Chernousova and Reitlinger, in
Rauzer- Chernousova and Fursenko, 1937

Omphalotis sp.

Pl. 2, figs. 9, 10

Description:

Test is enrolled, involute and biumbilicate. Early coiling is slightly variable (endothyroid), later coiling is planispiral. It has usually more than eight chambers in last whorl. Wall is calcareous and trilamellar. It has a dark and thin outer layer, a thick middle layer and a dark, thin inner layer. Septa are long and straight. Well developed secondary deposits are present in the final chamber and these secondary deposits located between septa and parallel to them.

Dimensions (mm):

Diameter of test: 0.567-0.584

Thickness of wall: 0.022

Remarks:

External shape of the test of this genus and the nature of coiling in inner whorls are very close to representatives of *Endothyra*, but distinctly differ from the latter by the complex wall structure and nature of secondary deposits.

The most characteristic features of this species are the distinct endothyroid stage of coiling, numerous chambers, and well developed secondary deposits.

Stratigraphic Distribution:

The stratigraphic range of *Omphalotis* sp. is Lower Carboniferous to Upper Carboniferous (Loeblich and Tappan, 1988). According to Poty et al. (2006), *Omphalotis* appears in the Ivorian (MFZ7) and survived into the Viséan.

Subfamily Endothyranopsinae Reytlinger, 1958

Genus *Latiendothyranopsis* Lipina, 1977

Type species: *Endothyra latispirali* var. *grandis* Lipina, 1955

Latiendothyranopsis sp.

Pl. 2, figs. 5-7

Description:

Test is large and slightly concave. Periphery is rounded. The early whorls are streptospiral. Later whorls are planispiral with rapidly enlarging whorl. Septa are long, thick and slightly oblique. Wall is thick, dark and microgranular.

Dimensions (mm):

Diameter of test: 0.486-0.529

Thickness of wall: 0.025-0.029

Remarks:

The characteristic features of this species are its rapidly growing coiling and its dark, thick wall. The specimens in this study are quite close to the species illustrated by Conil et al. (1989). Thick wall, long septa and large test are the main features recognized in the specimens of Conil et al. (1989) and these characteristic features of *Latiendothyranopsis* are also observed in our specimens. Moreover, coiling pattern of the illustrated species of Conil et al. (1989) resembles to coiling pattern of our specimens.

Stratigraphic Distribution:

The stratigraphic range of *Latiendothyranopsis* sp. is Lower Carboniferous. Our specimens were also recovered through Upper Tournaisian (Loeblich and Tappan, 1988). In Hance et al. (1997), *Latiendothyranopsis* is recognized in Ivorian (Association B) and defined as the most common Upper Tournaisian elements in Guangxi region within South China. According to Poty et al. (2006), the first appearance of *Endothyranopsis* is in Ivorian (MFZ5) and survived into Viséan.

SUPERFAMILY FUSULINACEA VON MOLLER, 1878

Family Eostaffellidae Mamet in Mamet, Mikhailoff and Mortelmans, 1970

Genus *Mediocris* Rozovskaya, 1961

Type species: *Eostafella mediocris* Vissarionova, 1948

Mediocris sp.

Pl. 2, fig. 4

Description:

Test is free and discoidal. Periphery is rounded. Test consists of three to four planispiral volutions. The chamber height gradually increases. Wall is calcareous and microgranular. Secondary deposits are present as lateral fills.

Dimensions (mm):

Diameter of test: 0.313

Width of test: 0.134

Thickness of wall: 0.011

Remarks:

The coiling of this species is usually planispiral but sometimes early whorls show some oscillations. Our specimens are quite close to forms illustrated by Dil (1976). *Mediocris* presented by Dil (1976) shows similar coiling pattern with our specimens and the secondary deposits are also interpreted in the specimens of Dil (1976). Moreover, the wall of his specimens are calcareous, like our specimens.

Stratigraphic Distribution:

The stratigraphic range of *Mediocris* sp. is from Lower Carboniferous to Upper Carboniferous (Loeblich and Tappan, 1988). According to Hance et al. (1997), the first appearance of *Mediocris* is in Moliniacian (Association B) and survived into the Viséan. Moreover, in Poty et al. (2006), *Mediocris* appeared in Ivorian (MFZ8) and survived into the Viséan.

Class Foraminifera d'Orbigny, 1826

Order Fusulinida Wedekind, 1937

Family Ozawainellidae Thompson and Foster, 1937

Genus *Eoparastaffella* Vdovenko, 1954

Type species: *Parastaffella (Eoparastaffella) simplex* Vdovenko, 1954

Eoparastaffella Morphotype 1 Vdovenko, 1954

Pl. 4, figs. 5-11

Description:

Test is involute to weakly evolute. Periphery in axial section is well rounded. Coiling is endothyroid. Basal deposits are present as pseudo-chomata which is more microgranular and darker than of the wall itself.

Dimensions (mm):

Diameter: 0.263-0.318

Width: 0.145-0.181

e/r : 0.285-0.375

Thickness of wall: 0.008-0.011

Remarks:

The genus *Eoparastaffella* was originally described by Vdovenko (1954) from the Donets Basin (Donbass) in the Ukraine. Genus *Eoparastaffella* is an essential component of Latest Tournaisian to Early Visean foraminiferal fauna. This genus is a key taxon not only for biostratigraphy, but also for understanding the underpinnings of the evolutionary relationships among certain foraminiferal groups during a time of significant environmental change (Devuyst and Kalvoda, 2007). *Eoparastaffella* Morphotype 1 differs from *Eoparastaffella* Morphotype 2 with its evolutionary stage. Hance et. al. (1997) introduced a criterion as e/r ratio to calibrate the evolution of *Eoparastaffella* where “e” is defined as the elevation of the outer and “r” is the radius of the largest interior circle. *Eoparastaffella* that has an e/r ratio <0.5 are termed as morphotype 1 species (Hance et. al., 1997), whereas specimens that have an e/r ratio >0.5 are termed as morphotype 2 species

(Hance et. al. 1997). In this study the e/r ratio for the samples consisting *Eoparastaffella* are less than 0.5, therefore, these species are *Eoparastaffella* M1.

Stratigraphic Distribution:

The stratigraphic range of *Eoparastaffella* M1 is from Late Tournaisian to late Moliniacian in Western Europe (e.g., Conil et al. 1991); from Late Tournaisian to Early Livian in Southern China (e.g., Wu and others, 1998; Devuyst and others, 2003), Late Tournaisian and Early Visean in Urals (e.g., Malakhova, 1975; Simonova, 1975; Postoyalko, 1975), Late Tournaisian to Warnantian (?); e.g., Poletaev and others, 1990; Vdovenko, 2001) in the Ukraine (Donbass), Late Tournaisian to Visean of Tengiz, Kazakhstan (Gibshman, 1997; Kulagina and others, 2003; Brenckle and Milkina, 2003), Late Tournaisian to Early Visean of northern Iran (Bozorgina, 1973; this work), Late Tournaisian to Early Visean of Belgium and northern France (Poty et al., 2006) and Early Visean of Turkey (e.g., Altner, 1981) (Devuyst and Kalvoda, 2007).

Eoparastaffella interiacta Vdovenko, 1971

Pl. 4, figs. 12-14

1971. *Eoparastaffella interiacta* Vdovenko in Vdovenko, pl. 1, fig. 18

1973. *Eoparastaffella interiacta* Vdovenko in Brazhnikova and Vdovenko, pl. 33, fig. 15

1971. *Endostaffella* sp. 1 in Michelsen, pl. 14, fig. 2

1975. *Eoparastaffella interiacta* Vdovenko in Postoyalko, pl. 13, fig. 11

1981. *Eoparastaffella interiacta* Vdovenko and others, pl. 6, fig. 1, 2

1986. *Eoparastaffella interiacta* Vdovenko in Vdovenko, pl. 5, fig. 6

2003. *Eoparastaffella interiacta* Vdovenko in Kulagina and others, pl. 1, figs. 9

2007. *Eoparastaffella interiacta* Devuyst and Kalvoda, p. 74, pl. 1, figs. 1- 10

Description:

Periphery of this species is well rounded and slightly pointed on lower side. Basal deposits are well developed as massive pseudochomata. Coiling is irregular in first two initial volutions and then becoming rapidly subplanispiral in the later volutions.

Dimensions (mm):

Diameter: 0.272-0.309

Width: 0.145-0.191

e/r : 0.327-0.412

Thickness of wall: 0.008-0.009

Remarks:

Eopasrataffella interiacta is differentiated from the other species of *Eoparastaffella* by its lower elevation of the last volutions and better developed and more massive pseudochomata. *Eoparastaffella interiacta* is characterized by a more slender morphology in axial section than other species of *Eoparastaffella*.

Stratigraphic Distribution:

Eopasrataffella interiacta is first recorded in the latest Tournaisian of the Gaduk section in the upper part of the range of *D. monilis* and *E. parvula* (Devuyst and Kalvoda, 2007). The stratigraphic range of this species is from Late Tournaisian to Viséan (Loeblich and Tappan, 1988). Our specimens were also recovered through Upper Tournaisian. According to Hance et al. (1997), *Eoparastaffella* is recognized in Association of B of Hance et al. (1997) in Late Tournaisian. In Poty et al. (2006), *Eoparastaffella* appeared in Ivorian (MFZ8) and survived into the Viséan.

CHAPTER 5

DISCUSSION AND CONCLUSION

In this study, a 27.01 m thick stratigraphic section was measured across the well exposed carbonate deposits of the Yarıcak Formation which is one of the fundamental lithostratigraphic units of the Upper Paleozoic of the Aladağ Unit. The Upper Tournaisian substage within the measured section was investigated based on the benthic foraminifers. In order to explain the sequence stratigraphic evolution of this carbonate succession, the cyclicity of meter-scale shallowing upward cycles of the measured section was defined and the response of benthic foraminifera to cyclicity was discussed.

A detailed systematic micropaleontological study was carried out based on the thin sections of benthic foraminifera obtained from the collected samples of the measured section. 21 different species were identified based on the taxonomic parameters including wall structure, wall composition, type of coiling, number of volutions, number of chambers, peripheral shape, position of septa and secondary deposits. According to the benthic foraminiferal assemblages, the measured section was divided into two biozones as Ut1 and Ut2 within the Upper Tournaisian. Ut1 Zone covers the lower parts of the measured section corresponding to the uppermost part of the Çityayla Member. Ut1 Zone consisting of limestones intercalated with shale layers is composed of the Upper Tournaisian foraminifers including *Earlandia* sp., *Lugtonia monilis*, *Granuliferella* sp. and *Endothyra* sp. Ut2 Zone corresponding to the lowermost part of the Mantar Tepe Member overlies the Ut1 Zone. Ut2 Zone is characterized by its diversity of Upper-Tournaisian fauna including *Earlandia* sp., *Lugtonia monilis*, *Tournayella* sp., *Tournayellina* sp., *Eoforschia moelleri*, *Septabrunsiina* sp., *Eblanaia* sp., *Eotextularia diversa*, *Palaeospiroplectamina mellina*, *Dainella* sp., *Granuliferella* sp., *Planoendothyra* sp., *Endothyra* sp., *Globoendothyra* sp.,

Inflatoendothyra sp., *Laxoendothyra* ex. gr. *laxa*, *Omphalotis* sp., *Latiendothyranopsis* sp., *Mediocris* sp., *Eoparastaffella* Morphotype 1, *Eoparastaffella interiacta*. The base of Ut2 Zone is defined by the entry of first primitive *Eoparastaffella* Morphotype 1 (Morphotype 1 of Hance and Muchez, 1995 and Hance, 1997). Association B of Hance et al. (1997) and MFZ8 Zone of Devuyt and Hance in Poty and others (2006) are also characterized by the first primitive *Eoparastaffella* M1 (Morphotype 1 of Hance & Muchez, 1995 and Hance, 1997). Therefore, Ut2 Zone of Upper-Tournaisian age can be considered globally comprising the first occurrence of *Eoparastaffella* M1 (Morphotype 1 of Hance and Muchez, 1995 and Hance, 1997).

In order to construct a sequence stratigraphic framework and appreciate depositional environmental changes, microfacies studies were carried out. The studied section is mainly composed of subtidal carbonates interclated with shales and through the measured section 7 microfacies types were identified. These microfacies types are mudstone to sandstone microfacies (MS), silty peloidal mudstone microfacies (MS-P1), silty peloidal packstone microfacies (P1), peloidal and crinoidal wackestone-packstone microfacies (P1-P2), crinoidal wackestone-packstone microfacies (P2), crinoidal and foraminiferal packstone-grainstone microfacies (P2-P3), foraminiferal packstone-grainstone microfacies (P3). The vertical evolution of these microfacies represents the subtidal shallowing upward cycles. The measured section contains 25 shallowing-upward meter scale cycles show low and high energy facies according to their microfacies textures. Depending on the stacking patterns of the microfacies, two fundamental types, A and B, were recognized in this study. 4 subtypes of A-type cycle were defined as A1, A2, A3 and A4. A1 type cycles generally start at the base with mudstone to sandstone microfacies and are capped by the sandy peloidal packstone microfacies. A2 type cycles are generally characterized by silty peloidal packstone microfacies overlain by the crinoidal wackestone-packstone microfacies. A3 type cycles generally start at the base with mudstone to sandstone microfacies and are capped by the silty-peloidal packstone microfacies and ends with the peloidal and crinoidal packstone microfacies. A4 type cycles generally

are characterized by mudstone to sandstone microfacies overlain by crinoidal and foraminiferal packstone grainstone microfacies. Two subtypes of B type cycles, namely B1 and B2, are recognized. B1 type cycles are usually composed of silty peloidal packstone microfacies at the bottom and generally capped by crinoidal wackestone-packstone microfacies. These two microfacies are generally overlain by crinoidal and foraminiferal packstone-grainstone microfacies. The cycle ends with the foraminiferal grainstone-packstone microfacies. B2 type cycles are generally characterized by crinoidal wackestone-packstone microfacies at its base and followed upwards by the crinoidal and foraminiferal packstone microfacies and this type of cycle ends with foraminiferal grainstone-packstone microfacies. Stacking patterns of the meter scale cycles were used to define large scale sequences, system tracts and long term sea-level fluctuations. Since there is no exposure surface and erosional boundary, the vertical evolution of the microfacies and the interaction of the cycle types within the measured section are investigated to define the system tracts. Within the measured section, two main sequences and two sequence boundaries have been identified. A-type cycles dominated by sandstone and peloidal-crinoidal packstone facies are usually interpreted as transgressive system tracts since the vertical evolution of these cycles implies a change to higher energy conditions. B-type cycles dominated by crinoidal and foraminiferal grainstone-packstone facies are interpreted as highstand system tract in the level corresponding to samples from TD-81 to TD-100 where the environment has changed into higher energy conditions (Figure 3.10). This highstand system tract is followed by a transgressive system tract in the level corresponding to samples from TD-101 to TD-114 (Figure 3.10). Finally, a highstand system tract is defined in the level corresponding to samples from TD-115 to TD-129. Although the most important criteria for recognizing sequence boundaries are incised valleys and related unconformities, these criteria are difficult to trace on carbonate platforms. In the level corresponding to the sample TD-52 consists of mudstone to sandstone facies which overlies the foraminiferal packstone facies interpreted as sequence boundary. The second sequence boundary is interpreted in the level corresponding to top of the sample

TD-100 where the investigated section represents a significant change in sedimentation.

In order to understand the lateral relationship of meter scale cycles, a composite model illustrating the microfacies distribution of Upper Tournaisian beds in the investigated section is constructed. Since the types of cycles are defined based on the stacking patterns of microfacies, the cycle types are considered as major criteria while constructing the facies model. All types of cycles can be recognized within the composite model illustrating the microfacies distribution of Tournaisian beds in the investigated section with the exception of A4-type cycle which requires a rather abrupt facies change model. This composited model is a summary of the depositional environment model in which our stratigraphic section formed.

Response of benthic foraminifera to carbonate cyclicity in shallow subtidal carbonate deposit is investigated within the measured section. Since foraminifers are very sensitive to sea level changes, the abundance of foraminifera displays a good response to sedimentary cyclicity. The general trend obtained from the counting study is that the bottom of the cycles consists of less benthic foraminifera whereas the top of the cycles contains abundant benthic foraminifera within the cycle types in the measured section. The sequence boundaries within the measured section can easily be recognized by the evidence of decrease in foraminiferal assemblages. The number of foraminifera decreases abruptly at the levels corresponding to the sequence boundaries (Figure 3.10).

In order to apply a worldwide sequence stratigraphic correlation, the meter scale cycles of this study were compared with the relative sea-level fluctuations of South China and Western European Platform and Moscow Syncline. The sequence stratigraphy of the Tournaisian-Visean strata in South China was constructed by Hance et al. (1997). Both the biostratigraphical and the sedimentological data of these studied sections were used to construct the sequence stratigraphical framework in South China by Hance et al. (1997). To apply a sequence stratigraphical correlation between the investigated sections in

the Early Carboniferous carbonate platform of South China (Hance et al., 1997) and the studied Upper-Tournaisian carbonate succession within the measured section, a major key surface has been identified. This key surface is interpreted as the sequence boundary that is defined in the level corresponding to unit 30 within the Yajiao River section of Hance et al. (1997) where a significant change in sedimentation pattern was observed (Figure 3.13). This sequence boundary is interpreted in the Association B of Hance et al. (1997) (Figure 3.13) which is the equivalent of Ut2 zone in our study (Table 2.1). In the Ut2 zone of this study, a sequence boundary (SB2) has also been interpreted (TD-100). These two sequence boundaries most probably are equivalent to each other. Moreover, a highstand system tract is interpreted below the sequence boundary in Yajiao section of Hance et al (1997) and the equivalent highstand system tract under the SB2 has also been interpreted in our study (Figure 3.9). A major drop in relative sea level near the end of the Tournaisian has been recognized worldwide. Since the global inprints of these sea level changes are recognized in the studied Upper-Tournaisian carbonate succession, this study can be considered globally.

The Carboniferous Namur-Dinant Basin has been studied extensively since it is the type area for the Tournaisian and Viséan stages. Consequently, outcrops in Western European Platform have been used as worldwide references for Mississippian subsystem (Lower Carboniferous). Poty et al. (2006) carried out a detailed study in Belgium and Northern France. They used both biostratigraphical and sedimentological data to construct a sequence stratigraphical approach. The biostratigraphical data of Poty et al. (2006) is based on mainly on foraminifer associations. Based on foraminiferal assemblage and diversity of foraminifers, they identified sixteen Mississippian Foraminiferal Zones (MFZ1-MFZ16). The Mississippian Foraminiferal Zones including MFZ5, MFZ6, MFZ7 and MFZ8 were identified within the Upper-Tournaisian substage. Poty et al. (2006) reconstruct a sketch combining the foraminiferal zones of Poty et al (2006) and third-order sequences of Hance, Poty and Devuyst (2001). According to this correlation, Poty et al. (2006) observed a sequence boundary within the MFZ5 which is equivalent of Ut1 zone of this study and a second sequence boundary within the MFZ8 which

is the equivalent of Ut2 zone of this study (Table 3.2). Within Upper Tournaisian we recognized two sequence boundary named as SB1 and SB2 (Table 3.2). SB1 is identified in Ut1 zone whereas SB2 is identified within Ut2 zone. Therefore, the SB1 of this study corresponds to the sequence boundary observed bottom of sequence named 4 of Poty et al. (2006) and the SB2 is equivalent of the sequence boundary observed top of the sequence named 4 of Poty et al. (2006) (Table 3.2).

The time-calibrated sea level curves provide a very useful tool for detailed stratigraphic correlations. Alekseev et al. (1996) developed a relative sea-level curve for the Devonian and Carboniferous of the Moscow Syncline, using the Harland et al. (1990) geological times scale since the principles of construction and design of the curves of Aisenverg et al. (1985, 1986) are not compatible with modern sea-level curves. According to Alekseev et al. (1996), an Early Tournaisian transgression covered almost the entire Moscow Syncline with normal marine waters. The curve for the Carboniferous of the Moscow syncline is very similar to the marine onlap curve by Ross and Ross (1988). When the sequence boundaries interpreted within the shallowing upward cycles in this study are correlated with the sea level curves of Alekseev et al. (1996), the same imprints of sea level fluctuations are observed within the two study area. The sequence boundary SB 1 of this study (sample TD-52) is approximately equivalent to sequence boundary recognized in the Early Kizelian of Alekseev et al. (1996) and SB2 of this study (TD-101) is approximately equivalent to sequence boundary recognized in the early Kosvian of Alekseev et al. (1996) (Figure 3.14). Since the SB1 and SB2 of this study have equivalent sequence boundaries in the studied Upper Tournaisian succession in Western European Platform of Poty et al. (2006) (Figure 3.14), the Tournaisian transgression is also recognized in Western European Platform like in the Central Taurides with indicating a global sense when compared with the sea level curve for the Carboniferous of Moscow Syncline of Alekseev et al. (1996) and marine onlap curve of Ross and Ross (1988).

This study delineated the Upper Tournaisian substage within the well-exposed Carboniferous Aladağ Unit which is one of the tectonic units of the Central Taurides and showed that the Upper Tournaisian substage has been recorded in a similar pattern around the world in terms of benthic foraminiferal assemblages and sea level changes.

REFERENCES

- Aisenverg, D. Ye., Poletaev, V. I., Makharov, I. A., Makhlina, M. Kh. and Schebakov, O. A., 1986. On the changes of Carboniferous sea-level in East-European Platform, Donets Basin and Urals. *Geol J.*, 46, 35 – 42. (In Russian).
- Aisenverg, D. Ye., Poletaev, V. I., Makhlina, M. Kh. and Schebakov, O. A., 1985. Carboniferous sea level changes on the East-European Platform. In: *Dixieme Congress International de Stratigraphie et de Géologie du Carbonifere*, Madrid, 12-17 september, 1983. *Compre Rendu*, 4, 65 – 70.
- Alekseev, A. S., Kononova, L. I. and Nikishin, A. M., 1996. The Devonian and Carboniferous of the Moscow Syneclise (Russian Platform): stratigraphy and sea-level changes. *Tectonophysics*, 268, 149 – 168.
- Algeo, T. J., and Rich, M., 1992. Bangor Limestone: Depositional environments and cyclicity on a Late Mississippian carbonate shelf. *S. Southeastern Geology*. Vol. 32, no.3, 143-162.
- Altner D., 1981. *Recherches stratigraphiques et micropaleontologiques dans le Taurus Oriental au NW'de Pınarbaşı (Turquie)*. These Universite de Geneve, No. 2005, Geneve, 450 p.
- Altner D., 1984. Upper Permian foraminiferal biostratigraphy in some localities of the Taurus Belt. In: Tekeli O. and Göncüoğlu M.C. (ed.), *Geology of the Taurus Belt*. Mineral Research and Exploration Institute of Turkey Publication, 255 – 268.
- Altner, D. and Özgül, N., 2001. Paleoforams 2001; International Conference on Paleozoic Benthic Foraminifera; Carboniferous and Permian of the

allochthonous terranes of the Central Tauride Belt, Southern Turkey. Guide Book, 35 p.

Altner, D., Özkan-Altner, S. and Koçyiğit, A., 2000. Late Permian foraminiferal biofacies in Turkey. In: E. Bozkurt, J. A., Winchester and J. D. A., Piper (eds.), Tectonics and magmatism in Turkey and the surrounding area. Geological Society, London, Special publication, 173, 83-96.

Atakul, A., 2006. Lower-Middle Carboniferous boundary in Central Taurides, Turkey (Hadim Area): Paleontological and sequence stratigraphic approach. M. S. Thesis, Middle East Technical University, Ankara, Turkey, 202 pp.

Blumenthal, M. M., 1944. Bozkır Güneyinde Toros Sıradağlarının Serisi ve Yapısı. İstanbul Üniversitesi Fen Fakültesi Mec, V. B. 9, 95-125.

Blumenthal, M. M., 1947. Beyşehir-Seydişehir Hinterlandındaki Toros Dağlarının jeolojisi. Maden Tetkik Arama Ens., Ankara, seri D, 2, 242p.

Blumenthal, M. M., 1951. Batı Toroslarda Alanya Ard Ülkesinde Jeolojik araştırmalar. Maden Tetkik Arama Enst., Ankara, seri D, 5, 194p.

Blumenthal, M. M., 1956. Karaman Konya Havzası Güneybatısında Toros Kenar Silsileleri ve Şist Radyolarit Formasyonu Stratigrafi Meselesi. Maden Tetkik Arama Enst. Derg., C.48 p. 1- 36.

Bogush, O. I and Yuferev, O. V., 1962. Foraminifera and stratigraphy of the Carboniferous deposits of Karatau and Talas Alatau. Institut Geologii Geofiziki, Akademiya Nauk SSSR, Sibirskow Otdelenie, 1-234 (In Russian).

Bozorgnia, F., 1973. Paleozoic foraminiferal biostratigraphy of central and East Alborz Mountains, Iran: National Iranian Oil Company. Geological Laboratories Publication, No. 4, 185 p.

- Bozorgnia F. and Vdovenko, M. V., 1973. Early Visean foraminifers of Ukraine, Naukova Dumka, Kiev, 296 p. (in Ukrainian).
- Brazhnikova, N. E., 1962. *Quasiendothyra* and related forms from the Lower Carboniferous of the Donets Basin and other regions of Ukraine: Akademiya Nauk Ukrainskoy SSSR, Trudy Instituta Geologicheskikh Nauk, Seriya Stratigrafii i Paleontologii, 44, 3-48 (in Russian).
- Brady, H. B., 1876. A monograph of Carboniferous and Permian foraminifers (the genus *Fusulina* excepted). Paleontographical Society 30, 1-166.
- Brady, H. B., 1884. Report on the foraminifera dredged by H. M. S. Challenger, during the years 1873-1876. Report on the Scientific Results of the Voyage of the H. M. S. Challenger during the years 1873-1876. 9, 819 pp., 115 pls.
- Brenckle, P. L. and Milkina, N. V., 2003. Foraminiferal timing of carbonate deposition on the Late Devonian (Femennian) – Middle Pennsylvanian (Bashkirian) Tengiz Platform, Kazakhstan. Rivista Italiana di Paleontologia Stratigrafia, v. 109, no. 2, p. 131-158.
- Brunn, J. H., Dumont, J.F., Graciansky, P.C., Gutnic, M., Juteau, T., Marcoux, J., Monod, O. and Poisson, A., 1971. Outline of the Geology of the Geology of the Western Taurides. In: Geology and History of Turkey, Campbell (A.S. Ed.), Pet. Expl., Soci. of Libya, Tripoli, 225- 255.
- Chernysheva, N., 1948. Nekotororye novye vidyi foraminifer iz Vizeyskogo yarusa Makarovskogo raiona (Yuzhnyi Ural). (Some new species of Visean foraminifers from the Makarov area (southern Urals)). Akademiya Nauk SSSR, Trudy Instituta Geologicheskikh Nauk, 62, geologiskaya seriya 19, 246-250 (in Russian).
- Conil, R., 1976. Contribution a l'Etude des foraminiferes du Dinantien de l'Irlande. Annales de la Societe Geologique de Belgique, 99, 467-479.

- Conil, R., 1977. Contribution a l'étude des foraminifères du Dinantien de l'Irlande. *Annales de la Société Géologique de Belgique*, 99, 467-479.
- Conil, R. and Lees, A., 1974. Les transgressions Viséennes dans l'Ouest de l'Irlande. *Annales de la Société Géologique de Belgique*, 97, 463-484.
- Conil, R. and Lys, M., 1964. Matériaux pour l'Étude micropaléontologique du Dinantien de la Belgique et de la France (Avesnois). *Mémoires de l'Institut de Géologie de l'Université de Louvain*, 23, 1-296.
- Conil, R. and Lys, M., 1967. Aperçu sur les Associations de Foraminifères Endothyroïdes du Dinantien de la Belgique. *Ann. Soc. Géologique de Belgique*, T. 90, 4, 395-412.
- Conil, R. and Lys, M., 1968. Utilisation stratigraphique des Foraminifères du Dinantien. *Annales de la Société Géologique de Belgique*, 91, 491- 558.
- Conil, R. and Lys, M., 1977, Les transgressions Dinantiennes et leur influence sur la dispersion et l'Évolution des Foraminifères. *Mémoires de l'Institut Géologique de l'Université de Louvain*, 29, 9- 55.
- Conil, R., Groessens, E., Hibo, D., Laoux, M., Lees, A. and Poty, E., 1988. The Tournaisian-Viséan boundary in the type area. Guidebook, Field meeting, Paleontological Association Carboniferous Group, 22-25 April 1988. Institut de Géologie, Université Catholique de Louvain, Louvain-la-Neuve, 2 vols, 145 pp.
- Conil, R., Groessens, E., Laloux, M. and Poty, E. 1989. La limite Tournaisian/Viséen dans la région type. *Annales de la Société Géologique de Belgique*, 122, 177- 189.
- Conil, R., Longerstaey, P. J., Laloux, M., Poty, E., and Tourneur, F., 1991. Carboniferous guide foraminifers, corals and conodonts in the Franco-Belgian and Campine Basins. *Courier Forschungsinstitut Senckenberg*, 130, 5-30.

- Cozar, P. and Vachard, D., 2001. Dainellinae subfam. nov. (Foraminiferida du Carbonifere inferieur), revision et nouveaux taxons. *Geobios*, 34, 505-526.
- Cummings, R. H., 1955. New genera of foraminifers from the British Lower Carboniferous. *Journal of the Washington Academy of Sciences*, 45, 1-8.
- D'Orbigny, A. D., 1826. Tableau methodique de la Classe des Cephalopodes. *Annales des Sciences Naturelles*, Paris, ser. 1, v. 7, p. 245-314.
- Dain, L. G., and L. Grozdilova, 1953. Iskopaemye foraminifery SSSR: Turneiellidy i Arkhedistsidy. (Fossil Foraminifers of the USSR, Tourneiellidy i Arkhediscidae), *Trudy Vsesesoyuznogo Neftyanogo Nauchno-issledovatel'skogo Geologorazvedochnogo Instituta (VNIGRI)*, n. Ser. 74: 1-115.
- Demirtaşlı, E., 1984. Stratigraphy and tectonic of the area between Silifke and Anamur, Central Taurus Mountains. In: Tekeli O. and Göncüoğlu M.C. (Ed.), *Geology of the Taurus Belt. Mineral Research and Exploraion Institute of Turkey Publication*, 101 – 123.
- Devuyst, F. X., Hance, L., and Poty, E., 2006. Moliniacian, in Dejonghe, L. (ed.), *Current status of chronostratigraphic units named from Belgium and adjacent areas. Geologica Belgica*, v. 9, no. 1-2, p. 123-131.
- Devuyst, F. X. and Hance, L., 2003. Early evolution of the genus *Eoparastaffella* (foraminifer), a high-resolution biostratigraphical tool for the Tournaisian-Visean boundary: XVth International Congress on Carboniferous and Permian Stratigraphy, Utrecht, August 2003, Abstracts volume, 123-124.
- Devuyst, F. X., Hance, L., Hou, H., Wu, X., Tian, S., Coen, M. and Sevastopula, G. 2003. A proposed global stratotype section and point for the base of the Visean Stage (Carboniferous): the Pengchong section, Guangxi, South China. *Episodes*, 26 (2), 105-15.

- Devuyst, F. X. and Kalvoda, J., 2007. Early evolution of the genus *Eoparastaffella* (Foraminifera) in Eurasia: the *interiacta* group and related forms. Late Tournaisian to Early Visean. *Journal of Foraminiferal Research*, v.37, no. 1, p. 69-89.
- Dil, N., 1975. Etude micropaleontologique du Dinantien de Gökgöl et Kokaksu (Turquie). *Annales de la Societe Geologique de Belgique*, 98, 213-228.
- Dil, N., 1976. Assemblages caracteristiques de foraminiferes du Devonien superieur et du Dinantien de Turquie (Bassin Carbonifere de Zonguldak). *Annales de la Societe Geologique de Belgique*, 99, 373-400.
- Dunham, R. J. 1962. Classification of carbonate rocks according to depositional texture, in Ham, W. E. Ed. *Classification of carbonate rocks: American Association of Petroleum Geologists Memoir 1*, p. 108-121.
- Ellis, B. and Messina, A., 1941-2004. *Catalogue of Micropaleontology, Catalogue of Foraminifera*. American Museum of Natural History, Special Publication.
- Flügel, E., 2004. *Microfacies of carbonate rocks: analysis, interpretation and application*. Springer, 976 p.
- Gallagher, S. J., 1998. Controls on the distribution of calcareous foraminifera in the Lower Carboniferous of Ireland. *Marine Micropaleontology*, 34, 187-211.
- Gibshman, N. B., 1997. Foraminiferal zonation and paleogeography of Early Carboniferous PreCaspian depression (West Kazakhstan), in Ross, C. A., Ross, J. R. P., and Brenckle, P. L. (eds.), *Late Paleozoic Foraminifera: Their biostratigraphy, evolution, and paleoecology and the Mid-Carboniferous boundary*. Cushman Foundation for Foraminiferal Research, Special Publication, 36, 47-50.

- Goldhammer, R. K., Dunn, P. A. and Hardie, L. A., 1990. Depositional cycles, composite sea-level changes, cycle stacking patterns, and their hierarchy of stratigraphic forcing: examples from Alpine Triassic platform carbonates. *Geol. Soc. of Am. Bull.*, 102, 663.
- Gutnic, M., Monod, O., Poisson, A. and Dumont, J. F., 1979. *Geologie des Taurides Occidentals (Turquie)*. *Mem. Soci. Geol., France*, 58, 109p.
- Hance, L., 1997. *Eoparastaffella*, its evolutionary pattern and biostratigraphic potential in C. A. Ross, J. R. P. Ross, and P. L. Brenckle, editors, *Late Paleozoic Foraminifera; thier biostratigraphy, evolution, and paleoecology; and the Mid Carboniferous boundary*. Cushman Foundation for Foraminiferal Research, Special Publication, 36 p.
- Hance, L., and Muchez, P., 1995. Study of the Tournaisian-Visean transitional strata in South China (Guangxi). XIII International Congress on Carboniferous and Permian, Krakow, Poland, 1995, Abstracts, 51 p.
- Hance, L., Laloux, M., Muchez, P., Groessens, E., Peeters, C. and Poty, E., 1994. An outline of the Moliniacian (Upper Tournaisian – Lower Visean) in Southern Belgium. Introduction to a field excursion in honour of Prof. Dr. Raphael Conil 12 October 1991. *Memoires de l'Institut geologique de l'Universite de Louvain* 35, 27- 50.
- Hance, L., Muchez, P. H., Hou, H. F. and Wu, X. 1997. Biostratigraphy, sedimentology, and sequence stratigraphy of the Tournaisian – Visean transitional strata in South China (Guangxi). *Geological Journal*, 32, 337-357.
- Hance, L., Poty, E. and Devuyst, F. X. 2001. Stratigraphie sequentielle du Dinantien type (Belgique) et correlation avec le Nord de la France (Boulonnais, Avesnois). *Bulletin de la Societe Geologique de France*, 172 (4), 411-26.

- Harland, W. B., Armstrong, R. L., Cox, A.V., Craig, L. E., Smith, A.G. and Smith, D. G., 1990. A Geologic Time Scale 1989. Cambridge University Press, Cambridge, 236 pp.
- Işık, A., 1981. Foraminiferal biostratigraphy of the Nohutluk tepe Lower Carboniferous sequence (Aladağ Region, Eastern Taurus Mountains). Bulletin of Geological Society of Turkey, V. 24, 79-84.
- Kalvoda, J. and Ondrackova, L., 1999. Lower Carboniferous subdivision and paleogeography: XIV International Congress on Carboniferous and Permian, Pander Society and Canadian Paleontology Conference, Abstracts, 71 p.
- Kalvoda, J., Devuyst, F. X., Mergl, M., and Rak, S., 2005. The Tournaisian-Visean boundary and evolutionary trends in the *Eoparastaffella interiacta* group in Mokra near Brno (Czech Republic). SCCS Mid-congress Field-Conference, May 2005, Liege (no page number).
- Kobayashi, F. and Altner, D., 2008. Late Carboniferous and Early Permian Fusulinoideans in the Central Taurides, Turkey: Biostratigraphy, faunal composition and comparison. Journal of Foraminiferal Research, v. 38, no. 1, p. 59-73.
- Kulagina, E. I., Gibshman, N. B. and Pazukhin, V. N. 2003. Foraminiferal zonal standard for the Lower Carboniferous of Russia and its correlation with the conodont zonation. Rivista Italiana di Paleontologia e Stratigrafia 109(2), 173-85.
- Lebedeva, N. S. 1954. Foraminifery nizhnego kurbona Kuznetskogo bassenya. Mikrofauna SSSR, Sbornik, 7, Vsesoyuznogo Neftyanogo Nauchno-Issledevatel'skogo Geologorazvedochnogo Institut, Trudy, 81, 237-295.
- Lipina, O. A., 1948. Tekstulyariidy verkhnei chasti nizhnego Karbona Yuzhnogo Kryla Podmoskovnogo Basseina. (Textulariids of the upper part of Early Carboniferous from southern margin of Submoscow Basin). Akademiya

- Nauk SSSR, Trudy Instituta Geologicheskikh Nauk 62, geologicheskaya, 19, 196-215 (in Russian).
- Lipina, O. A., 1955. Foraminifera of the Tournaisian and Upper Devonian of the Volga-Ural region and western slopes of the Middle Urals, U.S.S.R.: Acad. Nauk. U.S.S.R. Inst. Geol. Nauk., Trudy, Vypusk 163 (Geol. Ser., 70), 55.
- Lipina, O. A., 1965. Sistematika Turneyellid, (Systematics of the Tournayellidae). Akad. Nauk SSSR, Geologicheskii Institut, Moscow, 130, 1-115.
- Lipina, O. A., 1977. On the systematics and evolution of Lower Carboniferous endothyrids: Akademiya Nauk SSSR, Geologicheskii Institut, Voprosy Mikropaleontologii, 20, 3-20 (in Russian).
- Loeblich, A.R. and Tappan, H., 1984. Some new proteaceous and agglutinated genera of Foraminiferida. *Journal of Paleontology*, 58, 1158-1163.
- Loeblich, A.R. and Tappan, H., 1988. Foraminiferal genera and their classification. Von Nostrand Reinhold Company, New York, 2 v, 970 p.
- Malakhova, N. P., 1956. Foraminifers of the Upper Tournaisian on the western slope of the northern and central Urals. Akademiya Nauk SSSR, Ural'skii Filial, Trudy Gorno-Geologicheskogo Instituta, Vypusk 24, Sbornik po Voprosam Stratigrafi, 3, 72-155 (in Russian).
- Malakhova, N. P., 1963. New foraminiferal species from Lower Visean sediments of the Urals. *Paleontologicheskii Zhurnal*, 4, 110-112 (in Russian).
- Malakhova, N. P., 1975. Foraminifers of the Lower Visean of the eastern slopes of the southern Urals. *Trudy Instituta Geologii i Geokhimii*, 112, 5-45 (in Russian).
- Malpica, R. 1973. E'tude micropaleontologique du Viseen de Chokier. *Annales de la Societe Geologique de Belgique*, 96, 219-232.

- Mamet, B. L., 1970. Carbonate microfacies of the Windsor Group (Carboniferous), Nova Scotia and New Brunswick. *Geol. Surv. Can.*, 1-23; Protozoa, article 4.
- Mamet, B., Mikhailoff, N. and Mortelmans, G., 1970. La stratigraphie du Tournaisien et du Viséen inferieur de Landelies. Comparisons avec les coupes du Tournaisis et du bord nord du synclinal de Namur. *Memoires de la Societe belge de Geologie*, 9, 1-81.
- Marchant, T. R., 1974. Preliminary note on the micropalaentology of the Dinantian Dublin Basin, Ireland. *Annales de la Societe Geologique de Belgique*, 97, 447-461.
- McKee, E. D. and Gutschick, R. C., 1969. History of Redvfall limestone Arizona. *Mem. Geol. Soc. America*, 114, 711-726
- Michelsen, O., 1971. Lower Carboniferous foraminiferal fauna of the Boring Oslev No 1. Island of Falster, Denmark. *Geological survey of Denmark, Series II*, 98, 1-87.
- Monod, O., 1967. Presence d'une faune Ordovicienne dans les schistes de Seydişehir ala base des calcaries du Taurus occidental. *MTA Bul.* 69, 79-89.
- Monod, O., 1977. *Researches geologiques Dans le Taurus occidental au sud de Beyşehir (Turquie): These, Universite Paris XI Orday*, 422 p.
- Möller, V., 1878. Die spiral-gwunden foraminiferen des russischen Kohlenkalkes. *Mem. l'Acad. Imp. Sci. St. Petersburg*, 7, 1-131.
- Osleger, D. and Read, J. F., 1991. Relation of eustacy to stacking patterns of meter-scale Carbonate cycles, Late Cambrian, U.S.A. *Journal of Sed. Pet.*, 61 (7), 1225-1252.

- Özgül, N., 1971. Batı Torosların kuzey kesiminin yapısal gelişiminde blok hareketlerin önemi. Türkiye Jeoloji Kur. Bül., 14, 75- 87.
- Özgül, N., 1976. Toroslar'ın bazı temel jeolojik özellikleri. Türkiye Jeol. Kur. Bül., 19, 65- 78.
- Özgül, N., 1984. Stratigraphy and tectonic evolution of the Central Taurides; In Tekeli O., and Göncüoğlu M.C. (eds.), Geology of Taurus Belt. Mineral Research and Exploration Institute of Turkey Publication, 77- 90.
- Özgül, N., 1997. Stratigraphy of the tectono-stratigraphic units in the region Bozkır-Hadim-Taskent (northern central Taurides). Mineral Research and Exploration Institute of Turkey (MTA) Bulletin, 119, 113-174 (in Turkish with English abstract).
- Özgül, N. and Gedik, İ., 1973. Orta Toroslar'da Alt Paleozoyik yaşta Çaltepe Kireçtaşı ve Seydişehir Formasyonu'nun stratigrafisi ve konodont faunası hakkında yeni bilgiler. Türkiye Jeoloji Kurumu Bülteni, 16, 39- 52.
- Peynircioğlu, A., 2005. Micropaleontological analysis and facies evolution across the Tournaisian-Visean boundary in Aladağ Unit (Central Taurides, Turkey). M. Sc. Thesis, Middle East Technical University, Ankara, Turkey, 76 pp.
- Phillips, J. 1846. On the remains of microscopic animals in the rocks of Yorkshire. Geol. Polytech. Soc., West Riding, Yorkshire, 2, 274-285.
- Plummer, H. J., 1930. Calcareous foraminifera in the Brownwood shale near Bridgeport, Texas. Texas Univ. Bull. (Bur. Econ. Geol.), 3019, 5-21.
- Poletaev, V. I., Brazhnikova, N. E., Vasilyuk, N. P., and Vdovenko, M. V., 1990. Local zones and major Lower Carboniferous biostratigraphic boundaries of the Donets Basin (Donbass), Ukraine, U.S.S.R. Courier Forschungstintstitut Senckenberg, 130, 47-59.

- Postoyalko, M. V., 1975. Foraminifers and stratigraphy of the EarlyVisean of the western slope of the Urals. *Trudy Instituta Geologii i Geokhimii*, 112, 110-143 (in Russian).
- Poty, E., Devuyt, F. X., and Hance, L., 2006. Upper Devonian and Mississippian foraminiferal and rugose coral zonations of Belgium and northern France, a tool for Eurasian correlations. *Geological Magazine*, v. 143, no. 6, p. 829-857.
- Rauser-Chernousova, D. M. and Fursenko, A. V. 1937. Determination of foraminifera from the oil-producing regions of the USSR. *Glavnova Redaktsya Gorno-Toplivnoi Literaturny Leningrad, Moskoca*, 315 p. (in Russian).
- Reitlinger, E. A. 1950. Foraminifera from Middle Carboniferous deposits of the central part of the Russian Platform (excluding family Fusulinidae). *Akademiya Nauk SSSR. Trudy Institut Geologicheskii Nauk*, 126 (47), 1-127 (in Russian).
- Reitlinger, E. A. 1958. K voprosy systematiki i filogenii nadsemeystva Endothyrida. *Voprosy Mikropaleontologii*, no. 2, *Akademiya Nauk SSSR, Geol.* 53-73.
- Reitlinger, E. A. 1959. Foraminifery progranichnykh sloev devona i karbona zapadnoy chasti tsentralnogo Kazakhstana. *Doklady Akademiya Nauk SSSR*, 659-662.
- Ross, C. A. and Ross, J. R. P., 1988. Late Paleozoic transgressive-regressive deposition. In: C. K. Wilgus, B. S. Hastings, C. G. St. C. Kendall, H.
- Rozovskaya, S. E. 1961. On the systematics of the families Endothyridae and Ozawainellidae. *Paleontologicheskii Zhurnal*, 3, 19-21 (Russian).

- Posamentier, C. A. Ross and J. C. Van Wagoner (Editors), *Sea-Level Changes: An Integrative Approach*. Soc. Econ. Paleontol. Mineral., Spec. Publ., 42: 227-243.
- Rhumbler, L., 1895. Entwurf eines natürlichen Systems der Thalamorphoren. K. Ges. Wiss. Göttingen, M. P. Kl., Nachr., 1, 51-98.
- Segura, L. R., 1973. Revision des foraminifères de la coupe type de Sovet. *Annales de la Société Géologique de Belgique*, 96, 223-251.
- Shlykova, T. I., 1969. Novy rod rannekamennougol'nykh foraminifer (New Early Carboniferous genus), *Voprosy Mikropaleontologii*, 12, 47-50.
- Simonova, Z. G., 1975. Gumbei and Ust'Grekhov foraminiferal complexes of the Magnitogorsk Synclinorium. *Trudy Instituta Geologii i Geokhimii*, 112, 177-209 (in Russian).
- Şen, A., 2002. Meter-scale subtidal cycles in the Middle Carboniferous Carbonates of Central Taurides, Southern Turkey and Response of Fusulinacean Foraminifers to Sedimentary Cyclicity. M. Sc. Thesis, Middle East Technical University, Ankara Turkey, 110 pp.
- Thompson, M. L. and Foster, C. L., 1937. Middle Permian Fusulinids from Szechuan, China. *Journal of Paleontology*, vol. 11, no. 2, pp. 126-144.
- Van Wagoner, J. C., Posamentier, H. W., Mithchum, R. M., Vail, P. R., Sarg, J. F., Loutit, T. S. and Hardenbol, J., 1988. An overview of the fundamentals of sequence stratigraphy and key definitions. *Sea-Level Changes-An Integrated Approach*, The Society of Economic Paleontologist and Mineralogist, Special Publication, 42, 39-45.
- Vdovenko, M. V., 1954. Some new foraminiferal species from lower Viséan deposits of Donets Basin. *Geologichnyi Zbirnik*, 5, 63-76 (in Ukrainian).

- Vdovenko, M. V., 1964. Evolution of the genus *Eoparastaffella* – *Pseudoendothyra*. Akademiia Nauk Ukrainskoi SSR. Trudy Institut Geologii Nauk, Serii stratigrafiia i paleontologiiia, 48, 16-30 (in Russian)
- Vdovenko, M. V., 1971. New species and forms of the genus *Eoparastaffella*. Paleontologicheskii Sbornik, v. 7, no. 2, p. 6-12 (in Russian).
- Vdovenko, M. V., 1986. Early Carboniferous foraminifera from the Pridobrudzha Depression. Paleontology, stratigraphy and lithology, 22, 3-15 (in Russian).
- Vdovenko, M. V., 2001. Atlas of foraminifera from the Upper Visean and Serpukhovian (Lower Carboniferous) of the Donets Basin (Ukraine). Abhandlungen and Berichte für Naturkunde, 23, 93-178.
- Vdovenko, M. V., and Poletaev, V. I., 1981. Paleontological characterization and substantiation of the age of Carboniferous formations of the Lvov-Volyn Coal Basin based on foraminifers and brachiopods. Institut Geologicheskikh Nauk Akademii Nauk, USSR, Kiev, 62 p. (in Russian).
- Vissarionova, A. Ya., 1948. Primitivnye fuzulinidy iz nizhnego Karbona Evropiskoi chasti SSSR. (Primitive fusulinids from the Early Carboniferous of the European part of the USSR). Akademiya Nauk SSSR, Trudy Instituta Geologicheskikh Nauk 62, geologicheskaya seriya 19, 216-226 (in Russian).
- Wedeking, P. R., 1937. Einführung in die Grundlagen der historischen Geologie. Mikrobiostratigraphie die Korallen und Foraminiferenzeit Stuttgart: Ferdinand Enke, 136 pp.
- Wedekind, P. R., 1973. Einführung in die Grundlagen der historischen Geologie. Band II. Mikrobiostratigraphie die Korallen- und Foraminiferenzeit. Ferdinand Enke, Stuttgart, 136 p.

Wilson, J. L., 1975. Carbonate facies in geologic history. Springer-Verlag, New York, 469 p.

Wu, X. H., Ji, Q., and Chen, X. Y., 1998. The origin of fusulinid and a new Tournaisian-Visean boundary. *Acta Micropaleontologica Sinica*, v. 15, no. 4, p. 367-379 (in Chinese with English abstract).

Zeller, E. J., 1950. Stratigraphic significance of Mississippian endothyroid Foraminifera. *University of Kansas Paleontological Contributions*, Art. 4, 23 p., 6 pls.

Zeller, E. J., 1957. Mississippian endothyroid Foraminifera from the Cordilleran Geosynclin. *Journal of Paleontology*, v. 31, no. 4, p. 679-704.

Web Site References:

www.scotese.com/newpage4.htm

APPENDIX A

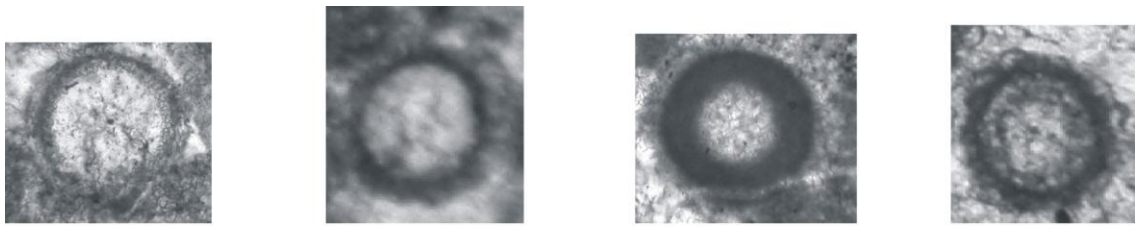
EXPLANATION OF PLATES

PLATE I

Figures

1. Calcispharidae, TD-128, X160, axial section.
2. Calcispharidae, TD-107, X160, axial section.
3. Calcispharidae, TD-124, X160, axial section.
4. Calcispharidae, TD-107, X160, axial section.
5. Calcispharidae, TD-123, X160, axial section.
6. *Lugtonia monilis* (Malakhova, 1963), TD-102, X120, axial section.
7. *Lugtonia monilis* (Malakhova, 1963), TD-61, X120, axial section.
8. *Lugtonia monilis* (Malakhova, 1963), TD-123, X120, axial section.
9. *Lugtonia monilis* (Malakhova, 1963), TD-79, X120, axial section.
10. *Earlandia* sp. TD-69, X90, axial section.
11. *Earlandia* sp. TD-103, X90, axial section.
12. *Earlandia* sp. TD-111, X90, axial section.
13. *Eoforchia moelleri* (Malakhova, 1953), TD-127, X100, axial section.
14. *Eoforchia moelleri* (Malakhova, 1953), TD-124, X100, axial section.
15. *Eoforchia moelleri* (Malakhova, 1953), TD-124, X100, axial section.
16. *Paleospiroplectamma mellina* (Malakhova, 1956), TD-127, X80, axial section.
17. *Paleospiroplectamma mellina* (Malakhova, 1956), TD-93, X80, axial section.
18. *Paleospiroplectamma mellina* (Malakhova, 1956), TD-93, X80, axial section.

PLATE I

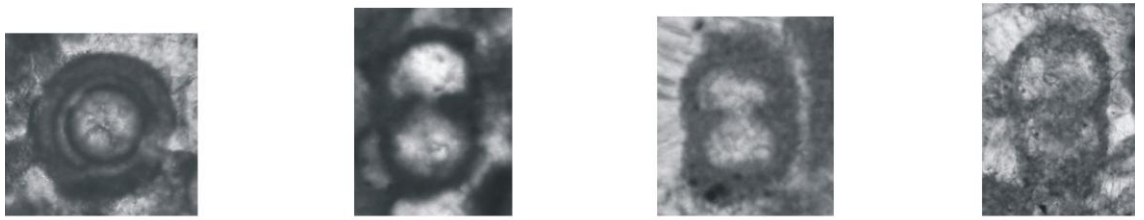


1

2

3

4

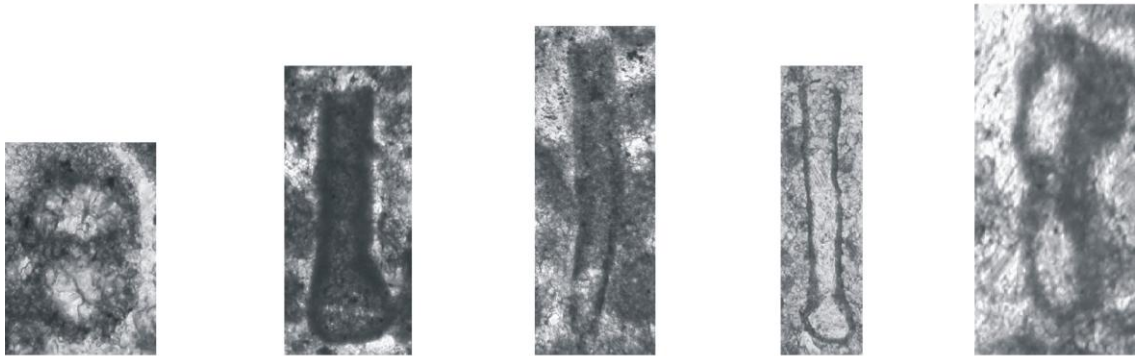


5

6

7

8



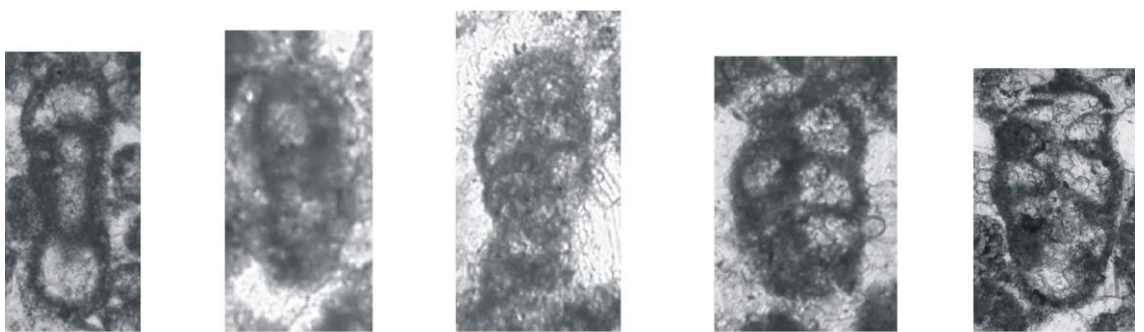
9

10

11

12

13



14

15

16

17

18

PLATE II

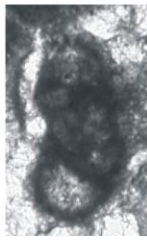
Figures

1. *Granuliferella* sp., TD-127, X95, axial section.
2. *Granuliferella* sp., TD-124, X95, axial section.
3. *Granuliferella* sp., TD-61, X95, axial section.
4. *Globoendothyra* sp., TD-127, X70, oblique section.
5. *Latiendothyranopsis* sp., TD-129, X70, axial section.
6. *Latiendothyranopsis* sp., TD-129, X70, axial section.
7. *Latiendothyranopsis* sp., TD-71, X70, axial section.
8. *Mediocris* sp., TD-123, X80, axial section.
9. *Omphalotis* sp., TD-93, X60, oblique section.
10. *Omphalotis* sp., TD-129, X60, oblique section.
11. *Dainella* sp., TD-127, X90, oblique section.
12. *Dainella* sp., TD-116, X90, oblique section.
13. *Tournayellina* sp. TD-120, X100, oblique section.
14. *Tournayellina* sp. TD-126, X100, oblique section.
15. *Tournayella* sp. TD-77, X70, axial section.
16. *Tournayella* sp. TD-127, X70, axial section.

PLATE II



1



2



3



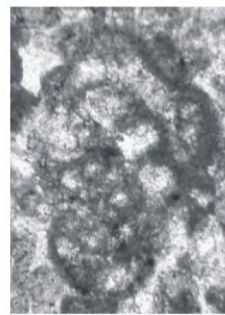
4



5



6



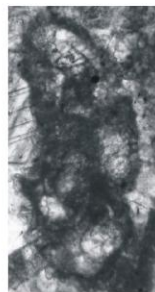
7



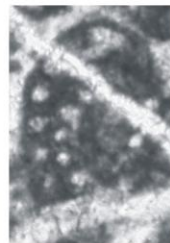
8



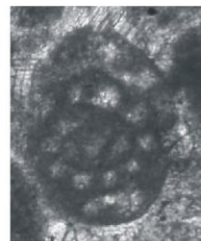
9



10



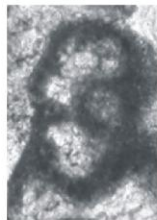
11



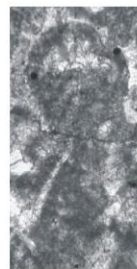
12



13



14



15



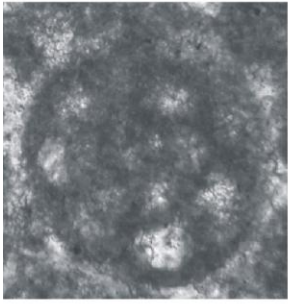
16

PLATE III

Figures

1. *Inflatoendothyra inflata* (Lipina, 1955), TD-120, X110, equatorial section.
2. *Inflatoendothyra inflata* (Lipina, 1955), TD-128, X110, equatorial section.
3. *Inflatoendothyra inflata* (Lipina, 1955), TD-128, X110, equatorial section.
4. *Inflatoendothyra inflata* (Lipina, 1955), TD-128, X110, equatorial section.
5. *Inflatoendothyra inflata* (Lipina, 1955), TD-122, X110, equatorial section.
6. *Inflatoendothyra inflata* (Lipina, 1955), TD-120, X110, equatorial section.
7. *Inflatoendothyra inflata* (Lipina, 1955), TD-127, X110, equatorial section.
8. *Inflatoendothyra inflata* (Lipina, 1955), TD-91, X110, equatorial section.
9. *Inflatoendothyra inflata* (Lipina, 1955), TD-92, X110, equatorial section.
10. *Inflatoendothyra inflata* (Lipina, 1955), TD-127, X110, equatorial section.
11. *Inflatoendothyra inflata* (Lipina, 1955), TD-81, X110, equatorial section.
12. *Inflatoendothyra inflata* (Lipina, 1955), TD-127, X110, equatorial section.

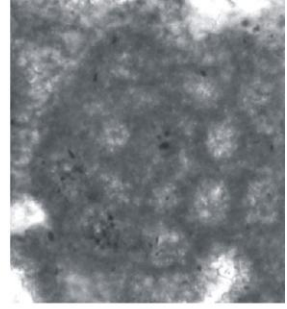
PLATE III



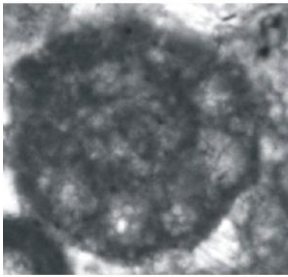
1



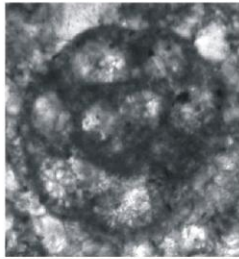
2



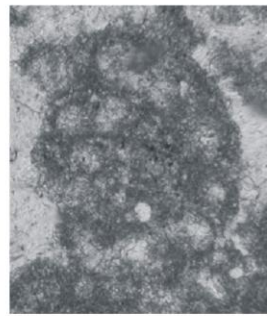
3



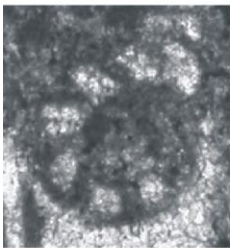
4



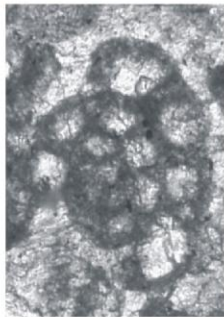
5



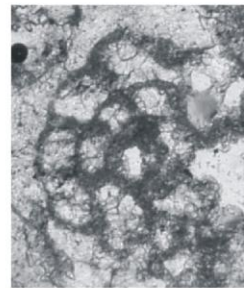
6



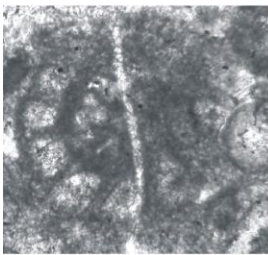
7



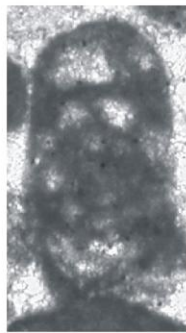
8



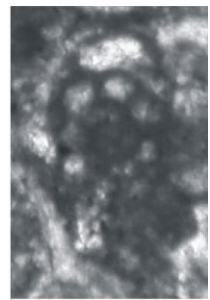
9



10



11



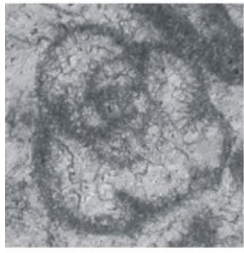
12

PLATE IV

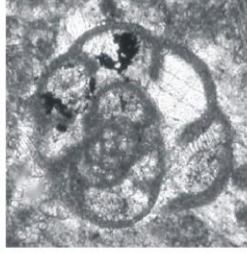
Figures

1. *Laxaendothyra* ex. gr. *laxa*. (Conil and Lys, 1964), TD-103, X90, oblique section.
2. *Laxaendothyra* ex. gr. *laxa*. (Conil and Lys, 1964), TD-127, X90, equatorial section.
3. *Laxaendothyra* ex. gr. *laxa*. (Conil and Lys, 1964), TD-128, X90, axial section.
4. *Laxaendothyra* ex. gr. *laxa*. (Conil and Lys, 1964), TD-128, X90, axial section.
5. *Eoparastaffella* (morphotype 1) sp. TD-129, X110, axial section.
6. *Eoparastaffella* (morphotype 1) sp. TD-129, X110, axial section.
7. *Eoparastaffella* (morphotype 1) sp. TD-127, X110, axial section.
8. *Eoparastaffella* (morphotype 1) sp. TD-93, X110, axial section.
9. *Eoparastaffella* (morphotype 1) sp. TD-127, X110, axial section.
10. *Eoparastaffella* (morphotype 1) sp. TD-129, X110, axial section.
11. *Eoparastaffella* (morphotype 1) sp. TD-126, X110, axial section.
12. *Eoparastaffella interiacta* (Vdovenko, 1971), TD-126, X110, axial section.
13. *Eoparastaffella interiacta* (Vdovenko, 1971), TD-127, X110, axial section.
14. *Eoparastaffella interiacta* (Vdovenko, 1971), TD-128, X110, axial section.
15. *Planoendothyra* sp., TD-102, X100, oblique section.
16. *Planoendothyra* sp., TD-77, X100, oblique section.

PLATE IV



1



2



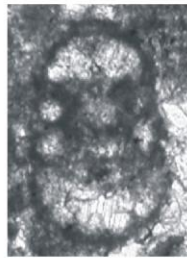
3



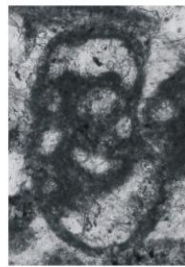
4



5



6



7



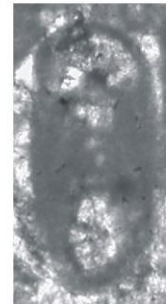
8



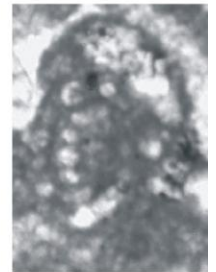
9



10



11



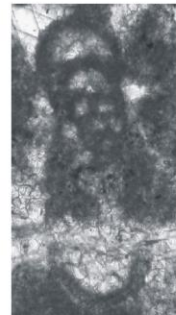
12



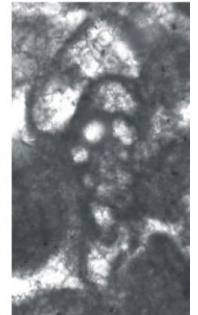
13



14



15



16

PLATE V

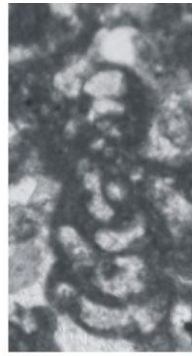
Figures

1. *Eblanaia* sp., TD-92, X90, oblique section.
2. *Eblanaia* sp., TD-95, X90, oblique section
3. *Endothyra* sp., TD-76, X85, equatorial section.
4. *Endothyra* sp., TD-127, X80, equatorial section.
5. *Endothyra* sp., TD-127, X80, oblique section
6. *Endothyra* sp., TD-115, X80, equatorial section.
7. *Endothyra* sp., TD-96, X80, oblique section
8. *Endothyra* sp., TD-96, X80, oblique section
9. *Endothyra* sp., TD-102, X80, oblique section
10. *Endothyra* ? sp., TD-120, X80, oblique section
11. *Septabrunsiina* sp. TD-89, X80, oblique section
12. *Septabrunsiina* sp. TD-120, X80, oblique section
13. *Eotextularia diversa* (Chernysheva, 1948), TD-123, X70, axial section

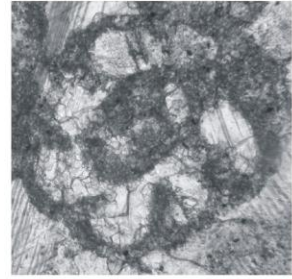
PLATE V



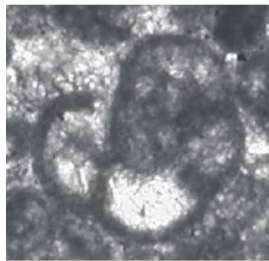
1



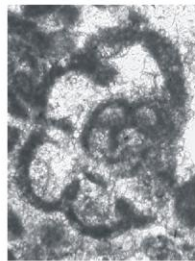
2



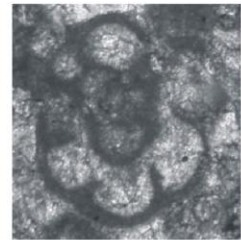
3



4



5



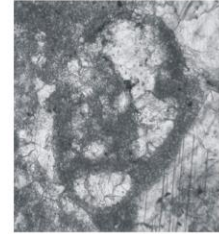
6



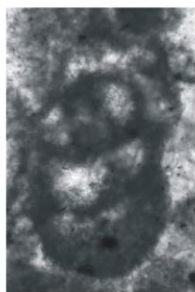
7



8



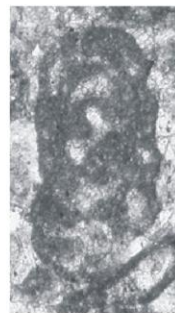
9



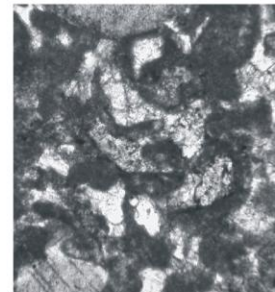
10



11



12



13

APPENDIX B

Table B: NUMBER OF BENTHIC FORAMINIFERA COUNTED IN THE MEASURED SECTION

Sample_No	Number of Foraminifera
51	118
52	0
53	10
54	8
55	8
56	0
57	3
58	4
59	0
60	0
61	61
62	42
63	23
64	0
65	0
66	10
67	0
68	0
69	16
70	0
71	171
72	0
73	0
74	0
75	0
76	118
77	240
78	174
79	220
80	172
81	15
82	218
83	107
84	182
85	106
86	380
87	310
88	115
89	140
90	180

Sample_No	Number of Foraminifera
91	162
92	360
93	206
94	62
95	104
96	220
97	110
98	190
99	150
100	96
101	24
102	250
103	340
104	57
105	66
106	52
107	210
108	93
109	D
110	D
111	20
112	42
113	58
114	97
115	47
116	72
117	94
118	62
119	310
120	420
121	87
122	96
123	127
124	120
125	132
126	140
127	210
128	280
129	150